ANALYTICAL ENERGY GRADIENTS IN MØLLER-PLESSET PERTURBATION AND QUADRATIC CONFIGURATION INTERACTION METHODS:

THEORY AND APPLICATION

Jürgen Gauss[‡] *and Dieter Cremer*

Theoretical Chemistry,
University of Göteborg, Kemigården 3,
S-41296 Göteborg, Sweden

‡ *present address: Lehrstuhl für Theoretische Chemie, Institut für Physikalische Chemie und Elektrochemie der Universität Karlsruhe, D-7500 Karlsruhe, Federal Republic of Germany*

ADVANCES IN QUANTUM CHEMISTRY
VOLUME 23

1. Introduction

During the last decades, quantum chemistry has become a rapidly expanding field of active research with many applications to pending chemical problems [1]. The breath-taking progress in quantum chemistry is strongly coupled to the successful construction of high speed computers, and, in particular, to the recent development of vector and parallel processors [2]. Their enormous computational capacity provides the basis to routinely apply quantum chemical methods to interesting chemical problems [3] thus revealing more and more the importance and relevance of quantum chemistry to all fields of chemistry. Of course, all the accomplishments in computer technology could only have such a large impact on quantum chemistry, because

quantum chemical methods have been improved at the same rapid pace leading to more efficient and more accurate algorithms almost on a daily basis. Thus, progress in computer technology and improvement of quantum chemical methods have gone hand in hand pushing quantum chemical research projects forward. High speed computers have provided for the first time the possibility of going right away from the pencil-and-paper work of method development to the reality of computational work.

One field of quantum chemistry, which has strongly contributed to the current popularity and efficiency of quantum chemical calculations, is the field of analytical energy derivative methods [4,5]. The importance of these methods results from the fact that many characteristic features of molecules depend on the variation of the energy with respect to nuclear coordinates or some external perturbation parameter such as a static electric or magnetic field. When specifying the dependence of the energy on these parameters the corresponding derivatives of the energy play a key role. For example, derivatives of the energy with respect to nuclear coordinates are used to explore the potential energy surface of a molecule and to search for equilibrium geometries and transition states along reaction paths [6]. Both equilibrium geometries and transition states represent stationary points on the potential energy surface for which the forces on the nuclei, i.e. the first derivatives of the energy with respect to the nuclear coordinates, vanish. Stationary points on an energy surface can be further characterized by the Hesse matrix which comprises the second derivatives of the energy with respect to nuclear coordinates [6]. Second and higher derivatives are also used to calculate harmonic and anharmonic frequencies [7,8].

Variation of the energy with respect to an external electric or magnetic field provides the possibility of calculating molecular properties such as dipole moment, quadrupole moment, octupole moment, polarizabilities, magnetic moments, etc. [9]. Differentiating dipole moment and polarizability with respect to nuclear coordinates leads to IR and Raman intensities [10,11] which have turned out to be very useful when assigning vibrational modes to observed IR and Raman bands. Such an assignment just on the basis of vibrational frequencies is in most cases very difficult or even impossible and, therefore, additional information such as calculated intensities is needed [7].

In principle, it is possible to calculate all properties just mentioned with the aid of finite differentiation procedures. However, there are two arguments that suggest the use of analytical derivatives rather than finite differentiation methods [12,13]. First, the accuracy of the finite differentiation scheme is not very high and calculating higher derivatives in this way can be very troublesome. Analytical methods avoid these difficulties and provide sufficient

accuracy for all derivatives. Secondly, if the number of perturbation parameters increases (in a polyatomic molecule with K atoms there are 3K forces), the numerical procedures will become very expensive. The computational costs of numerical methods directly scale with the number of perturbations, while the costs of analytical derivative methods are more or less independent of the number of perturbation parameters [5,14]. Therefore, use of analytical methods is advantageous, especially when investigating larger molecules. Compared to numerical differentiation procedures, time savings by analytical methods are considerable.

The impact of analytical derivative methods in quantum chemistry is clearly demonstrated by the fact that nowadays most quantum chemical studies include (at least at all lower levels of theory) optimization of geometries by utilizing analytically evaluated forces.

Historically, Pulay [12,14] was the first who implemented an analytical derivative scheme for a quantum chemical ab initio method. As early as 1969, he presented analytical gradients for the Hartree-Fock (HF) energy and used them to calculate equilibrium geometries, and, by numerical differentiation of the analytically evaluated gradients, force constants [14,15]. However, it should be mentioned that during this time one of the major problems of analytical derivative methods was the evaluation of the derivatives of the one-electron and two-electron integrals over AO basis functions. A major step in direction of a more efficient implementation of analytical derivatives was done when new techniques for the evaluation of electron integrals were introduced into quantum chemistry. In this context, the gaussian quadrature based on the use of Rys polynominals [16] has to be mentioned. This new technique for evaluating electron integrals was especially designed to calculate integrals over higher order Cartesian gaussian functions and this feature could be used with great advantage when computing integral derivatives [17].

In 1979, Pople and co-workers [18] implemented analytical second derivatives for HF energies thus significantly reducing the computational costs for the calculation of HF force constants. The key to their successful implementation of analytical second derivatives was the development of an efficient scheme to solve the Coupled-perturbed HF (CPHF) equations [19-21] in order to get perturbed orbitals. These are not needed for HF energy gradients but they become necessary for HF second derivatives. Pople and co-workers also presented for the first time analytical first derivatives for a correlation method, namely for second order Møller-Plesset (MP2) perturbation theory. Again, the solution of the CPHF equations was an important prerequisite for the calculation of analytical derivatives. This is due to the fact that all correlation methods, which do not optimize orbitals, require the derivatives

of the MO coefficients (given in form of perturbed orbitals) or at least some equivalent information in form of the so-called z-vector [22].

In the following, analytical first derivatives of the energy were coded for CI methods with single (S) and double (D) excitations (CISD) with respect to a HF reference function [23,24] and for the MCSCF ansatz [25,26]. Also, analytical methods for higher derivatives, which are of special interest for the calculation of vibrational spectra, were developed. For example, analytical HF third derivatives [27], analytical MCSCF- [28,29] and CI second derivatives [30] as well as analytical dipole [31] and polarizability derivatives [32,33] were coded and successfully applied in a large number of calculations.

After these developments had taken place, it was clear that the main thrust of any further developments in analytical gradient techniques would concentrate on more sophisticated electron correlation methods. Especially attractive were three groups of single determinant based correlation methods, namely the many-body perturbation techniques in the form introduced by Møller and Plesset (MP) [34], the CI methods [35] and, finally, the coupled cluster (CC) methods [36,37]. MPn methods with n = 3 and 4 were implemented by the Pople and co-workers in the late seventies [38-40] and after generally usable MP3 and MP4 programs had been released by Pople group in the early eighties [41], perturbation methods became soon very popular. The main advantage of the MP methods in particular and many-body perturbation theory in general results from the fact that these methods are size-consistent [38] (or size-extensive [37]) thus allowing a consistent description of molecules independent of size and number of electrons. Contrary to perturbation methods, CI methods truncated to single and double excitations are not size-consistent and, therefore, a CI description of chemical reaction systems has to be corrected in most cases by some empirical correction terms [42].

Apart from being size-consistent, MP methods are attractive since they can be used to investigate electron correlation in a systematic way. MP2 is certainly the simplest method of treating dynamical correlation. Of course, MP2 often exaggerates effects of D excitations, i.e. electron pair correlation, but this is largely corrected at third order MP (MP3) perturbation theory, which introduces coupling between D excitations. Fourth order MP (MP4) perturbation theory provides a simple way of including effects of higher order excitations, namely (beside those of S and D excitations) those of triple (T), and quadruple (Q) excitations [40]. T excitations can be handled at the MP4 level in a routine way even when calculating larger molecules [43]. This, however, is very difficult at the CI level [44].

Since many-body perturbation theory is not a variational theory, it does

not lead to an upper bound for the energy and this may be considered as a disadvantage of MP methods. However, in practise it turns out that lack of the variational property does not lead to serious problems. A much more severe restriction of MP methods is the fact that they are based on the single determinant ansatz of HF theory. In this context, new developments such as spin projected MP [45,46], MP with GVB [47] or CASSCF reference function [48] have to be mentioned since they may be considered as promising generalizations of the MP approach.

The CC approach [37] is related to MP perturbation theory but, although a non-variational method, it is iterative and, therefore, more expensive to carry out. Within CC theory, the wave function is written in exponential form, namely as exp(T) acting on a reference wave function where T is the excitation operator covering all possible excitations of a given type. Restricting excitations to, e.g., S and D and projecting the Schrödinger equation on all S- and D-excited forms of the reference wave function leads to a closed set of equations which can be solved iteratively [49-51]. The CC approach is size-consistent and is invariant with regard to unitary transformations among occupied (virtual) orbitals [37]. Furthermore, it seems to be applicable on a larger scale than MP theory. At least in some cases, CC methods turned out to provide reasonable descriptions of molecular systems that actually require a multi-determinant approach.

Recently, Pople, Head-Gordon, and Raghavachari [52] introduced a modified method for calculating correlation energies starting from a HF wave function. Their method corrects CI for its size-consistency error by adding to the CI equations new terms, which are quadratic in the CI coefficients. Therefore, the method was coined, perhaps unfortunately [54], quadratic CI (QCI). Alternatively, the QCI method may be considered as an approximate CC method [52-54], but since the general strategy of QCI differs from that of CC, QCI results are not necessarily inferior to those obtained with the CC methods. Both CC and QCI are correct to the same order of perturbation theory if the same excitations are considered. Thus, QCISD, i.e. QCI with S and D excitations, is correct in the SDQ space of MP4 and QCISD(T), which also considers triple excitations in an approximated way, is fully correct in fourth order perturbation theory. The more recent QCISD(TQ) method is even fully correct in fifth order perturbation theory [55]. Work carried out with the QCI methods clearly shows that these methods will establish themselves beside MP and CC methods as promising ways of getting electron correlation corrections.

During the eighties, work on analytical energy derivatives was aimed at getting appropriate formulas and efficient computer programs for MP,

CC, and QCI methods. In 1983, Jørgensen and Simons worked out the formulas for the analytical MP3 and CCD energy gradient [56]. A first attempt to implement analytical MP3 gradients was made in 1985 by Bartlett and co-workers [57]. The computer program these authors developed was not very efficient and, certainly, was not intended for routine applications. The main drawback of their program was that it required a full transformation of the two-electron integral derivatives from AO to MO basis which is a very expensive and unnecessary step [58,59]. An implementation of analytical MP3 energy gradients for routine calculations was presented by Gauss and Cremer in 1987 [58], followed shortly afterwards by a similar implementation by Bartlett's group [60]. Later, Alberts and Handy extended analytical MP3 gradient methods to unrestricted HF (UHF) reference wave functions [61].

In 1986, Fitzgerald, Harrison, and Bartlett formulated the theory for analytical MP4 energy gradients [62]. The first computer implementation of the analytical MP4 gradient restricted to S, D, and Q excitations was published by Gauss and Cremer in 1987 [58]. Full MP4 gradient calculations including T excitations were reported by Gauss and Cremer [63] and, independently, by Bartlett and co-workers [64,65] in 1988.

In the early eighties, analytical gradients for CC methods seemed to be more complicated than either MP or CI gradients. Due to the nonvariational character of the CC method the derivatives of the excitation amplitudes seemed to be needed for the CC energy gradient. In 1985, Bartlett and co-workers succeeded in solving the Coupled-perturbed CC (CPCC) equations for CCD to determine the derivatives of the D excitation amplitudes [66]. This, however, was not the final solution of the CC gradient problem. In 1984, Handy and Schaefer showed that in all gradient expressions perturbation dependent quantities which have to be determined by some additional set of equations, e.g. by the CPHF or CPCC equations, can be replaced by a vector z [22]. The z-vector is the solution of only one set of equations that does not depend on the perturbation. Adamowicz, Laidig, and Bartlett [67] applied the z-vector method to derive expressions for the analytical CCSD energy gradient. In 1987, Schaefer and co-workers presented the first computer implementation of analytical CCSD gradients based on these ideas [68]. Later, Scuseria and Schaefer extended this work by including T excitations via the CCSDT-1 ansatz [69,70]. However, most of these developments were restricted so far to RHF reference functions. A generalization to UHF and ROHF reference functions as well as some special classes of non-HF reference functions in the case of the CCSD method was recently carried out by Gauss, Stanton, and Bartlett [71].

In 1988, the theory of analytical QCISD energy gradients as well as the

first computer implementation for routine calculations was reported by Gauss and Cremer [72]. In this work, the z-vector method was used to determine the derivatives of the QCI amplitudes. Recently, Gauss and Cremer were also able to derive the analytical energy gradient for QCISD(T) [73] utilizing techniques which had previously been developed to handle T excitations at the MP4 level [63]

2. Comparison of Møller-Plesset and Quadratic CI Electron Correlation Theories

2.1 Møller-Plesset Perturbation theory

In Møller-Plesset (MP) perturbation theory [34] the unperturbed Hamiltonian $\mathbf{H}_0$ is chosen as a sum of Fock operators $\mathbf{F}$

$$\mathbf{H}_0 = \sum_{\xi} \mathbf{F}(\xi). \tag{2.1}$$

and the perturbed Hamiltonian $\mathbf{H}'$ is given as the difference between the exact Hamiltonian $\mathbf{H}$ and the zeroth order Hamiltonian $\mathbf{H}_0$. The Fock operator $\mathbf{F}(\xi)$ of the ξth electron in eq.(2.1) is defined as

$$\mathbf{F}(\xi) = \mathbf{h}(\xi) + \sum_{\tau}(\mathbf{J}_\tau(\xi) - \mathbf{K}_\tau(\xi)), \tag{2.2}$$

where $\mathbf{h}(\xi)$ denotes the one-electron part of the Hamiltonian and $\mathbf{J}_\tau(\xi)$ and $\mathbf{K}_\tau(\xi)$ are the Coulomb and exchange operators which describe two-electron interactions between the τth and the ξth electron. For the perturbation expansion the Hartree-Fock (HF) wave function is used as zeroth order function. In the following the HF spin orbitals are denoted by φ_p. It is assumed that they are eigen functions of the Fock operator $\mathbf{F}$ with eigen value ε_p. Following a widespread convention we will use indices $i, j, k, \ldots$ to label occupied orbitals and indices $a, b, c, \ldots$ to label unoccupied (virtual) orbitals. In cases where the formulas hold for both type of orbitals indices $p, q, r, \ldots$ are used.

The energy corrections are calculated in MP theory using the Rayleigh-Schrödinger expansion. At second order, this gives the following energy contribution [34,38]

$$\mathrm{E(MP2)} = \frac{1}{4}\sum_{i,j}\sum_{a,b} a(ij,ab)\langle ij\|ab\rangle, \tag{2.3}$$

where $a(ij,ab)$ denotes the first order correction to the wave function

$$a(ij,ab) = \langle ij\|ab\rangle/(\varepsilon_i + \varepsilon_j - \varepsilon_a - \varepsilon_b) \tag{2.4}$$

and $\langle pq\|rs\rangle$ is the usual anti-symmetrized two-electron integral

$$\langle pq\|rs\rangle = \int \varphi_p(1)\varphi_q(2)\frac{1}{|\mathbf{r_1} - \mathbf{r_2}|}[\varphi_r(1)\varphi_s(2) - \varphi_s(1)\varphi_r(2)]d\tau_1 d\tau_2. \tag{2.5}$$

At third order the energy correction is given by [38]

$$\mathrm{E(MP3)} = \frac{1}{4}\sum_{i,j}\sum_{a,b} a(ij,ab)w(ij,ab) \tag{2.6}$$

with

$$\begin{aligned} w(ij,ab) = {} & \frac{1}{2}\sum_{k,l}\langle kl\|ij\rangle a(kl,ab) + \frac{1}{2}\sum_{c,d}\langle ab\|cd\rangle a(ij,cd) \\ & - \sum_{k}\sum_{c}\{\langle ka\|ic\rangle a(kj,cb) + \langle ka\|jc\rangle a(ik,cb) \\ & + \langle kb\|ic\rangle a(kj,ac) + \langle kb\|jc\rangle a(ik,ac)\}. \end{aligned} \tag{2.7}$$

While second and third order MP perturbation theory include only double(D) excitations with respect to the HF reference function, fourth order MP theory considers in addition single(S), triple(T), and quadruple(Q) excitations [39]. The energy correction at this level of theory is usually given as [39,40]

$$\begin{aligned} \mathrm{E(MP4)} = {} & \sum_{i}\sum_{a} w(i,a)d(i,a) + \frac{1}{4}\sum_{i,j}\sum_{a,b} w(ij,ab)d(ij,ab) \\ & + \frac{1}{36}\sum_{i,j,k}\sum_{a,b,c} w(ijk,abc)d(ijk,abc) \\ & + \frac{1}{4}\sum_{i,j}\sum_{a,b} a(ij,ab)v_q(ij,ab). \end{aligned} \tag{2.8}$$

In eq.(2.8), the first term denotes the energy correction due to S, the second due to D, the third due to T, and the fourth due to Q excitations. The various arrays in eq.(2.8) are defined as

$$w(i,a) = \frac{1}{2}\sum_{j}\sum_{b}\Big(\sum_{c}\langle aj\|cb\rangle a(ij,cb) - \sum_{k}\langle ib\|kj\rangle a(kj,ab)\Big), \tag{2.9}$$

$$d(i,a) = w(i,a)/(\varepsilon_i - \varepsilon_a), \tag{2.10}$$

$$d(ij,ab) = w(ij,ab)/(\varepsilon_i + \varepsilon_j - \varepsilon_a - \varepsilon_b), \tag{2.11}$$

$$\begin{aligned} w(ijk,abc) = \sum_d \{ & a(ij,ad)\langle bc\|dk\rangle + a(ij,bd)\langle ca\|dk\rangle + a(ij,cd)\langle ab\|dk\rangle \\ & + a(ki,ad)\langle bc\|dj\rangle + a(ki,bd)\langle ca\|dj\rangle + a(ki,cd)\langle ab\|dj\rangle \\ & + a(jk,ad)\langle bc\|di\rangle + a(jk,bd)\langle ca\|di\rangle + a(jk,cd)\langle ab\|di\rangle \} \\ - \sum_l \{ & a(il,ab)\langle cl\|jk\rangle + a(il,bc)\langle al\|jk\rangle + a(il,ca)\langle bl\|jk\rangle \\ & + a(jl,ab)\langle cl\|ki\rangle + a(jl,bc)\langle al\|ki\rangle + a(jl,ca)\langle bl\|ki\rangle \\ & + a(kl,ab)\langle cl\|ij\rangle + a(kl,bc)\langle al\|ij\rangle + a(kl,ca)\langle bl\|ij\rangle \}, \end{aligned} \tag{2.12}$$

$$d(ijk,abc) = w(ijk,abc)/(\varepsilon_i + \varepsilon_j + \varepsilon_k - \varepsilon_a - \varepsilon_b - \varepsilon_c), \tag{2.13}$$

and

$$\begin{aligned} v_q(ij,ab) = \frac{1}{4} \sum_{k,l} \sum_{c,d} \langle kl\|cd\rangle \big[& a(ij,cd)a(kl,ab) \\ & - 2\{a(ij,ac)a(kl,bd) + a(ij,bd)a(kl,ac)\} \\ & - 2\{a(ik,ab)a(jl,cd) + a(ik,cd)a(jl,ab)\} \\ & + 4\{a(ik,ac)a(jl,d) + a(ik,bd)a(jl,ac)\}\big]. \end{aligned} \tag{2.14}$$

Note that in order to reduce computational costs the formula for the energy contribution due to quadruple excitations has been rearranged [39] and combined with the renormalization term.

An alternative formula which turns out to be useful when deriving formulas for the energy gradient with respect to some external perturbation (see chapter 3), is given by eq.(2.15) [58] :

$$\begin{aligned} \mathrm{E(MP4)} = \frac{1}{4} \sum_{i,j} \sum_{a,b} a(ij,ab)\{ & v_s(ij,ab) + v_d(ij,ab) \\ & + v_t(ij,ab) + v_q(ij,ab)\}, \end{aligned} \tag{2.15}$$

where the various v-arrays are defined by [58,63]

$$\begin{aligned} v_s(ij,ab) = \sum_c \{ & \langle ab\|cj\rangle d(i,c) + \langle ab\|ic\rangle d(j,c)\} \\ & - \sum_k \{\langle kb\|ij\rangle d(k,a) + \langle ka\|ji\rangle d(k,b)\}, \end{aligned} \tag{2.16}$$

$$\begin{aligned} v_d(ij,ab) = & \frac{1}{2} \sum_{k,l} \langle kl\|ij\rangle d(kl,ab) + \frac{1}{2} \sum_{c,d} \langle ab\|cd\rangle d(ij,cd) \\ & - \sum_k \sum_c \{\langle ka\|ic\rangle d(kj,cb) + \langle ka\|jc\rangle d(ik,cb) \\ & + \langle kb\|ic\rangle d(kj,ac) + \langle kb\|jc\rangle d(ik,ac)\}. \end{aligned} \tag{2.17}$$

$$\begin{aligned} v_t(ij,ab) = & \frac{1}{2} \sum_k \sum_{c,d} \{\langle cd\|bk\rangle d(ijk,acd) - \langle cd\|ak\rangle d(ijk,bcd)\} \\ & + \frac{1}{2} \sum_{k,l} \sum_c \{\langle cj\|kl\rangle d(ikl,abc) - \langle ci\|kl\rangle d(jkl,abc)\}. \end{aligned} \tag{2.18}$$

Recently, also formulas for the energy correction at fifth order MP theory have been given and implemented [55,74,75]. Compared to MP4, no additional excitations are included and only couplings between S, T, and Q excitations, respectively, are introduced in MP5. However, since MP5 is computationally very expensive (the evaluation of the T-T coupling terms requires $O(N^8)$ operations compared to the most expensive $O(N^7)$ step in MP4), it is not expected that MP5 will be in the near future a standard method for large scale calculations.

2.2 Quadratic Configuration Interaction Theory

The coupled cluster (CC) [36] ansatz for the description of electron correlation is based on the following exponential form of the wave function

$$\Psi = \exp(\mathbf{T})\Psi_0, \tag{2.19}$$

where Ψ_0 denotes a single determinant reference function, usually the HF wave function, and $\mathbf{T}$ denotes a general excitation operator which considers all possible types of excitations up to n-tuple excitations when n is the number of electrons. Equations for the energy and for the amplitudes of the various excitations are obtained in CC theory by projecting the Schrödinger equation with Ψ given by eq. (2.19) onto the various determinants, namely Ψ_0, the singly excited determinants Ψ_i^a, etc. [36,37].

Similar to the CI method [35] CC calculations including all possible types of excitations are not feasible in most cases and several restrictions have to be imposed. Limitation of $\mathbf{T}$ to double excitations yields the CC doubles (CCD) method [49,50], additional inclusion of single excitations leads to the CC singles and doubles (CCSD) method [51] and so on.

The QCI approach of Pople and co-workers [52] can be regarded as an approximate CC method in which only those of the non linear terms are kept which are needed to guarantee size consistency. QCID including only double excitations is identical with CCD, while QCISD including single and double excitations neglects all cubic and quartic terms compared to CCSD [52].

With single and double excitation amplitudes denoted by a_i^a and a_{ij}^{ab} respectively, projection of the Schrödinger equation onto Ψ_0, Ψ_i^a, and Ψ_{ij}^{ab} yields for the QCISD correlation energy [52]

$$\mathrm{E(QCISD)} = \frac{1}{4}\sum_{i,j}\sum_{a,b} a_{ij}^{ab}\langle ij\|ab\rangle \tag{2.20}$$

and for the equations, which determine the amplitudes a_i^a and a_{ij}^{ab} [52]

$$(\varepsilon_a - \varepsilon_i)a_i^a + w_i^a + v_i^a = 0, \tag{2.21}$$

$$(\varepsilon_a + \varepsilon_b - \varepsilon_i - \varepsilon_j)a_{ij}^{ab} + w_{ij}^{ab} + v_{ij}^{ab} + \langle ij\|ab\rangle = 0. \tag{2.22}$$

The arrays w_i^a and w_{ij}^{ab} depend linearly on the configuration coefficients a_i^a and a_{ij}^{ab},

$$w_i^a = -\sum_j\sum_b \langle ja\|ib\rangle a_j^b - \frac{1}{2}\sum_j\sum_{b,c}\langle ja\|bc\rangle a_{ij}^{bc} - \frac{1}{2}\sum_{j,k}\sum_b \langle jk\|ib\rangle a_{jk}^{ab} \tag{2.23}$$

and

$$\begin{aligned} w_{ij}^{ab} = {} & \sum_c\{\langle ab\|cj\rangle a_i^c - \langle ab\|ci\rangle a_j^c\} + \sum_k\{-\langle kb\|ij\rangle a_k^a + \langle ka\|ij\rangle a_k^b\} \\ & + \frac{1}{2}\sum_{k,l}\langle kl\|ij\rangle a_{kl}^{ab} + \frac{1}{2}\sum_{c,d}\langle ab\|cd\rangle a_{ij}^{cd} - \sum_k\sum_c\{\langle kb\|jc\rangle a_{ik}^{ac} \\ & + \langle ka\|jc\rangle a_{ik}^{cb} + \langle kb\|ic\rangle a_{kj}^{ac} + \langle ka\|ic\rangle a_{kj}^{cb}\}, \end{aligned} \tag{2.24}$$

while v_i^a and v_{ij}^{ab} are quadratic in the amplitudes :

$$v_i^a = \frac{1}{2}\sum_{j,k}\sum_{b,c}\langle jk\|bc\rangle\{a_i^b a_{jk}^{ca} + a_j^a a_{ik}^{cb} + 2a_j^b a_{ik}^{ac}\} \tag{2.25}$$

and

$$\begin{aligned} v_{ij}^{ab} = \frac{1}{4}\sum_{k,l}\sum_{c,d}\langle kl\|cd\rangle[a_{ij}^{cd}a_{kl}^{ab} - 2\{a_{ij}^{ac}a_{kl}^{bd} + a_{ij}^{bd}a_{kl}^{ac}\} \\ - 2\{a_{ik}^{ab}a_{jl}^{cd} + a_{ik}^{cd}a_{jl}^{ab}\} + 4\{a_{ik}^{ac}a_{jl}^{bd} + a_{ik}^{bd}a_{jl}^{ac}\}]. \end{aligned} \tag{2.26}$$

The QCISD equations are solved iteratively via eq.s (2.27) and (2.28)

$$a_i^{a(n+1)} = [w_i^{a(n)} + v_i^{a(n)}]/(\varepsilon_i - \varepsilon_a), \tag{2.27}$$

$$a_{ij}^{ab(n+1)} = [\langle ij\|ab\rangle + w_{ij}^{ab(n)} + v_{ij}^{ab(n)}]/(\varepsilon_i + \varepsilon_j - \varepsilon_a - \varepsilon_b), \tag{2.28}$$

using as initial guess for the amplitudes

$$a_i^{a(0)} = 0, \tag{2.29}$$

$$a_{ij}^{ab(0)} = \langle ij\|ab\rangle/(\varepsilon_i + \varepsilon_j - \varepsilon_a - \varepsilon_b). \tag{2.30}$$

Convergence is usually significantly accelerated by applying extrapolation schemes of the DIIS type [76-79].

Since an explicit treatment of triple excitations in QCI theory is in most cases impractical [80] but on the other side often necessary, Pople and coworkers [52] proposed an useful approximation for treating them within the QCI approach. Their approximation is based on the assumption that triple excitations are small perturbations on the solution obtained at the QCISD level. Perturbation theory yields then for the energy correction due to triples [52]

$$\Delta\mathrm{E(T)} = \frac{1}{36}\sum_{i,j,k}\sum_{a,b,c} d_{ijk}^{abc}(w_{ijk}^{abc} + 2\tilde{w}_{ijk}^{abc}) \tag{2.31}$$

with

$$\begin{aligned} w_{ijk}^{abc} = {} & \sum_d\{a_{ij}^{ad}\langle bc\|dk\rangle + a_{ij}^{bd}\langle ca\|dk\rangle + a_{ij}^{cd}\langle ab\|dk\rangle + a_{ki}^{ad}\langle bc\|dj\rangle \\ & + a_{ki}^{bd}\langle ca\|dj\rangle + a_{ki}^{cd}\langle ab\|dj\rangle + a_{jk}^{ad}\langle bc\|di\rangle + a_{jk}^{bd}\langle ca\|di\rangle + a_{jk}^{cd}\langle ab\|di\rangle\} \\ & + \sum_l\{a_{il}^{ab}\langle cl\|jk\rangle + a_{il}^{bc}\langle al\|jk\rangle + a_{il}^{ca}\langle bl\|jk\rangle + a_{jl}^{ab}\langle cl\|ki\rangle \\ & + a_{jl}^{bc}\langle al\|ki\rangle + a_{jl}^{ca}\langle bm\|ki\rangle + a_{kl}^{ab}\langle cl\|ij\rangle + a_{kl}^{bc}\langle al\|ij\rangle + a_{kl}^{ca}\langle bm\|ij\rangle\}, \end{aligned} \tag{2.32}$$

$$\tilde{w}_{ijk}^{abc} = a_i^a\langle jk\|bc\rangle + a_i^b\langle jk\|ca\rangle + a_i^c\langle jk\|ab\rangle + a_j^a\langle ki\|bc\rangle + a_j^b\langle ki\|ca\rangle + a_j^c\langle ki\|ab\rangle + a_k^a\langle ij\|bc\rangle + a_k^b\langle ij\|ca\rangle + a_k^c\langle ij\|ab\rangle, \quad (2.33)$$

and

$$d_{ijk}^{abc} = w_{ijk}^{abc}/(\varepsilon_i + \varepsilon_j + \varepsilon_k - \varepsilon_a - \varepsilon_b - \varepsilon_c). \quad (2.34)$$

In these equations, a_i^a and a_{ij}^{ab} denote the converged QCISD amplitudes of single and double excitations, respectively. It has been demonstrated [52,83-86] that this approximate treatment of triple excitations leads to highly accurate results, which are in many cases comparable to those of full CI calculations.

Recently, Raghavachari et. al. [55] proposed a new non-iterative correction to the QCISD approach which considers beside triple excitations also connected quadruple excitations [87]. This method, which was named QCISD(TQ) is correct to fifth order of MP theory [55,74,75] and should yield as long as the single reference ansatz is appropriate, excellent result. However, since this method contains a $O(N^8)$ step which should be compared with the most expensive $O(N^7)$ of the QCISD(T) method, it is certainly not a method which can routinely be applied in large scale calculations.

2.3 The Relationship between QCISD Theory and MP Perturbation Theory

As it has been shown by several authors [74,76] there is a close relation between MP perturbation theory on one side and CC and QCI theory on the other side. The results of MP perturbation theory can be recovered by collecting various terms of the first iterations of QCISD (and as well as CCSD), which in the language of perturbation theory is a method that sums up several terms to infinite order [74,76].

When we write the MPn energy contribution in n-th order in the form

$$\mathrm{E(MPn)} = \frac{1}{4}\sum_{i,j}\sum_{a,b} a_{ij}^{ab}(\mathrm{MPn})\langle ij\|ab\rangle, \quad (2.35)$$

we obtain for the amplitudes a_{ij}^{ab}(MPn) in second, third, and fourth order

$$a_{ij}^{ab}(\mathrm{MP2}) = a(ij,ab), \quad (2.36)$$

$$a_{ij}^{ab}(\mathrm{MP3}) = d(ij,ab), \quad (2.37)$$

and

$$a_{ij}^{ab}(\mathrm{MP4}) = \{v_s(ij,ab) + v_d(ij,ab) + v_t(ij,ab) + v_q(ij,ab)\}/(\varepsilon_i + \varepsilon_j - \varepsilon_a - \varepsilon_b). \quad (2.38)$$

The first iteration of QCISD yields (with a_i^a and a_{ij}^{ab} set to zero in the initial guess)

$$a_{ij}^{ab}(\mathrm{QCISD, 1.Iteration}) = \langle ij\|ab\rangle/(\varepsilon_i + \varepsilon_j - \varepsilon_a - \varepsilon_b) \quad (2.39)$$

and, therefore, recovers the MP2 result. The second iteration gives

$$a_{ij}^{ab}(\mathrm{QCISD, 2.Iteration}) = a(ij,ab) + d(ij,ab) + v_q(ij,ab)/(\varepsilon_i + \varepsilon_j - \varepsilon_a - \varepsilon_b) \quad (2.40)$$

and produces the MP3 amplitudes as well as those due to the quadruple part of MP4. Note that while $d(ij,ab)$ is linear in the amplitudes $a(ij,ab)$ (see eq.s (2.7) and (2.8)) and thus a third order term, $v_q(ij,ab)$ is quadratic in $a(ij,ab)$ and hence a fourth order term. The third iteration of the QCISD method finally yields

$$a_{ij}^{ab}(\mathrm{QCISD, 3.Iteration}) = a(ij,ab) + d(ij,ab) + \{v_s(ij,ab) + v_d(ij,ab) + v_q(ij,ab)\}/(\varepsilon_i + \varepsilon_j - \varepsilon_a - \varepsilon_b) + \textit{higher order terms}. \quad (2.41)$$

Beside several higher order terms the third iteration gives the remaining single and double excitation terms of MP4. However, a theory which includes only single and double excitations cannot account for the triple excitation terms in MP4 and, therefore, is not exact to fourth order. The triple term in MP4 on the other side is closely related to the additional terms in QCISD(T) theory which are obtained in the perturbational treatment of triple excitations. The differences are that the fully converged QCISD amplitudes rather than $a(ij,ab)$ are used to calculate the triple corrections, and, second, that an additional coupling of single and double excitations which corresponds to a fifth order term in MP theory is introduced. The recently introduced QCISD(TQ) method [55] is finally correct to fifth order of MP theory.

3. Energy gradients

Analytical expressions for the energy gradients in MP and QCI theory with respect to an external perturbation λ such as the displacements of nuclear coordinates, or the components of a static electric (magnetic) field are easily derived by straightforward differentiation of the energy formulas discussed in the previous paragraph. Since the energy formulas are given in terms of two-electron integrals and orbital energies, we first discuss (section 3.1) the derivatives of these quantities. This requires some discussion of the theory of energy derivatives in HF theory, in particular of the so called coupled-perturbed HF theory. After this we will derive formulas for MP2, MP3, MP4 (section 3.2), QCISD and QCISD(T) (section 3.3) energy gradients and discuss the relations between the various gradient formulas (section 3.4). Finally, these formulas are condensed into a form which is useful for the implementation of analytical gradient methods within computer programs (section 3.5).

3.1 Derivatives of Two-electron Integrals and Orbital Energies

Differentiation of the two-electron integrals $\langle pq\|rs\rangle$ and the orbital energies ε_p with respect to an external perturbation λ is straightforward. The HF orbitals are given by

$$\varphi_p = \sum_\mu c_{\mu p}\chi_\mu, \tag{3.1}$$

where the χ_μ are the AO basis functions and the $c_{\mu p}$ the usual MO coefficients as determined in the SCF procedure. The derivatives of the orbitals are usually given in terms of the derivatives $\partial c_{\mu p}/\partial\lambda$ of the MO coefficients. Within standard Coupled-perturbed HF (CPHF) theory [18,21]), the derivatives $\partial c_{\mu p}/\partial\lambda$ are expanded in terms of the unperturbed coefficients $c_{\mu p}$ [18]

$$\frac{\partial c_{\mu p}}{\partial\lambda} = \sum_q U^\lambda_{qp} c_{\mu q}, \tag{3.2}$$

where the U^λ_{qp} are the perturbation dependent expansion coefficients. Orthonormality of the perturbed orbitals requires further that

$$U^\lambda_{qp} + U^\lambda_{pq} + S^\lambda_{qp} = 0 \tag{3.3}$$

with

$$S^\lambda_{qp} = \sum_{\mu,\nu} c_{\mu p}\frac{\partial S_{\mu\nu}}{\partial\lambda}c_{\nu q} \tag{3.4}$$

and $S_{\mu\nu}$ being the overlap matrix of the AO basis functions. Note that the dependence of the AO basis functions on the perturbation λ is usually included into the derivatives of the one- and two-electron operators of the Hamiltonian within the AO representation, e.g.

$$\frac{\partial h_{\mu\nu}}{\partial\lambda} = \langle\frac{\partial\chi_\mu}{\partial\lambda}|\mathbf{h}|\chi_\nu\rangle + \langle\chi_\mu|\frac{\partial\mathbf{h}}{\partial\lambda}|\chi_\nu\rangle + \langle\chi_\nu|\mathbf{h}|\frac{\partial\chi_\mu}{\partial\lambda}\rangle \tag{3.5}$$

and

$$\begin{aligned}\frac{\partial\langle\mu\nu\|\sigma\rho\rangle}{\partial\lambda} = {}&\langle\frac{\partial\chi_\mu}{\partial\lambda}\chi_\nu\|\chi_\sigma\chi_\rho\rangle + \langle\chi_\mu\frac{\partial\chi_\nu}{\partial\lambda}\|\chi_\sigma\chi_\rho\rangle\\ &+ \langle\chi_\mu\chi_\nu\|\frac{\partial\chi_\sigma}{\partial\lambda}\chi_\rho\rangle + \langle\chi_\mu\chi_\nu\|\chi_\sigma\frac{\partial\chi_\rho}{\partial\lambda}\rangle.\end{aligned} \tag{3.6}$$

The coefficients U^λ_{pq} are determined by solving the CPHF equations [19-21] which are obtained by differentiating the HF equations with respect to λ. However, there exists some ambiguity with respect to the definition of the perturbed orbitals in a similar way as it exists for the unperturbed orbitals. Energy gradients and perturbed wave function are invariant to rotations among the perturbed occupied (virtual) orbitals. There is no unique choice for the corresponding mixing coefficients U^λ_{ij} and U^λ_{ab} [88]. The selection of canonical orbitals which turns out to be advantageous in the case of the unperturbed orbitals and which would diagonalize the matrix $\partial\varepsilon_{pq}/\partial\lambda$ of the derivatives of the Lagrangian multipliers is not the best choice. Computation of the mixing coefficients U^λ_{ij} and U^λ_{ab} within this specific choice of perturbed orbitals causes numerical difficulties as soon as degenerate or nearly degenerate orbitals are encountered [18,88]. It is more advantageous to fix the coefficients U^λ_{ij} and U^λ_{ab} to

$$U^\lambda_{ij} = -\frac{1}{2}S^\lambda_{ij} \tag{3.7}$$

and

$$U^\lambda_{ab} = -\frac{1}{2}S^\lambda_{ab} \tag{3.8}$$

respectively [89]. In this way, one avoids all numerical difficulties although one has to deal now with the off-diagonal elements of the $\partial\varepsilon_{pq}/\partial\lambda$ matrix [88]. The only derivatives U^λ_{pq} that have not been defined so far are the derivatives U^λ_{ai} which describe the mixing between occupied and virtual orbitals. They are determined by the CPHF equations [18,21]

$$\sum_b\sum_j(A_{aibj} + (\varepsilon_a - \varepsilon_i)\delta_{ab}\delta_{ij})U^\lambda_{bj} = B^\lambda_{ai} \tag{3.9}$$

which are obtained by differentiating the HF equations with respect to λ. The various terms in eq. (3.9) are defined as

$$A_{pqrs} = \langle pr\|qs\rangle + \langle ps\|qr\rangle \tag{3.10}$$

and

$$B^{\lambda}_{ai} = -F^{(\lambda)}_{ai} + \varepsilon_i S^{\lambda}_{ai} + \frac{1}{2}\sum_{k,l} A_{klai} S^{\lambda}_{kl}, \tag{3.11}$$

where $F^{(\lambda)}_{ai}$ denotes the following derivative of the Fock matrix $F_{\mu\nu}$ transformed to the MO basis

$$\begin{aligned} F^{(\lambda)}_{ai} &= \sum_{\mu,\nu} c_{\mu a} F^{(\lambda)}_{\mu\nu} c_{\nu i} \\ &= \sum_{\mu,\nu} c_{\mu a} \{ \frac{\partial h_{\mu\nu}}{\partial \lambda} + \sum_{k} \sum_{\sigma,\rho} c_{\sigma k} c_{\rho k} \frac{\partial \langle \mu\sigma\|\nu\rho\rangle}{\partial \lambda} \} c_{\nu i}. \end{aligned} \tag{3.12}$$

Although one can show that the solution of the CPHF equation is not required for the evaluation of analytical energy gradients in any of the methods considered [22,58,59], it is on the other side very convenient to use the derivatives U^{λ}_{pq} in the derivation of the gradient formulas. The elimination of the coefficient U^{λ}_{ai} from the gradient formulas is discussed later in chapter 3.5.

Using CPHF theory, we obtain the following expression for the derivatives of the two-electron integrals $\langle pq\|rs\rangle$:

$$\begin{aligned} \frac{\partial \langle pq\|rs\rangle}{\partial \lambda} &= \sum_{\mu\nu\sigma\rho} c_{\mu p} c_{\nu q} c_{\sigma r} c_{\rho s} \frac{\partial \langle \mu\nu\|\sigma\rho\rangle}{\partial \lambda} + \sum_{t} U^{\lambda}_{tp} \langle tq\|rs\rangle \\ &\quad + \sum_{t} U^{\lambda}_{tq} \langle pt\|rs\rangle + \sum_{t} U^{\lambda}_{tr} \langle pq\|ts\rangle + \sum_{t} U^{\lambda}_{ts} \langle pq\|rt\rangle. \end{aligned} \tag{3.13}$$

Explicit specification of the orbitals φ_p, φ_q, φ_r, and φ_s allows further simplification of eq. (3.13) using eq.s (3.3), (3.7), and (3.8). E.g., the derivatives of the integrals $\langle ij\|ab\rangle$ are given by

$$\begin{aligned} \frac{\partial \langle ij\|ab\rangle}{\partial \lambda} &= \sum_{\mu\nu\sigma\rho} c_{\mu i} c_{\nu j} c_{\sigma a} c_{\rho b} \frac{\partial \langle \mu\nu\|\sigma\rho\rangle}{\partial \lambda} \\ &\quad + \sum_{c} U^{\lambda}_{ci} \langle cj\|ab\rangle - \frac{1}{2}\sum_{k} S^{\lambda}_{ki} \langle kj\|ab\rangle \end{aligned}$$

$$\begin{aligned} &+ \sum_{c} U^{\lambda}_{cj} \langle ic\|ab\rangle - \frac{1}{2}\sum_{k} S^{\lambda}_{kj} \langle ik\|ab\rangle \\ &- \sum_{k} \{U^{\lambda}_{ak} + S^{\lambda}_{ak}\} \langle ij\|kb\rangle - \frac{1}{2}\sum_{c} S^{\lambda}_{ca} \langle ij\|cb\rangle \\ &- \sum_{k} \{U^{\lambda}_{bk} + S^{\lambda}_{bk}\} \langle ij\|ak\rangle - \frac{1}{2}\sum_{c} S^{\lambda}_{cb} \langle ij\|ac\rangle. \end{aligned} \tag{3.14}$$

For the Lagrangian multipliers which are in HF theory given as

$$\varepsilon_{pq} = \sum_{\mu,\nu} c_{\mu p} F_{\mu\nu} c_{\nu q} \tag{3.15}$$

straightforward differentiation yields

$$\frac{\partial \varepsilon_{pq}}{\partial \lambda} = F^{(\lambda)}_{pq} + \sum_{a}\sum_{i} U^{\lambda}_{ai} A_{pqai} - \frac{1}{2}\sum_{k,l} S^{\lambda}_{kl} A_{pqkl} - \frac{1}{2} S^{\lambda}_{pq} (\varepsilon_p + \varepsilon_q). \tag{3.16}$$

By this, the derivatives of the orbital energies and two-electron integrals are given which are needed to derive analytic expressions for MP and QCI gradients.

3.2 Gradients in MP Perturbation Theory

In MP perturbation theory differentiation of the energy is straightforward, because the MP energies at all orders are given as "fixed" expressions in terms of two-electron integrals $\langle pq\|rs\rangle$ and orbital energies ε_p. Thus, the formulas for the energy gradients contain only derivatives of these quantities and beside the derivatives of one- and two-electron integrals as well as the derivatives of the MO coefficients no additional perturbation dependent quantities are required.

For second [18], third [58], and fourth order [58,63], one obtains

$$\begin{aligned} \frac{dE(\mathrm{MP2})}{d\lambda} &= \frac{1}{2}\sum_{i,j}\sum_{a,b} \frac{\partial \langle ij\|ab\rangle}{\partial \lambda} a(ij,ab) \\ &\quad - \frac{1}{2}\sum_{i,j} \frac{\partial \varepsilon_{ij}}{\partial \lambda} \sum_{k}\sum_{a,b} a(ik,ab) a(jk,ab) \\ &\quad + \frac{1}{2}\sum_{a,b} \frac{\partial \varepsilon_{ab}}{\partial \lambda} \sum_{c}\sum_{i,j} a(ij,ac) a(ij,bc), \end{aligned} \tag{3.17}$$

$$\frac{dE(\mathrm{MP3})}{d\lambda} = \frac{1}{2}\sum_{i,j}\sum_{a,b}\frac{\partial\langle ij\|ab\rangle}{\partial\lambda}d(ij,ab)$$
$$+\sum_{i,j}\sum_{a,b}a(ij,ab)\{\frac{1}{8}\sum_{k,l}\frac{\partial\langle kl\|ij\rangle}{\partial\lambda}a(kl,ab)$$
$$+\frac{1}{8}\sum_{c,d}\frac{\partial\langle ab\|cd\rangle}{\partial\lambda}a(ij,cd)-\sum_{k}\sum_{c}\frac{\partial\langle ka\|ic\rangle}{\partial\lambda}a(kj,cb)\}$$
$$-\sum_{i,j}\frac{\partial\varepsilon_{ij}}{\partial\lambda}\sum_{k}\sum_{a,b}a(ik,ab)d(jk,ab)$$
$$+\sum_{a,b}\frac{\partial\varepsilon_{ab}}{\partial\lambda}\sum_{c}\sum_{i,j}a(ij,ac)d(ij,bc), \qquad (3.18)$$

and

$$\frac{dE(\mathrm{MP4})}{d\lambda} = \frac{1}{2}\sum_{i,j}\sum_{a,b}\frac{\partial\langle ij\|ab\rangle}{\partial\lambda}\{e(ij,ab)+x(ij,ab)\}$$
$$+\sum_{i,j}\sum_{a,b}a(ij,ab)\{\frac{1}{4}\sum_{k,l}\frac{\partial\langle kl\|ij\rangle}{\partial\lambda}d(kl,ab)$$
$$+\frac{1}{4}\sum_{c,d}\frac{\partial\langle ab\|cd\rangle}{\partial\lambda}d(ij,cd)-\sum_{k}\sum_{c}\frac{\partial\langle ka\|ic\rangle}{\partial\lambda}d(kj,cb)\}$$
$$+\sum_{i,j}\sum_{a,b}a(ij,ab)\{\sum_{c}\frac{\partial\langle ab\|cj\rangle}{\partial\lambda}d(i,c)-\sum_{k}\frac{\partial\langle kb\|ij\rangle}{\partial\lambda}d(k,a)\}$$
$$+2\sum_{i,j,k}\sum_{a}\frac{\partial\langle ij\|ka\rangle}{\partial\lambda}r(ijk,a)+2\sum_{i}\sum_{a,b,c}\frac{\partial\langle ia\|bc\rangle}{\partial\lambda}s(i,abc)$$
$$-\sum_{i,j}\frac{\partial\varepsilon_{ij}}{\partial\lambda}\{\sum_{k}\sum_{a,b}a(ik,ab)\{e(jk,ab)+\frac{1}{2}x(jk,ab)\}$$
$$+\sum_{a}d(i,a)d(j,a)+\frac{1}{12}\sum_{k,l}\sum_{a,b,c}d(ikl,abc)d(jkl,abc)\}$$
$$+\sum_{a,b}\frac{\partial\varepsilon_{ab}}{\partial\lambda}\{\sum_{c}\sum_{i,j}a(ij,ac)\{e(ij,bc)+\frac{1}{2}x(ij,bc)\}$$
$$+\sum_{i}d(i,a)d(i,b)+\frac{1}{12}\sum_{i,j,k}\sum_{c,d}d(ijk,acd)d(ijk,bcd)\} \qquad (3.19)$$

with

$$e(ij,ab) = \{v_s(ij,ab)+v_d(ij,ab)$$
$$+v_t(ij,ab)+v_q(ij,ab)\}/(\varepsilon_i+\varepsilon_j-\varepsilon_a-\varepsilon_b), \qquad (3.20)$$

$$x(ij,ab) = \frac{1}{4}\sum_{k,l}\sum_{c,d}a(kl,cd)\{a(ij,cd)a(kl,ab)$$
$$-2\{a(ij,ac)a(kl,bd)+a(ij,bd)a(kl,ac)\}$$
$$-2\{a(ik,ab)a(jl,cd)+a(ik,cd)a(jl,ab)\}$$
$$+4\{a(ik,ac)a(jl,bd)+a(ik,bd)a(jl,ac)\}\}, \qquad (3.21)$$

$$r(ijk,a) = \frac{1}{4}\sum_{l}\sum_{b,c}a(kl,bc)d(ijl,abc), \qquad (3.22)$$

and

$$s(i,abc) = \frac{1}{4}\sum_{j,k}\sum_{d}a(jk,ad)d(ijk,bcd). \qquad (3.23)$$

3.3 Gradients in QCI Theory

The calculation of QCISD energy gradients is somewhat more complicated, because straightforward differentiation of the QCISD energy expression (eq. (2.20)) with respect to λ yields a formula (eq. (3.24)) which contains, in addition to the derivatives of the two-electron integrals $\langle pq\|rs\rangle$, derivatives of the double excitation amplitudes a_{ij}^{ab} :

$$\frac{dE(\mathrm{QCISD})}{d\lambda} = \frac{1}{4}\sum_{i,j}\sum_{a,b}\frac{\partial\langle ij\|ab\rangle}{\partial\lambda}a_{ij}^{ab}+\frac{1}{4}\sum_{i,j}\sum_{a,b}\langle ij\|ab\rangle\frac{\partial a_{ij}^{ab}}{\partial\lambda}. \qquad (3.24)$$

As has been shown in section 3.1, evaluation of the two-electron integral derivatives causes no serious problems. However, computation of the derivatives of a_{ij}^{ab} requires the solution of the Coupled-perturbed QCISD (CPQCISD) equations which are obtained by differentiating the QCISD equations (eq.s (2.27) and (2.28)) with respect to λ. The CPQCISD equations can be written in the following form [72]

$$B_i^{a(\lambda)} = \sum_{j}\sum_{b}C_{i,j}^{a,b}\frac{\partial a_j^b}{\partial\lambda}+\sum_{j<k}\sum_{b<c}C_{i,jk}^{a,bc}\frac{\partial a_{jk}^{bc}}{\partial\lambda} \qquad (3.25)$$

and

$$B_{ij}^{ab(\lambda)} = \sum_k \sum_c C_{ij,k}^{ab,c} \frac{\partial a_k^c}{\partial \lambda} + \sum_{k<l} \sum_{c<d} C_{ij,kl}^{ab,cd} \frac{\partial a_{kl}^{cd}}{\partial \lambda}. \tag{3.26}$$

For a definition of the various B and C terms see appendix I. Note that the C terms are independent of the perturbation λ, while the B terms contain derivatives of the two-electron integrals $\langle pq\|rs\rangle$ and of the Lagrangian multipliers ε_{pq} with respect to λ.

Explicit solution of the CPQCISD equations is very costly, since it requires for each perturbation parameter approximately the same time as needed for the solution of the corresponding QCISD equations. Computation of QCISD energy gradients by solving the CPQCISD equations (3.23) and (3.26) obviously presents no real advantage compared to a calculation via a numerical finite differentiation scheme. However, the explicit determination of the derivatives of a_{ij}^{ab} can be avoided by using the z-vector method of Handy and Schaefer [22,67,68,72]. If we define the z-amplitudes z_i^a and z_{ij}^{ab} by [72]

$$\sum_j \sum_b z_j^b C_{j,i}^{b,a} + \sum_{j<k} \sum_{b<c} z_{jk}^{bc} C_{jk,i}^{bc,a} = 0, \tag{3.27}$$

$$\sum_k \sum_c z_k^c C_{k,ij}^{c,ab} + \sum_{k<l} \sum_{c<d} z_{kl}^{cd} C_{kl,ij}^{cd,ab} = \langle ij\|ab\rangle, \tag{3.28}$$

the term in the QCISD energy gradient expression which contains the derivative of a_{ij}^{ab}, can be replaced using the following equality

$$\frac{1}{4} \sum_{i,j} \sum_{a,b} \langle ij\|ab\rangle \frac{\partial a_{ij}^{ab}}{\partial \lambda} = \sum_i \sum_a B_i^{a(\lambda)} z_i^a + \frac{1}{4} \sum_{i,j} \sum_{a,b} B_{ij}^{ab(\lambda)} z_{ij}^{ab}. \tag{3.29}$$

The main advantage of the z-vector method is that it requires only the solution of one set of linear equations in order to determine the perturbation independent quantities z_i^a and z_{ij}^{ab}. The corresponding costs are similar to those for the solution of the QCISD equations.

Using eq.(3.29) and the definition of $B_i^{a(\lambda)}$ and $B_{ij}^{ab(\lambda)}$ given in the appendix the QCISD energy gradient expression can be given in terms of derivatives of two-electron integrals $\langle pq\|rs\rangle$ and the Lagrangian multipliers ε_{pq} [72]

:

$$\begin{aligned}
\frac{dE(\mathrm{QCISD})}{d\lambda} &= \frac{1}{4} \sum_{i,j} \sum_{a,b} \frac{\partial \langle ij\|ab\rangle}{\partial \lambda} (a_{ij}^{ab} - z_{ij}^{ab} - x_{ij}^{ab}) \\
&\quad - \sum_{i,j} \sum_{a,b} z_{ij}^{ab} \{ \frac{1}{8} \sum_{c,d} \frac{\partial \langle ab\|cd\rangle}{\partial \lambda} a_{ij}^{cd} + \frac{1}{8} \sum_{k,l} \frac{\partial \langle kl\|ij\rangle}{\partial \lambda} a_{kl}^{ab} \\
&\quad - \sum_k \sum_c \frac{\partial \langle ka\|ic\rangle}{\partial \lambda} a_{kj}^{cb} \} + \sum_{i,j} \sum_{a,b} \frac{\partial \langle ja\|ib\rangle}{\partial \lambda} z_i^a a_j^b \\
&\quad + \frac{1}{2} \sum_{i,j} \sum_{a,b,c} \frac{\partial \langle ja\|bc\rangle}{\partial \lambda} \{ a_{ij}^{bc} z_i^a + z_{ij}^{bc} a_i^a \} \\
&\quad + \frac{1}{2} \sum_{i,j,k} \sum_{a,b} \frac{\partial \langle jk\|ib\rangle}{\partial \lambda} \{ a_{jk}^{ab} z_i^a + z_{jk}^{ab} a_i^a \} \\
&\quad + \sum_{i,j} \frac{\partial \varepsilon_{ij}}{\partial \lambda} \{ \sum_a a_i^a z_j^a + \frac{1}{2} \sum_k \sum_{a,b} a_{ik}^{ab} z_{jk}^{ab} \} \\
&\quad - \sum_{a,b} \frac{\partial \varepsilon_{ab}}{\partial \lambda} \{ \sum_i a_i^a z_i^b + \frac{1}{2} \sum_{i,j} \sum_c a_{ij}^{ac} z_{ij}^{bc} \}
\end{aligned} \tag{3.30}$$

with

$$\begin{aligned}
x_{ij}^{ab} &= \sum_k \sum_c z_k^c \{ a_{ij}^{ca} a_k^b - a_{ij}^{cb} a_k^a + a_{jk}^{ab} a_i^c - a_{ik}^{ab} a_j^c \\
&\quad + a_{jk}^{bc} a_i^a - a_{jk}^{ac} a_i^b - a_{ik}^{bc} a_j^a + a_{ik}^{ac} a_j^b \} \\
&\quad + \frac{1}{4} \sum_{k,l} \sum_{c,d} z_{kl}^{cd} \{ a_{ij}^{cd} a_{kl}^{ab} - 2(a_{ij}^{ac} a_{kl}^{bd} + a_{ij}^{bd} a_{kl}^{ac}) \\
&\quad - 2(a_{ik}^{ab} a_{jl}^{cd} + a_{ik}^{cd} a_{jl}^{ab}) + 4(a_{ik}^{ac} a_{jl}^{bd} + a_{ik}^{bd} a_{jl}^{ac}) \}.
\end{aligned} \tag{3.31}$$

Differentiation of the perturbation correction due to triple excitation within the QCISD(T) approach yields [73]

$$\begin{aligned}
\frac{\partial \Delta \mathrm{E(T,QCISD(T))}}{\partial \lambda} &= \frac{1}{2} \sum_{i,j} \sum_{a,b} \frac{\partial a_{ij}^{ab}}{\partial \lambda} v_{ij}^{ab} + 2 \sum_{i,j,k} \sum_a \frac{\partial \langle ij\|ka\rangle}{\partial \lambda} r_{ijk}^a \\
&\quad + 2 \sum_i \sum_{a,b,c} \frac{\partial \langle ia\|bc\rangle}{\partial \lambda} s_i^{abc} + \sum_i \sum_a \frac{\partial a_i^a}{\partial \lambda} \tilde{v}_i^a + \frac{1}{2} \sum_{i,j} \sum_{a,b} \frac{\partial \langle ij\|ab\rangle}{\partial \lambda} u_{ij}^{ab} \\
&\quad + \frac{1}{12} \sum_{a,b} \frac{\partial \varepsilon_{ab}}{\partial \lambda} \sum_{i,j,k} \sum_{c,d} d_{ijk}^{acd} \{ d_{ijk}^{bcd} + \tilde{d}_{ijk}^{bcd} \}
\end{aligned}$$

$$-\frac{1}{12}\sum_{i,j}\frac{\partial\varepsilon_{ij}}{\partial\lambda}\sum_{k,l}\sum_{a,b,c}d_{ikl}^{abc}\{d_{jkl}^{abc}+\tilde{d}_{jkl}^{abc}\}. \tag{3.32}$$

The arrays v, $\tilde{v}$, r, s, and u are defined as follows

$$v_{ij}^{ab}=\frac{1}{2}\sum_{k}\sum_{c,d}\{\langle cd\|bk\rangle[d_{ijk}^{acd}+\tilde{d}_{ijk}^{acd}]-\langle cd\|ak\rangle[d_{ijk}^{bcd}+\tilde{d}_{ijk}^{bcd}]\}$$
$$+\frac{1}{2}\sum_{k,l}\sum_{c}\{\langle cj\|kl\rangle[d_{ikl}^{abc}+\tilde{d}_{ikl}^{abc}]-\langle ci\|kl\rangle[d_{jkl}^{abc}+\tilde{d}_{jkl}^{abc}]\}, \tag{3.33}$$

$$r_{ijk}^{a}=\frac{1}{4}\sum_{l}\sum_{b,c}a_{kl}^{bc}\{d_{ijl}^{abc}+\tilde{d}_{ijl}^{abc}\}, \tag{3.34}$$

$$s_{i}^{abc}=\frac{1}{4}\sum_{j,k}\sum_{d}a_{jk}^{ad}\{d_{ijk}^{bcd}+\tilde{d}_{ijk}^{bcd}\}, \tag{3.35}$$

$$u_{ij}^{ab}=\sum_{k}\sum_{c}a_{k}^{c}d_{ijk}^{abc}, \tag{3.36}$$

and

$$\tilde{v}_{i}^{a}=\frac{1}{2}\sum_{j,k}\sum_{b,c}\langle jk\|bc\rangle d_{ijk}^{abc}. \tag{3.37}$$

Compared to the QCISD gradient expression, eq. (3.30), two additional terms that involve derivatives of a_i^a and a_{ij}^{ab} appear. While the CPQCI equations are identical for QCISD and QCISD(T), the corresponding z-vector equations are not. Triple excitations when treated as a perturbative correction to the QCISD result do no affect the unperturbed as well as the perturbed amplitudes of single and double excitations. However, since several terms in $\partial E(\Delta\mathrm{E(T,QCISD(T))})/\partial\lambda$ depend on the derivatives of a_i^a and a_{ij}^{ab}, the z-vector equations have to be modified in order to get rid of these terms in the final QCISD(T) energy gradient expression [73]. Thus, the z-vector equations in QCISD(T) theory are given by

$$\sum_{j}\sum_{b}z_{j}^{b}C_{j,i}^{b,a}+\sum_{j<k}\sum_{b<c}z_{jk}^{bc}C_{jk,i}^{bc,a}=\tilde{v}_{i}^{a}, \tag{3.38}$$

$$\sum_{k}\sum_{c}z_{k}^{c}C_{k,ij}^{c,ab}+\sum_{k<l}\sum_{c<d}z_{kl}^{cd}C_{kl,ij}^{cd,ab}=\langle ij\|ab\rangle+2v_{ij}^{ab}. \tag{3.39}$$

The terms dependent on $\partial a_i^a/\partial\lambda$ and $\partial a_{ij}^{ab}/\partial\lambda$ in the QCISD(T) energy gradient expression, eq. (3.32) are now replaced by

$$\sum_{i}\sum_{a}\tilde{v}_{i}^{a}\frac{\partial a_{i}^{a}}{\partial\lambda}+\frac{1}{2}\sum_{i,j}\sum_{a,b}v_{ij}^{ab}\frac{\partial a_{ij}^{ab}}{\partial\lambda}+\frac{1}{4}\langle ij\|ab\rangle\frac{\partial a_{ij}^{ab}}{\partial\lambda}$$
$$=\sum_{i}\sum_{a}B_{i}^{a(\lambda)}z_{i}^{a}+\frac{1}{4}\sum_{i,j}\sum_{a,b}B_{ij}^{ab(\lambda)}z_{ij}^{ab}. \tag{3.40}$$

In the final formula for the QCISD(T) energy gradient [73],

$$\frac{dE(\mathrm{QCISD(T)})}{d\lambda}=\frac{dE(\mathrm{QCISD})}{d\lambda}+2\sum_{i,j,k}\sum_{a}\frac{\partial\langle ij\|ka\rangle}{\partial\lambda}r_{ijk}^{a}$$
$$+2\sum_{i}\sum_{a,b,c}\frac{\partial\langle ia\|bc\rangle}{\partial\lambda}s_{i}^{abc}+\frac{1}{2}\sum_{i,j}\sum_{a,b}\frac{\partial\langle ij\|ab\rangle}{\partial\lambda}u_{ij}^{ab}$$
$$+\frac{1}{12}\sum_{a,b}\frac{\partial\varepsilon_{ab}}{\partial\lambda}\sum_{i,j,k}\sum_{c,d}d_{ijk}^{acd}\{d_{ijk}^{bcd}+\tilde{d}_{ijk}^{bcd}\}$$
$$-\frac{1}{12}\sum_{i,j}\frac{\partial\varepsilon_{ij}}{\partial\lambda}\sum_{k,l}\sum_{a,b,c}d_{ikl}^{abc}\{d_{jkl}^{abc}+\tilde{d}_{jkl}^{abc}\}, \tag{3.41}$$

the contribution of the triple excitations appears in two different ways. First, the QCISD energy gradient terms in eq. (3.41) have to be calculated using the modified z-amplitudes determined by eq.s (3.38) and (3.39). Second, eq. (3.41) includes several additional terms containing derivatives of the two-electron integrals and the Lagrangian multipliers.

Similar to MPn and QCISD energy gradients, the QCISD(T) energy gradient can be written in a form which contains only derivatives of the two-electron integrals $\langle pq\|rs\rangle$ and of the Lagrangian multipliers ε_{pq}. The z-vector equations are independent of the perturbation λ and have to be solved only once for all possible types of perturbations.

3.4 The Relationship between MP and QCI Energy Gradients

In the same way as there is a close relationship between the MP and QCI energy expressions, there also is a close connection between the energy gradient formulas of both methods. By expanding the QCISD amplitudes a_i^a

and a_{ij}^{ab} (see section 2.3) as well as the z-vector amplitudes z_i^a and z_{ij}^{ab} up to fourth order

$$\begin{aligned} a_{ij}^{ab} &= a(ij,ab) && \text{(second order)} \\ &\quad + d(ij,ab) && \text{(third order)} \\ &\quad + \{v_s(ij,ab) + v_d(ij,ab) \\ &\qquad + v_q(ij,ab)\}/(\varepsilon_i + \varepsilon_j - \varepsilon_a - \varepsilon_b) && \text{(fourth order)} \\ &\quad + \ldots && (3.42) \end{aligned}$$

$$\begin{aligned} a_i^a &= 0 && \text{(second order)} \\ &\quad + d(i,a) && \text{(third order)} \\ &\quad + v(i,a)/(\varepsilon_i - \varepsilon_j) && \text{(fourth order)} \\ &\quad + \ldots && (3.43) \end{aligned}$$

$$\begin{aligned} z_{ij}^{ab} &= -a(ij,ab) && \text{(second order)} \\ &\quad - d(ij,ab) && \text{(third order)} \\ &\quad - \{v_s(ij,ab) \\ &\qquad + v_d(ij,ab) + v_q(ij,ab)\}/(\varepsilon_i + \varepsilon_j - \varepsilon_a - \varepsilon_b) && \text{(fourth order)} \\ &\quad - \ldots && (3.44) \end{aligned}$$

$$\begin{aligned} z_i^a &= 0 && \text{(second order)} \\ &\quad - d(i,a) && \text{(third order)} \\ &\quad - v(i,a)/(\varepsilon_i - \varepsilon_j) && \text{(fourth order)} \\ &\quad - \ldots && (3.45) \end{aligned}$$

the relationship between the various gradient formulas becomes obvious. By substituting eq.s (3.41) - (3.45) in eq. (3.30) for the QCISD energy gradient, we obtain

$$\begin{aligned} \frac{dE(\text{QCISD})}{d\lambda} &= \frac{dE(\text{MP2})}{d\lambda} + \frac{dE(\text{MP3})}{d\lambda} \\ &\quad + \frac{dE(\text{MP4(SDQ)})}{d\lambda} + \textit{higher order terms} \end{aligned} \qquad (3.46)$$

Considering also triple excitations, a comparison of the QCISD(T) (eq. (3.32)) and the MP4(T) gradient (eq. (3.19)) reveals their similarity. Again, additional terms ($\tilde{d}_{ijk}^{abc}$,u_{ij}^{ab}, and $\tilde{v}_i^a$) are due to the fifth order coupling between single and double excitations.

3.5 General theory of MPn and QCI Gradients

As has been shown in the previous sections, the energy gradient expression for all methods considered can be casted in a form which contains only derivatives of the two-electron integrals and of the Lagrangian multipliers. Therefore, a general formula for the energy gradient is given by

$$\begin{aligned} \frac{dE(\text{METHOD})}{d\lambda} &= \sum_{i,j}\sum_{a,b} \frac{\partial\langle ij\|ab\rangle}{\partial\lambda} X_1^{METHOD}(ijab) \\ &\quad + \sum_{i,j,k,l} \frac{\partial\langle ij\|kl\rangle}{\partial\lambda} X_2^{METHOD}(ijkl) \\ &\quad + \sum_{i,j}\sum_{a,b} \frac{\partial\langle ia\|jb\rangle}{\partial\lambda} X_3^{METHOD}(iajb) \\ &\quad + \sum_{a,b,c,d} \frac{\partial\langle ab\|cd\rangle}{\partial\lambda} X_4^{METHOD}(abcd) \\ &\quad + \sum_{i,j,k}\sum_{a} \frac{\partial\langle ij\|ka\rangle}{\partial\lambda} X_5^{METHOD}(ijka) \\ &\quad + \sum_{i}\sum_{a,b,c} \frac{\partial\langle ia\|bc\rangle}{\partial\lambda} X_6^{METHOD}(iabc) \\ &\quad + \sum_{i,j} \frac{\partial\varepsilon_{ij}}{\partial\lambda} Y_1^{METHOD}(ij) \\ &\quad + \sum_{a,b} \frac{\partial\varepsilon_{ab}}{\partial\lambda} Y_2^{METHOD}(ab). \end{aligned} \qquad (3.47)$$

Appendix 2 summarizes for all methods discussed the explicit expressions of the various X and Y terms in eq.(3.47). It should be noted that eq. (3.47) also holds for gradients in CI [23,24] and CC theory [90] provided a single determinant reference function is used.

However, eq. (3.47) does not offer a convenient basis for implementation of computer programs for analytical calculation of energy gradients. In actual gradient calculations the derivatives $\partial\langle pq\|rs\rangle/\partial\lambda$ are never computed, since it is more advantageous to deal directly with the derivatives of the AO integrals and the derivatives of the MO coefficients. The computation of $\partial\langle pq\|rs\rangle/\partial\lambda$ would require for each perturbation a full transformation of the two-electron integral derivatives from the AO to the MO representation and, therefore, is too expensive.

An expression for the energy gradient in terms of the AO integral derivatives and the coefficients U_{pq}^{λ} is obtained by substituting eq. (3.13) into

eq.(3.47) [58]

$$\frac{dE(\mathrm{METHOD})}{d\lambda} = \sum_{\mu\nu\sigma\rho} T_{\mu\nu\sigma\rho}\frac{\partial\langle\mu\nu\|\sigma\rho\rangle}{\partial\lambda} + \sum_i\sum_a U_{ai}^{\lambda}L'_{ai} + \sum_i\sum_a U_{ia}^{\lambda}L''_{ia} - \frac{1}{2}\sum_{i,j} S_{ij}^{\lambda}L'_{ij} - \frac{1}{2}\sum_{a,b} S_{ab}^{\lambda}L''_{ab} + \sum_{i,j} K'_{ij}\frac{\partial\varepsilon_{ij}}{\partial\lambda} + \sum_{a,b} K''_{ab}\frac{\partial\varepsilon_{ab}}{\partial\lambda} \tag{3.48}$$

with

$$\begin{aligned} T_{\mu\nu\sigma\rho} = &\sum_{i,j}\sum_{a,b} c_{\mu i}c_{\nu j}c_{\sigma a}c_{\rho b}X_1^{METHOD}(ijab) \\ &+ \sum_{i,j,k,l} c_{\mu i}c_{\nu j}c_{\sigma k}c_{\rho l}X_2^{METHOD}(ijkl) \\ &+ \sum_{i,j}\sum_{a,b} c_{\mu i}c_{\nu a}c_{\sigma j}c_{\rho b}X_3^{METHOD}(iajb) \\ &+ \sum_{a,b,c,d} c_{\mu a}c_{\nu b}c_{\sigma c}c_{\rho d}X_4^{METHOD}(abc) \\ &+ \sum_{i,j,k}\sum_{a} c_{\mu i}c_{\nu j}c_{\sigma k}c_{\rho a}X_5^{METHOD}(ijka) \\ &+ \sum_{i}\sum_{a,b,c} c_{\mu i}c_{\nu a}c_{\sigma b}c_{\rho c}X_6^{METHOD}(iabc), \end{aligned} \tag{3.49}$$

$$\begin{aligned} L'_{pi} = &2\sum_{j}\sum_{a,b}\langle pj\|ab\rangle X_1^{METHOD}(ijab) \\ &+ 4\sum_{j,k,l}\langle pj\|kl\rangle X_2^{METHOD}(ijkl) \\ &+ 2\sum_{j}\sum_{a,b}\langle pa\|jb\rangle X_3^{METHOD}(iajb) \\ &+ 2\sum_{j,k}\sum_{a}\langle pj\|ka\rangle X_5^{METHOD}(ijka) \\ &+ \sum_{j,k}\sum_{a}\langle jk\|pa\rangle X_5^{METHOD}(jkia) \\ &+ \sum_{a,b,c}\langle pa\|bc\rangle X_6^{METHOD}(iabc), \end{aligned} \tag{3.50}$$

$$\begin{aligned} L''_{pa} = &2\sum_{i,j}\sum_{b}\langle ij\|pb\rangle X_1^{METHOD}(ijab) \\ &+ 2\sum_{i,j}\sum_{b}\langle ip\|jb\rangle X_3^{METHOD}(iajb) \\ &+ 4\sum_{b,c,d}\langle pb\|cd\rangle X_4^{METHOD}(abcd) \\ &+ \sum_{i,j,k}\langle ij\|kp\rangle X_5^{METHOD}(ijka) \\ &+ \sum_{i}\sum_{b,c}\langle ip\|bc\rangle X_6^{METHOD}(iabc) \\ &+ 2\sum_{i}\sum_{b,c}\langle ib\|pc\rangle X_6^{METHOD}(ibac), \end{aligned} \tag{3.51}$$

$$K'_{ij} = Y_1^{METHOD}(ij), \tag{3.52}$$

and

$$K''_{ab} = Y_2^{METHOD}(ab). \tag{3.53}$$

Using further the orthonormality condition (eq. (3.3)) and the explicit expression for the derivatives of the Lagrangian multipliers, eq. (3.16), eq. (3.48) is rewritten as

$$\frac{dE(\mathrm{METHOD})}{d\lambda} = \sum_{\mu,\nu,\sigma,\rho} T_{\mu\nu\sigma\rho}\frac{\partial\langle\mu\nu\|\sigma\rho\rangle}{\partial\lambda} + \sum_i\sum_a L_{ai}U_{ai}^{\lambda} + \sum_{p,q} M_{pq}S_{pq}^{\lambda} + \sum_{p,q} N_{pq}F_{pq}^{(\lambda)} \tag{3.54}$$

with

$$L_{ai} = L'_{ai} - L''_{ia} + 2\sum_{j,k} K'_{jk}\langle aj\|ik\rangle + 2\sum_{b,c} K''_{bc}\langle ab\|ic\rangle \tag{3.55}$$

$$M_{pq} = \begin{cases} -\frac{1}{2}(L'_{ij} + (\varepsilon_i+\varepsilon_j)K'_{ij}) + 2\sum_{k,l} K'_{kl}\langle ik\|jl\rangle \\ \qquad +2\sum_{a,b} K''_{ab}\langle ia\|jb\rangle & \mathrm{p = i,\ q = j} \\ -\frac{1}{2}(L''_{ab} + (\varepsilon_a+\varepsilon_b)K''_{ab}) & \mathrm{p = a,\ q = b} \\ -\frac{1}{2}L''_{ia} & \mathrm{p = i,\ q = a} \\ -\frac{1}{2}L''_{ia} & \mathrm{p = a,\ q = i} \end{cases}$$

and

$$N_{pq} = \begin{cases} K'_{ij} & \text{p = i, q = j} \\ K''_{ab} & \text{p = a, q = b} \\ 0 & \text{otherwise} \end{cases} \tag{3.57}$$

Following Handy and Schaefer [22], the derivatives U_{ai}^{λ} can be eliminated from the expression for the energy gradient (eq. (3.54)). By defining the Z-vector Z_{bj} for the CPHF equations (3.9) :

$$\sum_b \sum_j (A_{aibj} + (\varepsilon_a - \varepsilon_i)\delta_{ab}\delta_{ij}) Z_{bj} = L_{ai} \tag{3.58}$$

the second term in eq. (3.54), which contains the derivative U_{ai}^{λ}, is replaced by

$$\sum_a \sum_i L_{ai} U_{ai}^{\lambda} = \sum_b \sum_j B_{bj}^{(\lambda)} Z_{bj}. \tag{3.59}$$

The main advantage of this approach is that only one set of equations, eq. (3.58), rather than M sets of linear equations with M as the number of perturbations has to be solved. The idea, which is used to eliminate here U_{ai}^{λ} from the gradient expression, is actually the same which has been used to eliminate the derivatives of the excitation amplitudes from the gradient expression in QCI theory (see section 3.3). Both elimination procedures are based on the fact that the gradient expression is necessarily linear with respect to the perturbation λ. Thus, the original set of coupled perturbed QCI or HF equations can be replaced by one set of equations which is independent of λ. These equations are usually called the z-vector equations [22].

Using eq. (3.59) and transforming all remaining terms to the AO representation we get the following final formula for the energy gradient [58,59]

$$\frac{dE(\text{METHOD})}{d\lambda} = \sum_{\mu,\nu,\sigma,\rho} T_{\mu\nu\sigma\rho} \frac{\partial \langle \mu\nu \| \sigma\rho \rangle}{\partial \lambda} + \sum_{\mu,\nu} F_{\mu\nu}^{(\lambda)} D_{\mu\nu} + \sum_{\mu,\nu} S_{\mu\nu}^{\lambda} W_{\mu\nu}, \tag{3.60}$$

where $D_{\mu\nu}$ and $W_{\mu\nu}$ are defined as

$$D_{\mu\nu} = \sum_{p,q} N_{pq} c_{\mu p} c_{\nu q} - \frac{1}{2} \sum_i \sum_a Z_{ai} (c_{\mu a} c_{\nu i} + c_{\mu i} c_{\nu a}) \tag{3.61}$$

and

$$W_{\mu\nu} = \sum_{p,q} M_{pq} c_{\mu p} c_{\nu q} + \frac{1}{2} \sum_i \sum_a Z_{ai} \varepsilon_i (c_{\mu a} c_{\nu i} + c_{\mu i} c_{\nu a}) + \frac{1}{2} \sum_{i,j,k} \sum_a c_{\mu i} c_{\nu j} A_{akij} Z_{ak}. \tag{3.62}$$

The various quantities in eq. (3.60) might be interpreted as follows. $D_{\mu\nu}$ is a generalized density matrix which is usually called response density matrix [91-93]. $W_{\mu\nu}$ might be regarded as a generalized energy weighted density matrix and $T_{\mu\nu\sigma\rho}$ represents an effective two-particle density matrix.

Eq. (3.60) is a suitable basis for the implementation of computer programs for the calculation of analytical energy gradients within MP and QCISD theory.

4. Implementation of Analytical MPn and QCI Gradients

4.1 The Program System COLOGNE

The MPn and QCI gradient methods discussed in the previous section have been implemented into the ab initio program package COLOGNE [94]. The present version of COLOGNE has been developed at Cologne University and at the University of Göteborg during the years 1985 to 1990. While earlier versions of COLOGNE developed in the time period 1974 - 1984 [95] exclusively run on a CDC Cyber 176, the present version also runs on a CRAY XMP/48. COLOGNE is constantly improved and new features are added on a regular basis. Besides the MPn and QCI gradient methods, COLOGNE offers some other features not generally available in ab initio programs:

a) the calculation of IR and Raman intensities at the HF level [96] using analytically evaluated dipole and polarizability derivatives,

b) a direct and semi-direct SCF approach for calculation of large molecules [97-99],

c) a GVB program for calculating nondynamic correlation effects [100],

d) a pseudo-potential ansatz for calculation on transition metal compounds [101],

e) the use of puckering coordinates for optimizing and analyzing the geometries of ring compounds [102] ,

f) the calculation of CI, MPn, QCI, and CC response properties [93],

g) a topological analysis of the electron density [103-105] either for HF or correlated wave functions [93],

h) the PISA solvent model [122],

i) the IGLO- program for calculating magnetic properties of molecules [123],

j) determination of correlation energies with the LSD approach [124], and

k) graphics software for plotting molecular geometries, normal modes, IR and Raman spectra as well as various properties of the one-electron density.

In the following we will discuss only the implementation of MPn and QCI methods which are the focus of this review. Other features of COLOGNE are described in detail elsewhere [96,99].

4.2 MPn Calculations

MP calculations are carried out along the lines described by Pople and co-workers [41]. After the SCF part, first a partial integral transformation from the AO to the MO basis is performed. Single point energy calculations require in the case of second order MP theory the integrals of the type $\langle ij\|ab\rangle$, in third order integrals of the type $\langle ij\|kl\rangle$, $\langle ij\|ab\rangle$, $\langle ia\|jb\rangle$ and in fourth order integrals of the type $\langle ij\|ab\rangle$, $\langle ij\|ka\rangle$, $\langle ij\|ab\rangle$, $\langle ia\|jb\rangle$, and $\langle ia\|bc\rangle$. In MP3 and MP4 calculations a full transformation is avoided by evaluating the term, which requires in principle integrals of the type $\langle ab\|cd\rangle$,

$$w_3(ij,ab) = \frac{1}{2}\sum_{c,d}\langle ab\|cd\rangle a(ij,cd), \tag{4.1}$$

with the help of the AO integrals [38]. Therefore, the amplitudes $a(ij,ab)$ are partially transformed from the MO to the AO basis

$$\overline{a}(ij,\mu\nu) = \sum_{a,b} c_{\mu a}c_{\nu b}a(ij,ab), \tag{4.2}$$

then multiplied by the AO integrals,

$$\overline{w}_3(ij,\sigma\rho) = \frac{1}{2}\sum_{\mu,\nu}\langle\mu\nu\|\sigma\rho\rangle\overline{a}(ij,\mu\nu), \tag{4.3}$$

and, finally, transformed back to the MO basis

$$w_3(ij,ab) = \sum_{\sigma,\rho} c_{\sigma a}c_{\rho b}\overline{w}_3(ij,\sigma\rho). \tag{4.4}$$

The evaluation of the contribution (4.1) to the second order amplitude $w(ij,ab)$ with the AO integrals requires $O(n_{occ}^2 n_{vir}^2 n_{basis}^2)$ operations for the two transformations (eq.s (4.2) and (4.4)) and $O(n_{occ}^2 n_{basis}^4)$ operations for the multiplication (4.3). Computation of the term (4.1) using the MO integrals $\langle ab\|cd\rangle$ requires first $O(n_{basis}^5)$ multiplications for the full transformation instead of $O(n_{occ}n_{basis}^4)$ multiplication for the partial transformation and then $O(n_{occ}^2 n_{vir}^4)$ operations for multiplying the amplitudes $a(ij,ab)$ with the MO integrals. The AO algorithm as it has been suggested by Pople and coworkers [38] turns out to be very efficient when the number of virtual orbitals is large compared to the number of occupied orbitals. This condition is fulfilled in nearly all large scale calculations. In these calculations, the reduced disk space requirements of the AO algorithm are also of advantage and extend the applicability of the MPn methods significantly. All other terms, which contribute either to the amplitudes $w(ij,ab)$, $w(i,a)$, $w(ijk,abc)$, or $v_q(ij,ab)$, are calculated directly using the MO-integrals $\langle pq\|rs\rangle$ and first order amplitudes $a(ij,ab)$.

While in MP2 calculations the partial integral transformation is with $O(n_{occ}n_{vir}^4)$ operations the most expensive step, in MP3 and MP4(SDQ) calculations the multiplication of the amplitudes $a(ij,ab)$ with the two-electron integrals requires $O(n_{occ}^3 n_{vir}^3)$ and $O(n_{occ}^2 n_{vir}^4)$ operations, respectively. The additional inclusion of triple excitations increases the CPU requirements of a MP calculation further, since the evaluation of the triple amplitudes requires $O(n_{occ}^3 n_{vir}^4)$ multiplications. So far, symmetry is not used in the MP and QCI programs. It can only be exploited prior to the MPn calculation, namely in the AO integral evaluation, in the solution of the SCF problem [106], and in the integral transformation [107], in order to reduce mass storage and CPU requirements.

4.3 QCI calculations

The QCI method has been implemented in COLOGNE following the outline given by Pople and coworkers [52]. Contrary to the original implementation by Pople and coworkers, the simple iterative scheme based on eq.s (2.27), (2.28) together with a geometric extrapolation has been replaced by the more efficient DIIS method [76]. While for single point energy calculations a convergence threshold of 10^{-5} for the amplitudes is sufficient, higher accuracy is necessary in gradient calculations in order to get reliable results for the forces. Our experience shows that a convergence threshold of 10^{-8} is usually sufficient. However, due to the more stringent convergence threshold gradient calculations usually require more iterations to reach convergence in the QCI step than simple energy calculations. Therefore, methods to improve

convergence such as the DIIS method [76,77] are important and save a lot of computer time. The DIIS method is the optimal choice since it is ideally suited to speed up convergence in the last part of an iterative calculation, especially when high accuracy is required.

In most cases, the QCISD equations are solved up to the desired accuracy of 10^{-8} within 10 to 15 iterations. Only, in notorious cases where the single reference ansatz yields an insufficient description for the wave function, more iteration, usually up to 20 or 30, are necessary to reach convergence. However, this is not due to a failure of the QCI method itself, which has been proven successful to describe these systems (i.e. ozone [84] and carbonyl oxide [73]). It turns out that the slower convergence is more or less due to the insufficient MP2 guess for the amplitudes a_{ij}^{ab} used in the first iteration. In these cases MP2 usually exaggerates the influence of correlation effects by a large amount and leads to an insufficient description of the molecular wave function.

Contrary to MPn calculations, it is more advantageous in QCI calculations to perform a full integral transformation and to calculate the term (4.5)

$$w_3{}_{ij}^{ab} = \frac{1}{2}\sum_{c,d}\langle ab\|cd\rangle a_{ij}^{cd}, \tag{4.5}$$

using the transformed integrals $\langle ab\|cd\rangle$. The AO algorithm of Pople and coworkers, which has been originally designed for MP3 calculations is more expensive since it would require a large number of two-index transformation with a total of $n_{iteration}O(n_{occ}^2 n_{basis}^4)$ multiplications. The additional costs of the AO algorithm scale with the number of iterations required for convergence while the additional amount for the full integral transformation required for the MO algorithm is independent of the number of iterations. Only, if disk space is the bottleneck of a QCI calculation, the AO algorithm of Pople and co-workers will be more advantageous due to its reduced disk space requirements. Calculation of all other terms is carried out with the same algorithm as for MP3 and MP4 calculations, except that some additional terms have to be considered in the QCI approach [52].

As in MP3 and MP4(SDQ) calculations the most expensive steps in one QCI iteration are several multiplications of the amplitudes a_{ij}^{ab} with the two-electron integrals with $O(n_{occ}^3 n_{vir}^3)$ and $O(n_{occ}^2 n_{vir}^4)$ operations respectively. However, QCISD calculations are much more expensive than MP3 and MP4(SDQ) calculations since the computational costs scale with the number of iterations. The non-iterative inclusion of triple excitations requires $O(n_{occ}^3 n_{vir}^4)$ multiplications, which is a modest amount of additional

CPU time and can be routinely included in most cases. A thorough analysis of the computational costs of the QCISD and CCSD methods has recently been presented by Scuseria and Schaefer [53]. They showed that QCISD and CCSD actually require the same amount of computer time. Also, these authors suggested some improvements to the original QCI algorithm of Pople and coworkers. A similar analysis including also MPn methods and explicitly considering UHF reference functions has recently been carried out by Stanton and coworkers [108], who presented also a new efficient implementation of both the QCISD and CCSD method.

4.4 MPn Gradient Calculations

In principle, MP gradient calculations require the following additional steps compared to a single point energy calculation :

a) calculation of the perturbation independent matrices L_{pq},M_{pq}, and N_{pq} as well as of the two-particle density matrix $T_{\mu\nu\sigma\rho}$,

b) solution of the Z-vector equation within CPHF theory and the construction of the response density $D_{\mu\nu}$ as well as the energy-weighted response density matrix $W_{\mu\nu}$,

c) evaluation of the one- and two-electron integral derivatives, which are multiplied with the corresponding density matrix elements in order to obtain the desired forces.

We will discuss the various steps now in some more detail.

Integral transformations required for MPn gradient calculations. MPn gradient calculations require a larger subset of MO integrals than the corresponding MPn energy calculation. In second order, the formula for the gradients involves integrals of the type $\langle ij\|ka\rangle$ and $\langle ia\|bc\rangle$ in addition to the integrals $\langle ij\|ab\rangle$, which are sufficient to calculate the MP2 energy. Third-order gradient calculations require in addition to the integrals $\langle ij\|kl\rangle$, $\langle ij\|ab\rangle$, and $\langle ia\|jb\rangle$ also those of the type $\langle ij\|ka\rangle$ and $\langle ia\|bc\rangle$. As in the MP3 energy calculation all terms in the MP3 gradient expression, which involve the integrals $\langle ab\|cd\rangle$ can be evaluated with the AO procedure of Pople and co-workers. Fourth-order gradient calculations require the full set of MO integrals since the term involving triple amplitudes and the two-electron integrals $\langle ab\|cd\rangle$ can only be calculated efficiently in the MO basis. Only, when the MP4 ansatz is restricted to single, double, and quadruple excitations, MP4(SDQ), the full integral transformation might be avoided and these critical tems are evaluated in the same way as in third-order calculations.

The solution of the Z-vector equation requires integrals of the type $\langle ij\|ab\rangle$ and $\langle ia\|jb\rangle$. In principle, all terms needed for solving the Z-vector

equations might be computed using AO integrals (compare for example the AO-CPHF method [109,110]), but this offers in MPn gradient calculations no advantages. On the one hand, usually the MO integrals are available and, on the other hand, the AO-CPHF algorithm turns out to be more expensive than the MO-CPHF approach.

Calculation of L_{pq}, M_{pq}, and N_{pq}. The computation of the L_{pq}, M_{pq}, and N_{pq} matrices is straightforward with the formulas given in section 3.5 and in appendix 2. In second- and third-order, these formulas are solely given in terms of the MO integrals and the first (MP2) or first and second order amplitudes (MP3), respectively. The formulas in fourth-order are more advantageously written in a form which contains in addition to these quantities the third-order amplitudes $v_s(ij,ab)$, $v_d(ij,ab)$, $v_t(ij,ab)$, and $x(ij,ab)$, which are actually required for the first time in MP5 energy evaluations. However, calculation of these terms is straightforward. The array $v_d(ij,ab)$ is computed in the same way as $w(ij,ab)$ using only the second-order amplitudes $w(ij,ab)$ as input rather than the first-order amplitudes $a(ij,ab)$. $v_s(ij,ab)$ is evaluated in a similar way as the contributions of the singles to the array w_{ij}^{ab} in QCI theory using only $w(i,a)$ instead of a_i^a. The computation of $x(ij,ab)$ follows the same line as that of $v_q(ij,ab)$, the only difference being that the two-electron integrals $\langle pq||rs\rangle$ are substituted by the amplitudes $a(ij,ab)$.

The treatment of the triples in fourth-order theory, i.e. the calculation of $v_t(ij,ab)$, $r(ijk,a)$, $s(i,abc)$, but also the computation of the contributions of the triples to $Y_1(i,j)$ and $Y_2(a,b)$,

$$t_1(i,j) = \frac{1}{12}\sum_{k,l}\sum_{a,b,c} d(ikl,abc)d(jkl,abc), \tag{4.6}$$

$$t_2(a,b) = \frac{1}{12}\sum_{i,j,k}\sum_{c,d} d(ijk,acd)d(ijk,bcd), \tag{4.7}$$

poses much severe problems. In MP4 energy calculations, the contribution due to triple excitations is evaluated using a direct algorithm, where the amplitudes are never stored on disk [40]. This procedure ensures that the full MP4 method can be applied without any restriction in large-scale calculations. The storage of the triple amplitudes would require about $n_{occ}^3 n_{vir}^3$ words of disk space and thus be a serious bottleneck in large scale calculations. For example, a calculation with about 60 basis function (e.g DZ+P calculation on a molecule with three heavy atoms) would require about 10 to 50 Mwords, while a calculation with up to 100 and more basis functions (e.g. a TZ+2P calculation on a molecule with three, four and more heavy

atoms) would require several hundreds of Mwords of disk space and, thus, they would be prohibitive even on the largest available super computer. In addition, storage of the triple amplitudes if possible would increase the I/O significantly and, therefore, slow down the performance of a MP4 gradient calculation by several orders of magnitude.

A direct algorithm for the calculation of the triple amplitudes and their contribution to the gradients is more or less mandatory [63]. However, the implementation of such an algorithm is more complicated than in MP4 energy calculations, since there are five different terms which contain the triples either in a linear or quadratic way. The terms linear in the triple excitation amplitudes, actually the arrays $v_t(ij,ab)$, $r(ijk,a)$, and $s(i,abc)$, are relatively easy to handle, since all corresponding contributions can be immediately formed when the triple amplitudes are evaluated. More difficult are the quadratic terms, $t_1(i,j)$ and $t_2(a,b)$, since two different amplitudes $d(ijk,abc)$ are required simultaneously in order to evaluate the corresponding contribution. Fortunately, the required amplitudes differ only in one index, either in one of the labels of the occupied or the virtual orbitals and a direct computation of the two t-terms is possible. In the original implementation of MP4(T) energy calculation of Pople and co-workers [40], all triple amplitudes for fixed labels a, b, and c are calculated and processed together. Hence, computation of $t_1(i,j)$ causes no problems. To overcome the difficulties in calculating the second t-matrix, $t_2(a,b)$, where amplitudes differing in one virtual orbital index are multiplied, one recalculates the triple amplitudes in such a way that now all amplitudes with fixed labels i, j, and k [63] are obtained together. This recalculation of the triple amplitudes with a reversed loop structure ensures that a direct algorithm can be applied in full MP4 gradient calculation. However, it increases the computational costs by the order of $n_{occ}^3 n_{vir}^4$ operations. Nevertheless, the analytical procedure remains to be more efficient than the corresponding finite differentiation scheme.

Calculation of the two-particle density matrix $T_{\mu\nu\sigma\rho}$. In all MPn gradient calculations the two-particle density matrix $T_{\mu\nu\sigma\rho}$ is first evaluated in the MO basis using the MO integrals and the various amplitudes and, then, transformed to the AO basis. The expensive transformation step requires $O(n_{basis}^5)$ operations, but is independent of the number of perturbations. The alternative choice to multiply the two-particle density matrix in the MO basis with the integral derivatives includes a full transformation of the AO integral derivatives to the MO basis. It scales with the number of perturbations, is more expensive, requires in addition the storage of integral derivatives on disk, and, therefore, is not recommended.

MP3 and MP4 gradient calculations require for $T_{\mu\nu\sigma\rho}$ a full transforma-

tion from the MO to the AO basis and $O(n_{basis}^5)$ multiplications. In MP2 gradient calculations, a partial transformation with $O(n_{occ}n_{basis}^4)$ operations is sufficient, since the indices p,q (r,s) of T_{pqrs} run only over occupied (virtual) orbitals.

The transformed two-particle density matrix $T_{\mu\nu\sigma\rho}$ is stored on disk for latter use in the integral derivative calculation to form the appropriate contribution to the forces. In order to use a direct algorithm, which avoids the storage of the integral derivatives on disk, it must be ensured that the elements of $T_{\mu\nu\sigma\rho}$ are stored in the same (or at least a similar) order as the integral derivatives are evaluated. The transformation step produces an ordered list of $T_{\mu\nu\sigma\rho}$ elements with $\mu \geq \nu$, $\sigma \geq \rho$ and $[\mu\nu] \geq [\sigma\rho]$, while the integral derivatives are calculated in batches where all integral with indices belonging to the same shell combinations are computed together. In small calculations, the whole $T_{\mu\nu\sigma\rho}$-matrix can be kept in core memory and no problem exists to pick up the required $T_{\mu\nu\sigma\rho}$ elements. In large scale calculations, the whole $T_{\mu\nu\sigma\rho}$-matrix does no longer fit into core memory. However, it is sufficient that only this part of the $T_{\mu\nu\sigma\rho}$-matrix is kept in the core which contains for the indices μ of the first shell I all possible indices ν, σ, and ρ. With at most 6 or 10 basis functions per shell (i.e, 6 d- or 10 f-functions) such a procedure requires approximately $6n_{basis}^3/2$ or $10n_{basis}^3/2$ words of core memory, an amount, which on modern super computers is available even in large scale calculations. In this case, no preprocessing of the ordered list of $T_{\mu\nu\sigma\rho}$ elements is necessary. However, if there is not enough core memory for this procedure, the only solution will be a sort of the $T_{\mu\nu\sigma\rho}$ elements prior to the integral derivative calculation. By using an algorithm due to Yoshimine [111] this sort requires two additional reads and writes of the $T_{\mu\nu\sigma\rho}$ matrix. Since the sort of the $T_{\mu\nu\sigma\rho}$ elements increases the I/O requirements of a MPn gradient calculation, it should be avoided, whenever possible.

Solution of the z-vector equations in CPHF theory. The z-vector equations are solved using a procedure Pople and coworkers [18] originally developed for the solution of the CPHF equations. The z-vector Z_{ai} is expanded in a set of orthonormal vectors which are obtained by multiplying $L_{ai}/(\varepsilon_i - \varepsilon_a)$ n times with $A_{aibj}/(\varepsilon_i - \varepsilon_a)$ and then performing a Schmidt-orthogonalization. The expansion coefficients are determined by solving a small set of linear equations. The required accuracy of 10^{-8} for the z-vector is usually achieved in 10 to 15 iterations. The converged z-vector is used to construct the response density and energy weighted response density matrices in the MO representation. Both matrices are transformed in the AO representation which is needed for multiplication with the AO integral derivatives

to obtain the corresponding contributions to the energy gradients.

Evaluation of the integral derivatives. The contribution of integral derivatives to the forces are calculated using a direct algorithm. The one-electron integral derivatives $h_{\mu\nu}^{\lambda}$ and $S_{\mu\nu}^{\lambda}$ are multiplied with the total density and the total energy weighted matrix, respectively, while the two-electron integral derivatives are multiplied with the corresponding elements of the $T_{\mu\nu\sigma\rho}$ matrix and are used to build the two-electron contribution of the Fock-matrix derivatives $F_{\mu\nu}^{(\lambda)}$. Note that all contributions to the forces including the HF contribution must be considered in order to get the total force. When one-electron properties are evaluated, only the response density matrix $D_{\mu\nu}$ is multiplied with the corresponding property integrals, provided the basis is chosen to be independent of the corresponding perturbation.

The costs of an analytical evaluation of energy gradients at the various levels of MP theory are independent of the number of perturbations. They scale in a similar way with the number of occupied and virtual orbitals as the energy calculations and usually a gradient calculation requires about 2-3 times the costs of the foregoing energy evaluation.

4.5 QCI Gradient Calculations

QCISD and QCISD(T) gradient calculations are carried out using the same strategies as in the case of MPn gradient calculations. The only additional step is the solution of the z-vector equations within CPQCISD theory. Detailed formulas for the z-vector equations are given in appendix 2. However, evaluation of most arrays needed is straightforward and can be carried out with the same programs used for the solution of the QCI equations. The arrays $w[z]_i^a$ and $w[z]_{ij}^{ab}$ are calculated in the same way as w_i^a and w_{ij}^{ab}, only with the z-amplitudes z_i^a and z_{ij}^{ab} as input instead of the QCISD amplitudes a_i^a and a_{ij}^{ab}. $v[z]_i^a$ and $v[z]_{ij}^{ab}$ are closely related to the quadratic arrays v_i^a and v_{ij}^{ab}. Note that v_i^a and v_{ij}^{ab} are quadratic arrays, while $v[z]_i^a$ and $v[z]_{ij}^{ab}$ are actually linear with respect to the z-amplitudes. Therefore, it is possible to precalculate and store some intermediate arrays in order to reduce the computational requirements. The only new term in the z-vector equation is $y[z]_{ij}^{ab}$, but computation of this term causes no severe problems.

The z-vector equations within CPQCISD theory are solved in the same way as the QCISD equations. Again, convergence is accelerated using a DIIS procedure. As initial guess either the negative MP2 amplitudes or the negative QCISD amplitudes might be used.

$$z_i^{a(0)} = 0 \qquad \text{or} \qquad z_i^{a(0)} = -a_i^a \tag{4.8}$$

$$z_{ij}^{ab(0)} = -a(ij,ab) \qquad \text{or} \qquad z_{ij}^{ab(0)} = -a_{ij}^{ab}. \tag{4.9}$$

Our experience shows that the latter choice is more advantageous and saves usually a few iterations compared to the MP2 guess. When triple excitations are considered, the initial guess must be modified by subtracting $\tilde{v}_i^a$ and $\tilde{v}_{ij}^{ab}$, respectively

$$z_i^{a(0)} = -a_i^a - \tilde{v}_i^a/(\varepsilon_i - \varepsilon_a), \tag{4.10}$$

$$z_{ij}^{ab(0)} = -a_{ij}^{ab} - \tilde{v}_{ij}^{ab}/(\varepsilon_i + \varepsilon_j - \varepsilon_a - \varepsilon_b). \tag{4.11}$$

Since the z-vector equations are linear their solution usually requires less operations than the solution of the corresponding QCISD equations. The array x_{ij}^{ab} which includes both QCISD and z-amplitudes is evaluated after the solution of the z-vector equation using an algorithm similar to the evaluation of v_{ij}^{ab} and $y[z]_{ij}^{ab}$.

The calculation of the matrices L_{pq}, M_{pq}, N_{pq}, and $T_{\mu\nu\sigma\rho}$, the solution of the z-vector equation in CPHF theory and the integral derivative calculation are carried out after the z-amplitudes have been determined, since in this case both the QCISD amplitudes and the z-amplitudes are required.

As in MPn gradient calculations the costs of a QCISD gradient calculation are very similar to those of the corresponding energy evaluation. Actually, since the equations for the z-amplitudes are only linear in z_{ij}^{ab} while the original QCI equations are quadratic in a_{ij}^{ab}, the ratio of the computational costs for energy and gradient calculations are for the QCISD method usually more favorable than for MPn methods. Gradient calculations at the QCISD level usually require about 1-2 times the expenses of a single QCISD energy calculation thus proving the efficiency of analytical gradient methods for this type of quantum chemical methods.

5. Calculation of Molecular Properties at MPn and QCI Using Analytical Gradients

5.1 Response Densities and other One-Electron Properties

A one-electron property O of a molecule can be defined as the response of the molecule to an external perturbation λ. The Hamiltonian $\hat{\mathbf{H}}$ under

the impact of the perturbation has to be corrected by the term $\lambda\hat{O}$ where $\hat{O}$ is the quantum mechanical operator which corresponds to the property O

$$\hat{\mathbf{H}}(\lambda) = \hat{\mathbf{H}}(0) + \lambda\hat{\mathbf{O}}. \tag{5.1}$$

The energy in the presence of the perturbation depends on λ and, therefore, it can be expanded for small λ in a power series

$$E(\lambda) = E(\lambda = 0) + \lambda\frac{dE}{d\lambda}|_{\lambda=0} + \frac{1}{2}\lambda^2\frac{d^2E}{d\lambda^2}|_{\lambda=0} + \ldots \tag{5.2}$$

Applying the Hellmann-Feynman theorem leads to

$$\frac{dE}{d\lambda}|_{\lambda=0} = \langle\Psi|\hat{\mathbf{O}}|\Psi\rangle. \tag{5.3}$$

Eq. (5.3) shows that the definition of an one-electron property O as a response to an external perturbation requires the evaluation of an energy derivative, namely the derivative of the energy with respect to the external perturbation. The value obtained for O in this way will be identical to the expectation value $\langle\Psi|\hat{\mathbf{O}}|\Psi\rangle$ of the corresponding operator $\hat{O}$ as long as the Hellmann-Feynman theorem is satisfied. In cases where the Hellmann-Feynman theorem does not hold, the energy derivative approach should be the preferred way of calculating one-electron properties. In addition, the energy derivative approach offers the possibility to calculate one-electron properties even for methods for which a wave function is not defined and expectation values cannot be evaluated.

The total electron density distribution $\rho(\mathbf{r_p})$ at a point $\mathbf{r_p}$ is the response of the molecule to a perturbation λ that corresponds to the one-electron operator $\delta(\mathbf{r_p} - \mathbf{r})$, which is the Dirac delta operator.

$$\frac{dE(\lambda)}{d\lambda}|_{\lambda=0} = \langle\Psi|\delta(\mathbf{r_p} - \mathbf{r})|\Psi\rangle = \rho(\mathbf{r_p}). \tag{5.4}$$

When $\rho(\mathbf{r})$ is expanded in terms of basis functions used to calculate energy and wave function eq. (5.4) leads to

$$\frac{dE(\lambda)}{d\lambda}|_{\lambda=0} = \rho(\mathbf{r}) = \sum_{\mu\nu}\mathbf{D}_{\mu\nu}\chi_\mu(\mathbf{r})\chi_\nu(\mathbf{r}), \tag{5.5}$$

where $\mathbf{D}$ defines the response density matrix according to eq. (3.61) in Section 3. For a correlated wave function $\mathbf{D}$ can be decomposed into

$$\mathbf{D} = \mathbf{D}^{\mathbf{SCF}} + \mathbf{D}^{\mathbf{corr}} \tag{5.6}$$

indicating that **D** contains a SCF and a correlation part. In the same way $\rho(\mathbf{r_p})$ is expressed as a sum of the SCF density and a correlation correction

$$\rho(\mathbf{r})^{res} = \rho(\mathbf{r})^{SCF} + \rho(\mathbf{r})^{corr} \tag{5.7}$$

Using eq. (3.60) it is easily shown that one-electron properties calculated as energy derivatives are closely related to the response density. Provided that the basis set chosen is independent of the perturbation λ the corresponding one-electron property is simply given as the product of the response density matrix **D** with the corresponding property integrals.

$$O = \frac{dE(\lambda)}{d\lambda}|_{\lambda=0} = \sum_{\mu\nu} \mathbf{D}_{\mu\nu}\langle\chi_\mu|\hat{\mathbf{O}}|\chi_\nu\rangle. \tag{5.8}$$

In the following $\rho(\mathbf{r})$ and one-electron properties are investigated at various levels of theory using basis sets of valence DZ+P and valence TZ+2P quality [118]. As suitable test molecule carbon monosulfide, CS, has been chosen since its electron density distribution is sensitive to correlation effects. However, similar effects have been found for other molecules investigated recently [93].

For CS, one may expect that C carries a small negative and S a small positive charge in accordance with the fact that the electronegativity of C is slightly larger than that of S (2.50 vs. 2.44 on the Allred-Rochow scale). On the other hand, bonding in CS may be close to a triple bond since one of the electron lone pairs of S can be shared between the two atoms thus establishing a semipolar bond beside the two normal bonds.

$$C^{\delta-} \equiv S^{\delta+}$$

If this is true , C will carry a much larger negative charge and S a much larger positive charge as it can be expected from comparision of the electronegativities. However, HF theory predicts relatively small partial charges for C and S suggesting that there is no or only weak semipolar bonding. As a consequence the calculated dipole moment of CS is just 1.77 Debye (HF/MC-311G(2d)) while the experimental one is 1.98 Debye [112] (compare with Table 1). Obviously, HF underestimates the extent of semipolar bonding.

In Figure 1, $\rho(\mathbf{r})^{corr}(\mathrm{MP2}) = \rho(\mathbf{r})^{res}(\mathrm{MP2}) - \rho(\mathbf{r})^{res}(\mathrm{HF})$ of carbon monsulfide, CS, calculated with a VTZ + 2P basis set is given in form of a contour line diagram. Solid (dashed) contour lines are in regions of positive (negative) response densities. Obviously, correlation corrections at the MP2

Table 1. Energies, bond lengths, charges, dipole moments, and quadrupole moments of CS calculated with the MC-311G(2d) Basis.[a]

Method	Energy	R(CS)	Charge at S	Dipole Moment	Quadrupole Moment $Q_{xx} = Q_{yy}$	Quadrupole Moment Q_{zz}
HF	-435.341729	1.5132	188.3	-1.773	-18.64	-20.33
MP2	-435.758863	1.5413	273.4	-2.308	-18.38	-21.04
MP3	-435.767744	1.5269	253.2	-2.111	-18.45	-20.75
MP4(DQ)	-435.767665	1.5295	249.5	-2.106	-18.44	-20.68
MP4(SDQ)	-435.775175	1.5418	238.8	-2.063	-18.44	-20.72
MP4(SDTQ)	-435.797700	1.5646	240.3	-2.111	-18.42	-20.92
CCD	-435.768000	1.5298	248.4	-2.086	-18.45	-20.73
QCISD	-435.775721	1.5421	235.3	-2.010	-18.46	-20.66
QCISD(T)	-435.793730	1.5506	239.5	-2.028	-18.45	-20.73

[a] Energy in Hartree, bond length in Å, charge in melectron, dipole moment in Debye, quadrupole moment in Debye Å.

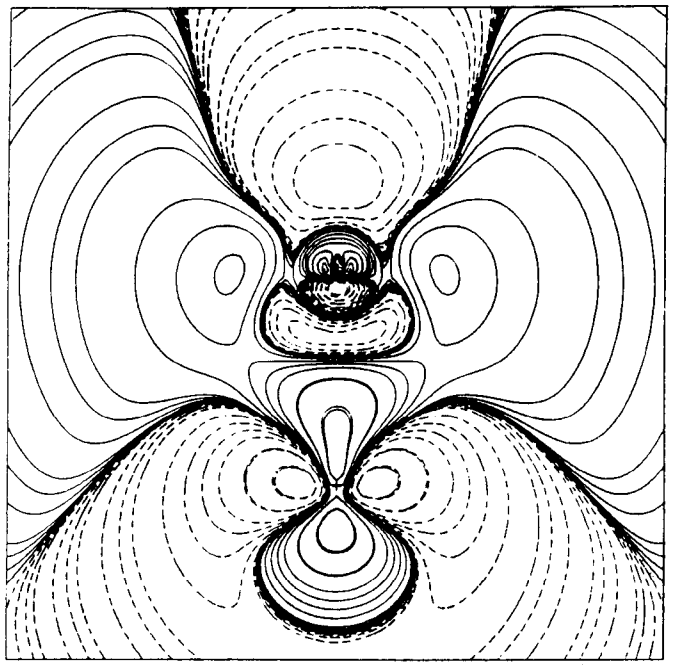

Figure 2. Contour line diagram of the difference electron density distribution $\Delta\rho(\mathbf{r})^{res}(MP3) = \rho(\mathbf{r})^{res}(MP3) - \rho(\mathbf{r})^{res}(MP2)$ of CS calculated with the 6-311G(2d) basis. Solid (dashed) contour lines are in regions of positive (negative) difference densities. The positions of the C and the S nucleus are indicated.

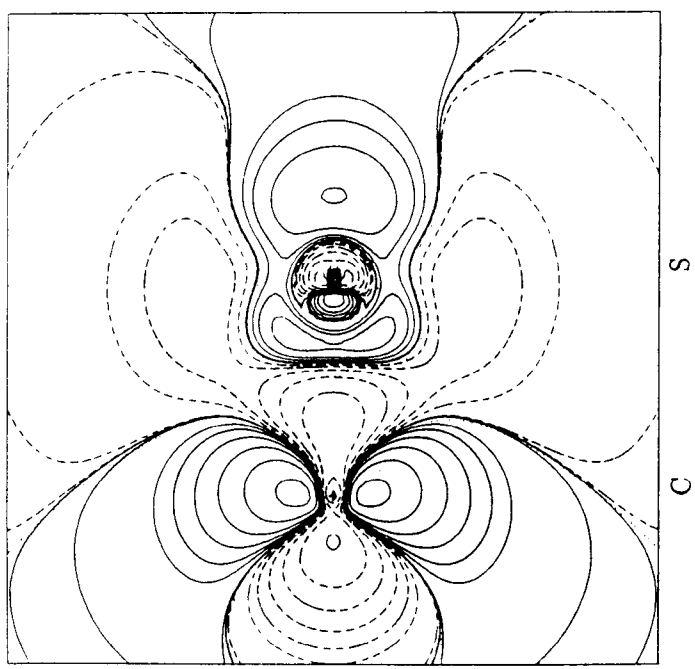

Figure 1. Contour line diagram of the difference electron density distribution $\Delta\rho(\mathbf{r})^{res}(MP2) = \rho(\mathbf{r})^{res}(MP2) - \rho(\mathbf{r})HF = \rho(\mathbf{r})^{corr}(MP2)$ of CS calculated with the 6-311G(2d) basis. Solid (dashed) contour lines are in regions of positive (negative) difference densities. The positions of the C and the S nucleus are indicated.

level lead to a transfer of π electronic charge from the sulfur to the carbon atom. At the same time, σ electronic charge is decreased at the C atom while it is increased in the valence shell of the S atom, both in the bonding and the lone pair region. Closer inspection of diagram 1 as well as an analysis of the corresponding Mulliken population values reveals that the transfer of π-charge from S to C depopulates the valence region of S. However in the $2p\pi$ core region of S, there is a build up of π-charge which envelopes another region of charge decrease. Thus, a complex pattern of alternating charge decrease and increase from valence to inner core region of S and from left to right along the CS bond axis results (Figure 1).

From inspection of Figure 1 and analysis of the response density contributions to the orbital populations it becomes clear that left-right correlation of $p\pi$ electrons is the most important correction of the HF electron distribution at the MP2 level of theory. They lead to an increase (decrease) of the negative (positive) charge at C (S). Less important but substantial are angular and in-out correlation.

The same features of $\rho(\mathbf{r})^{res}$ are found at the MP3, MP4(SDQ), MP4(SDTQ), CCD, QCISD, and QCISD(T) level. Qualitatively, there are no differences in the corresponding response densities which means that MP2 already includes the most important correlation corrections. In order to analyze the different correlation effects covered by the various methods difference response density plots have to be investigated.

In Figure 2, the difference density $\Delta\rho(\mathrm{MP3}) = \rho^{res}(\mathrm{MP3}) - \rho^{res}(\mathrm{MP2}) = \rho^{corr}(\mathrm{MP3}) - \rho^{corr}(\mathrm{MP2})$ is shown. It reveals that MP3 correlation corrections reduce MP2 effects, i.e. the MP2 response density is slightly changed back in the direction of the HF electron density distribution. Changes comprise a π electron transfer from C to S, transfer of σ electrons from outer valence functions to inner valence functions at C and vice versa at S, a transfer of σ electronic charge from S to C and depopulation (population) of the lone-pair region at S (C). These changes lead to a decrease of the CS bond polarity and decreased atomic charges relative to MP2. (Table 1)

Clearly, at MP3 the correlation effects of the double excitations are reduced relative to those calculated at the MP2 level. As has been outlined before this is due to the fact that at MP3 couplings between double excitations are introduced and, therefore, correlation between two electrons is no longer independent of the correlation between other electron pairs. At MP2 only interactions of the double excitations with the ground state wave function are considered and, as a consequence, correlation between two electrons is exaggerated.

In Figure 3, the calculated difference response density $\Delta\rho(\mathrm{MP4(SDQ)}) =$

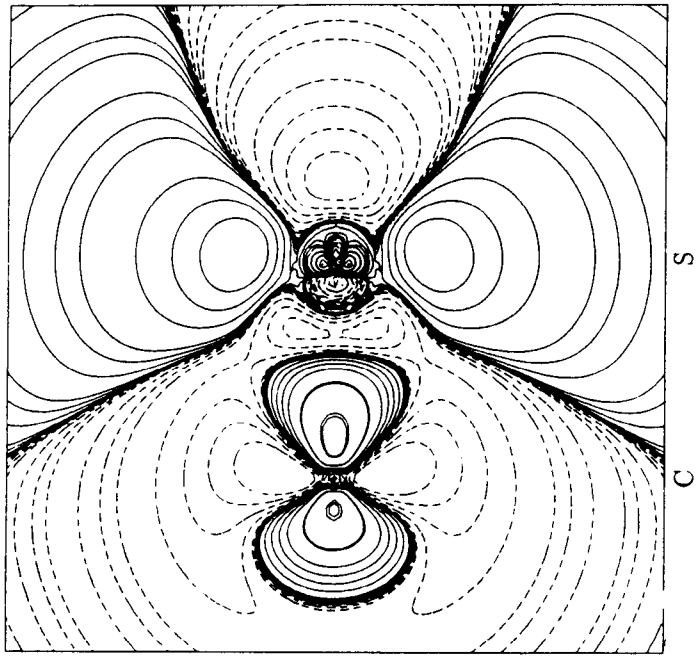

Figure 4. Contour line diagram of the difference electron density distribution $\rho(\mathbf{r})^{res}(MP4(SDQ))-\rho(\mathbf{r})^{res}(MP2)$ of CS calculated with the 6-311G(2d) basis. Solid (dashed) contour lines are in regions of positive (negative) difference densities. The positions of the C and the S nucleus are indicated.

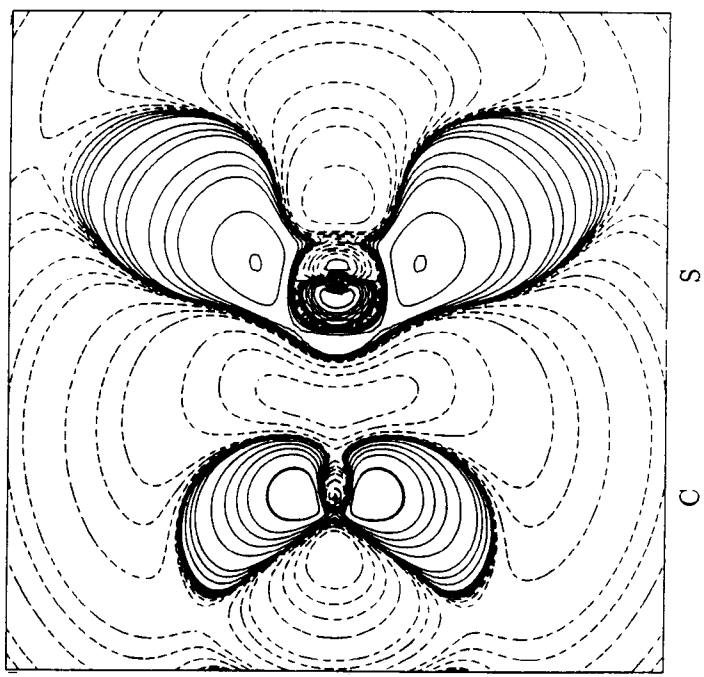

Figure 3. Contour line diagram of the difference electron density distribution $\Delta\rho(\mathbf{r})^{res}(MP4(SDQ)) = \rho(\mathbf{r})^{res}(MP4(SDQ))-\rho(\mathbf{r})^{res}(MP3)$ of CS calculated with the 6-311G(2d) basis. Solid (dashed) contour lines are in regions of positive (negative) difference densities. The positions of the C and the S nucleus are indicated.

$\rho^{res}(\text{MP4(SDQ)}) - \rho^{res}(\text{MP3})$ of CS is given. Its general features are similar to those of the MP2 response density, which means that MP4(SDQ) correlation corrections are in the same direction than MP2 correlation corrections. As a consequence, correlation corrections to charges, dipole moment, and other molecular properties are larger than those calculated at the MP3 level of theory. Apart from this, there are significant differences in the charge distribution at the MP4(SDQ) level. Both bonding and lone pair regions are depopulated relative to the MP3 charge distribution. Charge concentrates in the C 2pπ and S 2pπ and 3pπ region in such a way that electron repulsion is minimized (see Figure 3).

The charge distribution at the MP4(SDQ) level is even better understood when comparing it with the MP2 charge distribution with the help of the difference response density $\rho^{res}(\text{MP4(SDQ)}) - \rho^{res}(\text{MP2})$ shown in Figure 4. There, one sees that at MP4(SDQ) the charge transfer to the C 2pπ orbitals is smaller than at MP2. Hence, the pattern of changes is similar to that obtained at the MP3 level. Obviously, corrections due to single, double, and quadruple excitations at the MP4 level are between those obtained at the MP2 and the MP3 level.

Figure 5 gives the changes in the response density distribution that are due to triple excitations at the MP4 level of theory. They are in the same direction than those obtained from S, D, and Q excitations, i.e. they increase the charge transfer from the S to the C atom. A detailed analysis of calculated charges and dipole moments shows that the changes due to triples are larger than those of the S, D, and Q excitations at the MP4 level thus proving the importance of T excitations for multiple bonded systems.

The MP4 level is as far as we can go in MP perturbation theory. The results obtained clearly indicate that still considerable changes have to be expected for MP5, possibly correcting the MP4 response density back into the direction of the MP3 response density. This prediction is partially confirmed by the response density obtained at the QCISD and QCISD(T) level of theory. QCI is correct to fourth order perturbation theory in the space of the S, D, and Q excitations while QCISD(T) is correct to fourth order in the complete space of S, D, T, and Q excitations. Apart from that both methods contain important terms that first appear at MP5 [55]. Hence, they should indicate whether correlation effects are overestimated at MP4.

Figure 6 gives the difference response density $\Delta\rho(\text{QCISD}) = \rho^{res}(\text{QCISD}) - \rho^{res}(\text{MP4(SDQ)})$. It indicates that the MP4(SDQ) response density is primarily corrected by a transfer of π electrons from C to S. As a consequence, the QCISD atomic charge of S is less positive, the bond polarity and, thereby, the CS dipole moment smaller than that obtained at the MP4(SDQ) level.

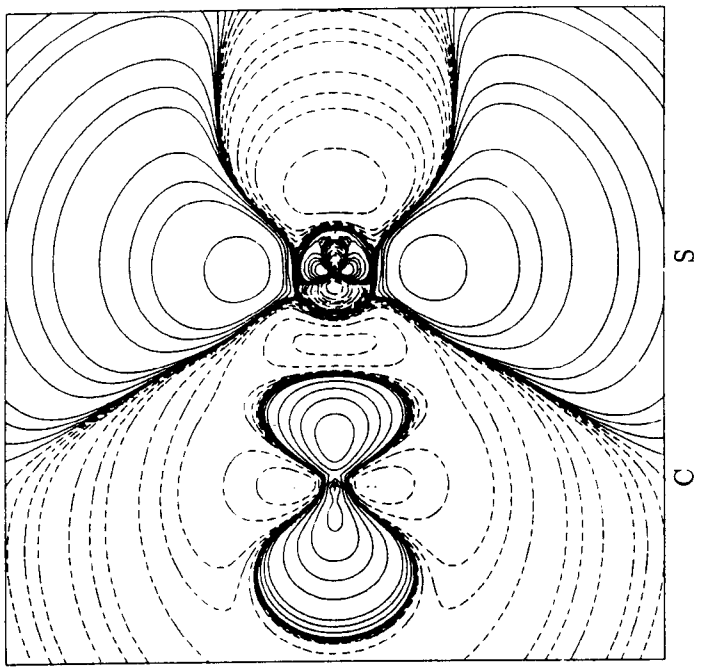

Figure 6. Contour line diagram of the difference electron density distribution $\Delta\rho(\mathbf{r})^{res}(QCISD) = \rho(\mathbf{r})^{res}(QCISD) - \rho(\mathbf{r})^{res}(MP4(SDQ))$ of CS calculated with the 6-311G(2d) basis. Solid (dashed) contour lines are in regions of positive (negative) difference densities. The positions of the C and the S nucleus are indicated.

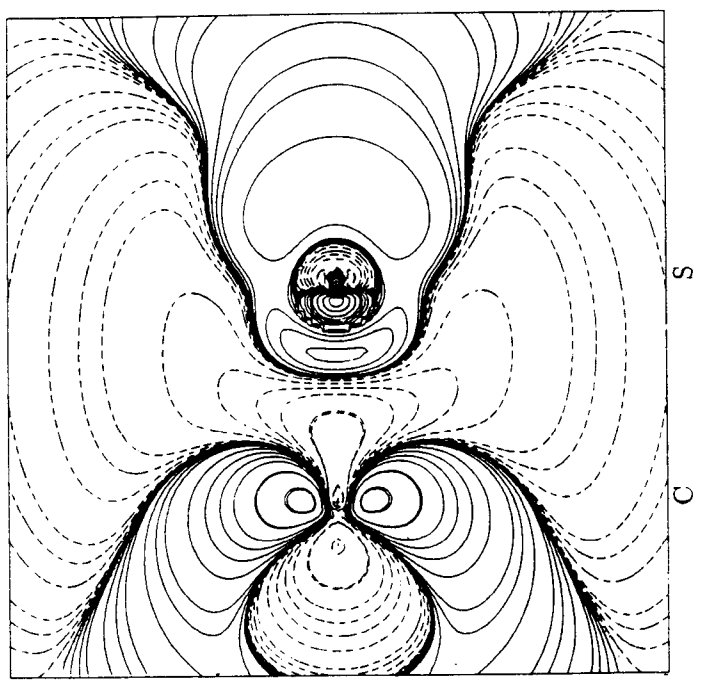

Figure 5. Contour line diagram of the difference electron density distribution $\Delta\rho(\mathbf{r})^{res}(MP4(SDQT)) = \rho(\mathbf{r})^{res}(MP4(SDQT)) - \rho(\mathbf{r})^{res}(MP4(SDQ))$ of CS calculated with the 6-311G(2d) basis. Solid (dashed) contour lines are in regions of positive (negative) difference densities. The positions of the C and the S nucleus are indicated.

The difference response density shown in Figure 6 is similar to that obtained for MP3 (Figure 2) and, therefore, it is reasonable to conclude that the coupling of S, D, and Q excitations at MP5 as well as the infinite order effects contained in QCISD lead to a correction of MP4(SDQ) back in the direction of MP3. The same conclusion is also true for the response density calculated at the QCISD(T) level as can be seen from the difference response density $\Delta\rho(\text{QCISD(T)}) = \rho^{res}(\text{QCISD(T)}) - \rho^{res}(\text{MP4(SDTQ)})$ shown in Figure 7. As a matter of fact the contour line diagrams in Figures 6 and 7 are very similar.

Nevertheless, the T corrections both at MP4 and at QCI are in the same direction which is reflected by the difference response density $\Delta\rho(\text{QCISD(T)}) = \rho^{res}(\text{QCISD(T)}) - \rho^{res}(\text{QCISD})$ given in Figure 8. They lead to transfer of π charge from S to C thus increasing gross atomic charges, bond polarity and dipole moment. Obviously, T effects are exaggerated at the MP4 level (compare Figure 7). A better account of T effects is given at QCISD(T).

The changes in the response density distribution of CS are parallel to calculated changes in atomic charges, dipole moment, quadrupole moment, and other one-electron properties, some of which are listed in Table 1. Figure 9 and 10 depict changes in atomic charge, dipole moment, and components of the quadrupole moment in dependence of the method. The multipole moments of CS oscillate in dependence of the order of perturbation theory applied where HF and MP2 results often represent upper and lower bound of computed values. Oscillations in calculated properties are observed in many cases [93]. Figure 11 gives as another example computed values of the CO dipole moment obtained at different levels of theory for a VDZ+P and a VTZ+2P basis set. Figure 11 also indicates that oscillations are largely independent of the basis set used.

Comparison of Figure 9, 10 and 11 leads to the following conclusions:

(1) The largest part of the correlation corrections to response properties is recovered at the MP2 level, but higher order effects are still considerable and cannot be neglected if accurate one-electron properties are needed.

(2) Correlation corrections due to D excitations are exaggerated at the MP2 level. They are reduced at the MP3 level where couplings between D excitations are first introduced.

(3) Single excitations lead only to relatively small changes in calculated response properties. This is opposite to the importance of S excitations when calculating one-electron properties as expectation values at the CI level [113]. There, S excitations are important to account for orbital relaxation effects which are covered within the energy derivative approach by solving the CPHF equations or the corresponding z-vector equation.

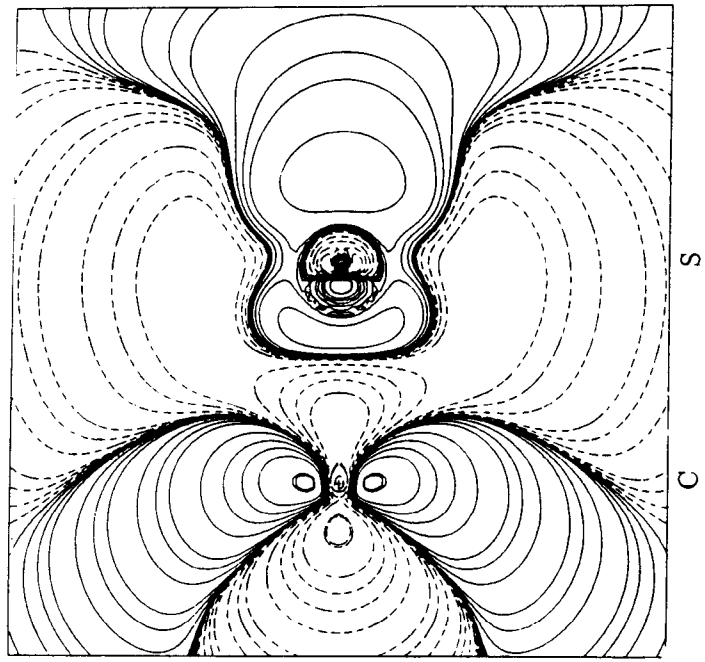

Figure 8. Contour line diagram of the difference electron density distribution $\rho(\mathbf{r})^{res}(QCISD(T)) - \rho(\mathbf{r})^{res}(QCISD)$ of CS calculated with the 6-311G(2d) basis. Solid (dashed) contour lines are in regions of positive (negative) difference densities. The positions of the C and the S nucleus are indicated.

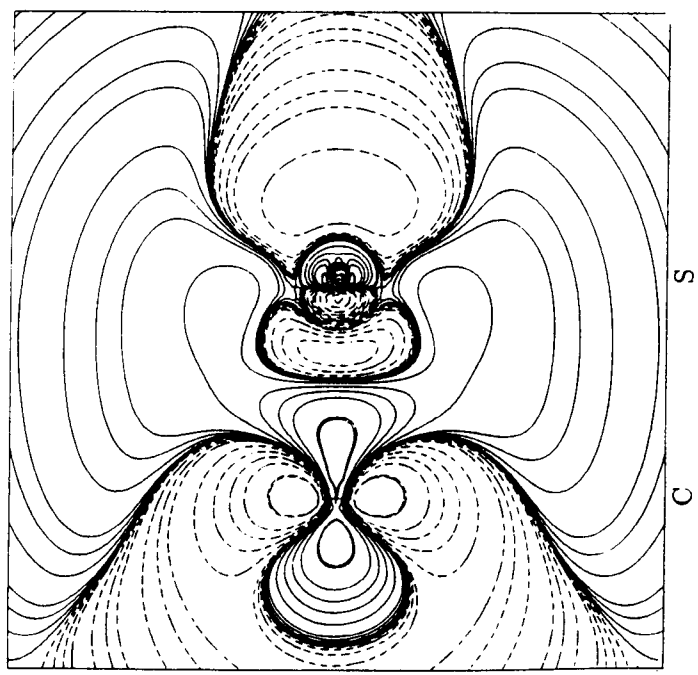

Figure 7. Contour line diagram of the difference electron density distribution $\Delta\rho(\mathbf{r})^{res}(QCISD(T)) = \rho(\mathbf{r})^{res}(QCISD(T)) - \rho(\mathbf{r})^{res}(MP4(SDQT))$ of CS calculated with the 6-311G(2d) basis. Solid (dashed) contour lines are in regions of positive (negative) difference densities. The positions of the C and the S nucleus are indicated.

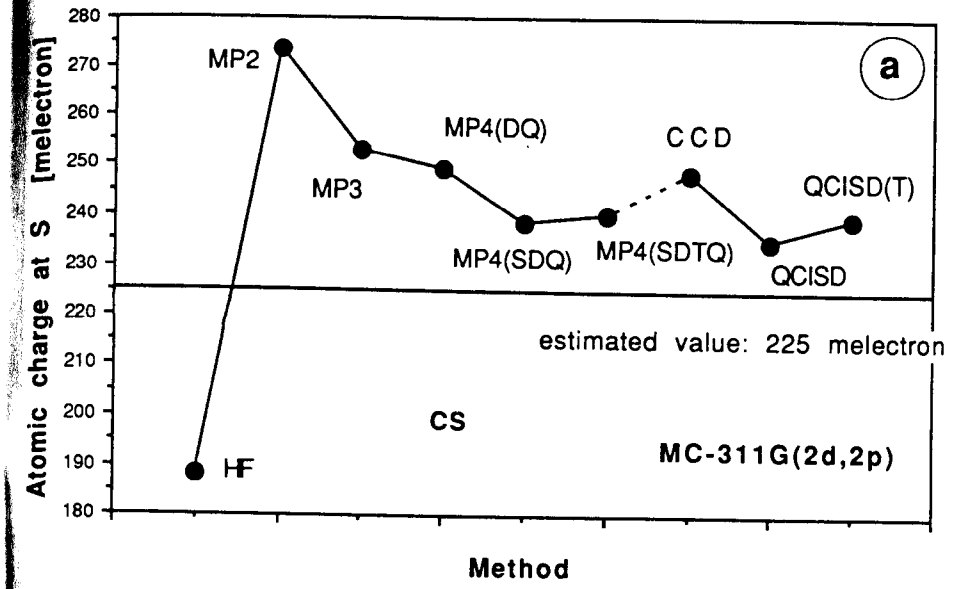

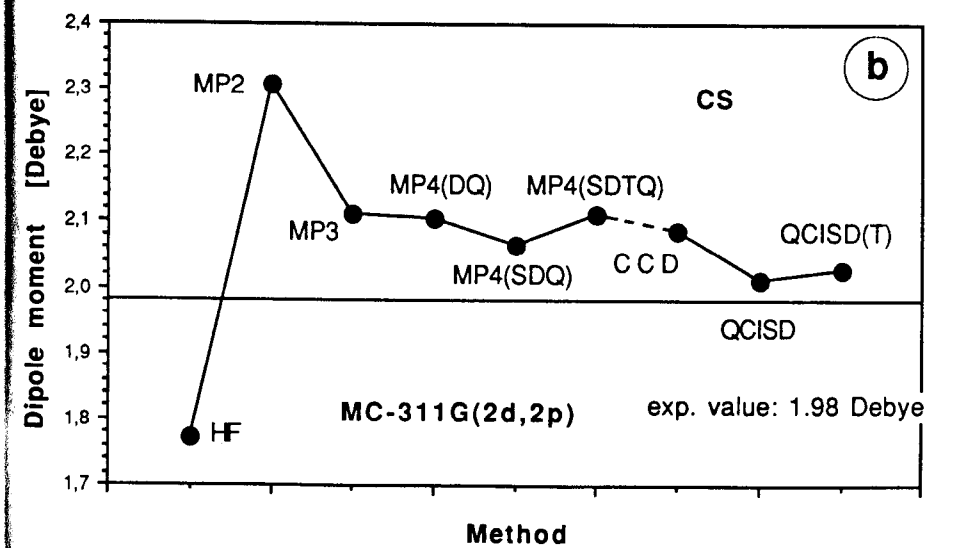

Figure 9. Dependence of calculated one-electron properties on the method used. (a) Charge of the S atom in carbon monosulfide. (b) Dipole moment of carbon monosulfide (6-311G(2d,2p) calculations).

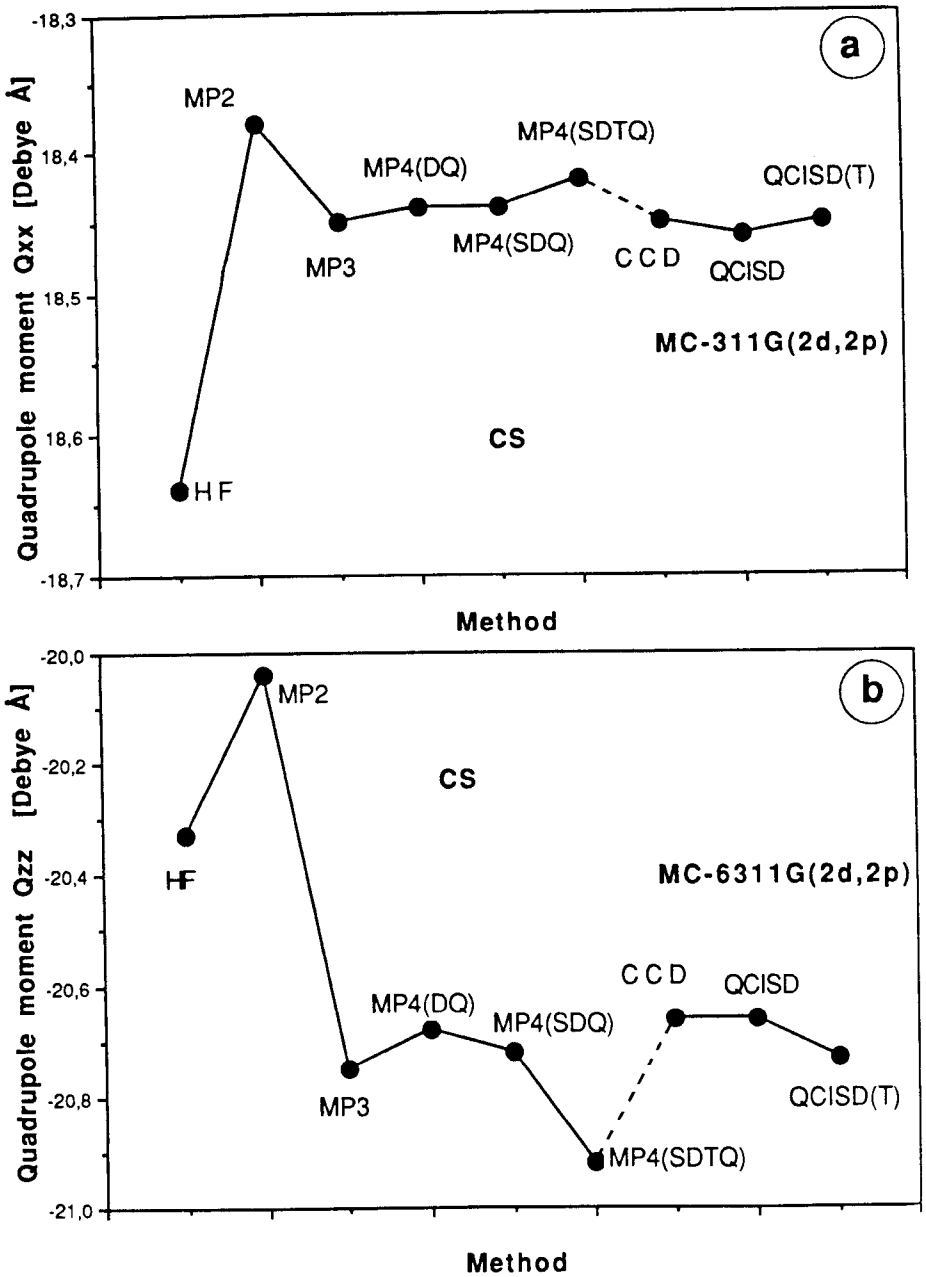

Figure 10. Dependence of calculated quadrupole moment Q of carbon monosulfide, CS, on the method used. (a) Q_{xx}. (b) Q_{zz} (6-311G(2d,2p) calculations; z-axis is identical with molecular axis).

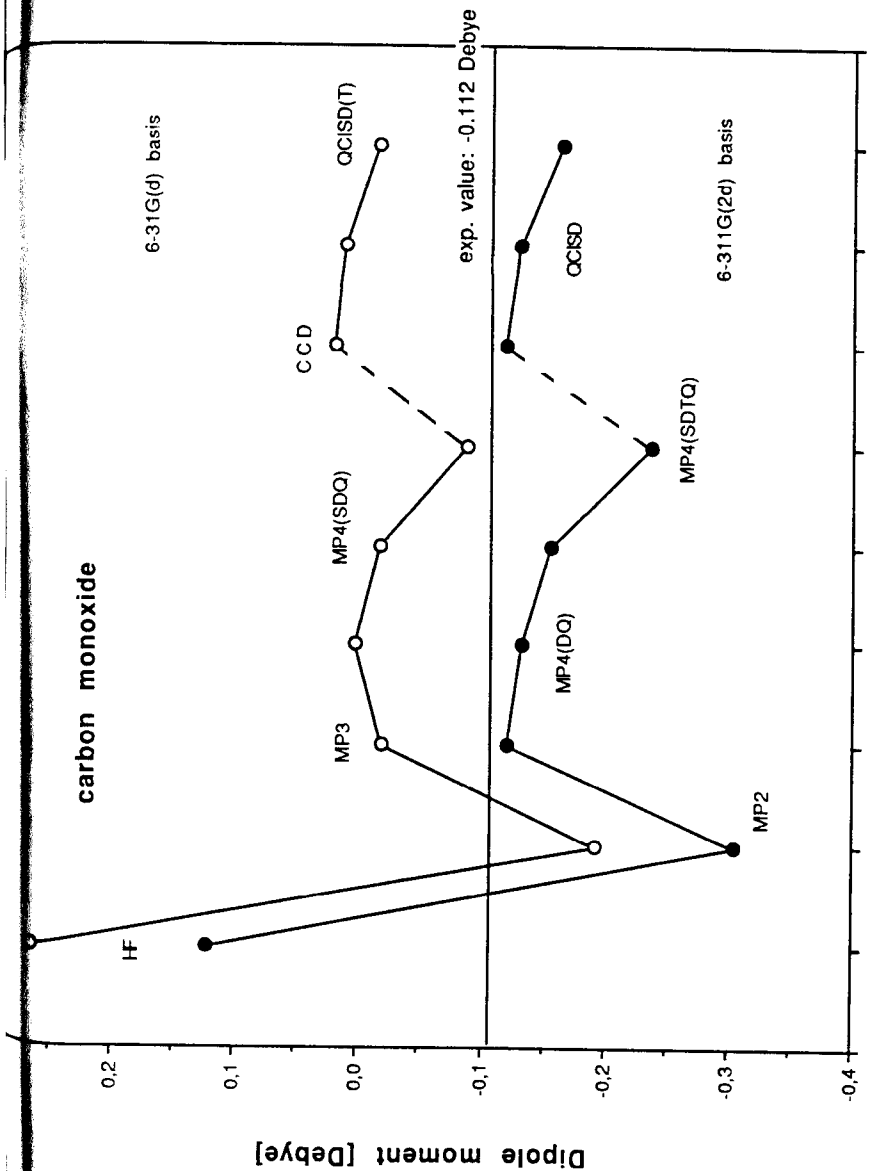

Figure 11. Dependence of the dipole moment of carbon monoxide, CO, on method and basis set.

(4) The influence of T excitations at MP4 is relatively large, at least for molecules with multiple bonds. However, comparison with QCISD(T) suggests that T effects are somewhat exaggerated at the MP4 level. This may also be true for S and Q effects at MP4 since couplings between these excitations are not considered at this level of theory.

(5) It is most likely that MP5, which introduces couplings between SDTQ excitations corrects MP4 values back in the direction of the MP3 result. On the other hand, MP6, which introduces P and H excitations may lead to response properties closer to MP4 than MP3 values. In other words, oscillations of response property values may only slowly damp out at the MPn level.

(6) Calculated response property values from CC and QCI methods that contain infinite order effects seem to converge to a limiting value rather than to oscillate in dependence of the excitation effects included. At least, this is suggested by the calculated CCD, QCISD, and QCISD(T) results. In any case the changes in the CC and QCI values are much smaller than those observed for the MPn results.

It is clear that changes in the response property that lead to an increase or decrease of the atomic charges (bond polarity) will also lead to similar changes in dipole moment and higher multipole moments. However, similar oscillations in the calculated values are also obtained for other properties such as for example nuclear quadrupole moments [114]. Figure 12 gives calculated values of the ^{14}N nuclear quadrupole moment Q of HCN. Actually, $Q(^{14}\mathrm{N})$ is largely independent of the molecular structure. Experimental and theoretical investigations have led to $Q(^{14}\mathrm{N})$ values of 19.3 ± 0.8 [115] and 20.5±0.5 mbarn [116], respectively. Theoretically, $Q(^{14}\mathrm{N})$ is derived from the computed electric field gradient q and the experimentally known nuclear quadrupole coupling constant χ according to

$$Q = 4.256\chi/q \tag{5.9}$$

with χ given in MHz and q in atomic units both determined for a particular molecule. Since the component of the nuclear quadrupole coupling constant of HCN along the molecular axis is accurately known (χ_{aa} = -4.7091(13) MHz) [117], calculated values of $Q(^{14}\mathrm{N})$ reflect the accuracy of computed electric field gradients q_{aa}.

The diagram in Figure 12 indicates that correlation corrections for $Q(^{14}\mathrm{N})$ calculated with a basis set of TZ+2P quality are substantial increasing the HF value by 3 to 5 mbarn. Again, the MP2 and (less strongly) the MP4 value are too large while the MP3 value is too small compared to the accepted $Q(^{14}\mathrm{N})$ value. Hence, MPn results oscillate between $Q(^{14}\mathrm{N})$ values

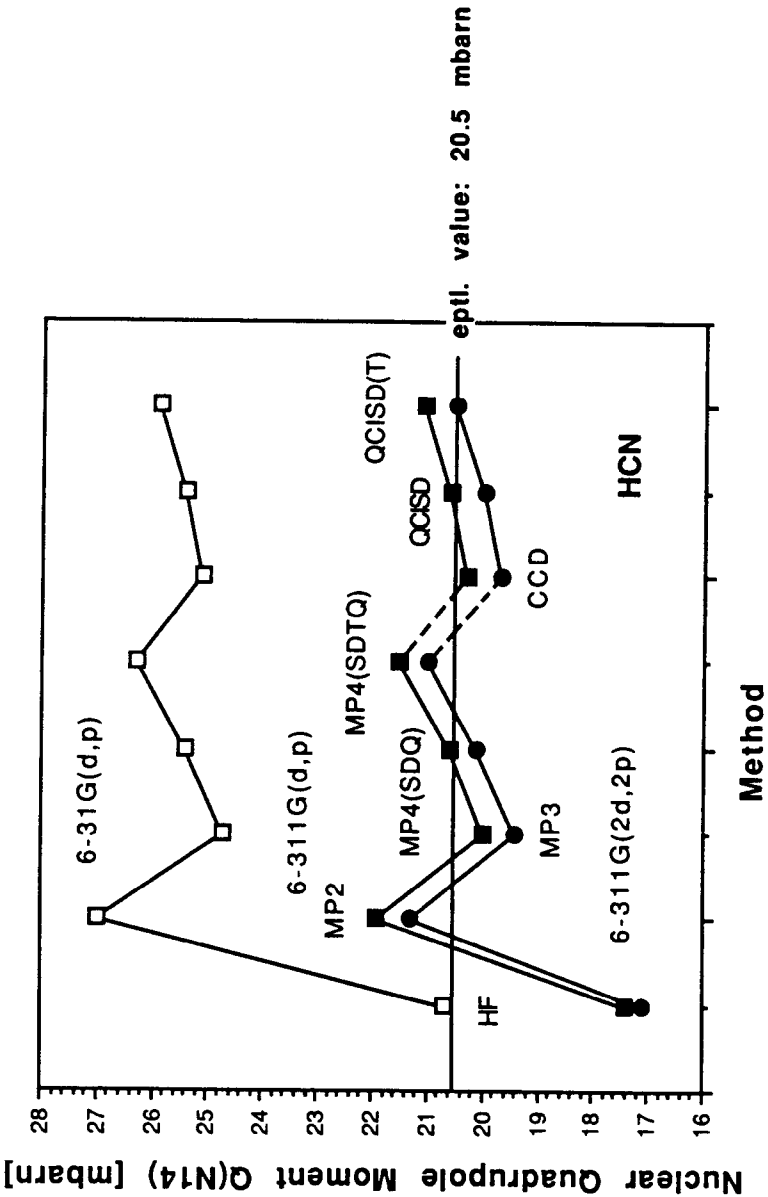

Figure 12. Dependence of the nuclear quadrupole moment $Q(^{14}N)$ of HCN on method and basis set.

obtained at the HF and MP2 level. CC and QCI values of $Q(^{14}N)$ quickly converge to the correct value of 20.5 mbarn (see Figure 12). Both at the MP and at the CC (QCI) level, the inclusion of T excitations has a substantial effect on the $Q(^{14}N)$ value.

The same trends have been found for electric field gradients and ^{14}N nuclear quadrupole moments of other molecules. In all cases investigated, correlation corrections are almost independent of the basis set used (compare with Figure 12).

In conclusion we stress the following points:

(1) Calculated MPn, CC, and QCI one-electron properties follow calculated changes in response densities due to correlation corrections. These changes are almost independent of the basis set used provided the basis is sufficiently large (at least DZ+P quality).

(2) At the MPn level of theory correlation corrections to response properties oscillate where in most cases the maximal values of the oscillation are given by HF and MP2. Oscillations clearly depend on the fact that at even orders of perturbation theory new types of correlation effects are included (D at MP2, STQ at MP4, etc.) while at odd orders these effects are reduced by introducing couplings between excitations included at the previous order (coupling between D excitations at MP3, between STQ excitations at MP5, etc.).

(3) Analysis of calculated response properties suggests that oscillations persist at MP5 and probably also at higher orders of MP theory. Convergence to a limiting MPn value seems to be much slower as one generally tends to believe. In many cases, MP4 is not sufficient to obtain an accurate value of the response property in question.

(4) CC and QCI values of response properties seem to converge very fast to a limiting value which in most cases is already reached when T excitations are included. This is due to the fact that CC and QCI methods contain infinite order effects that prevent overestimation (underestimation) of a particular correlation effect. Hence, CC and QCI methods are clearly superior to MP methods. If high accuracy is needed, QCISD(T) or CC methods including triple corrections such as CCSD(T) or even CCSDT will definitely be the methods of choice.

In the following we will investigate whether similar trends can be observed for other molecular properties calculated at either MP, CC or QCI.

5.2 Equilibrium Geometries

In Figure 13 calculated and experimental r_e geometries (compare with

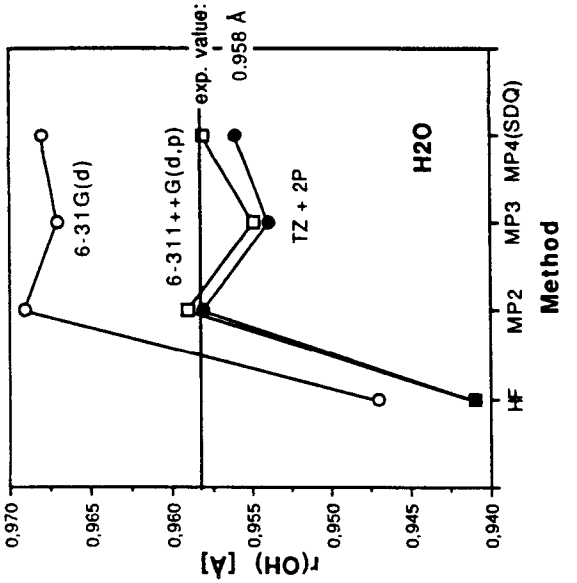

Figure 13b. Dependence of calculated equilibrium geometries on method and basis set. H_2O, bond length OH.

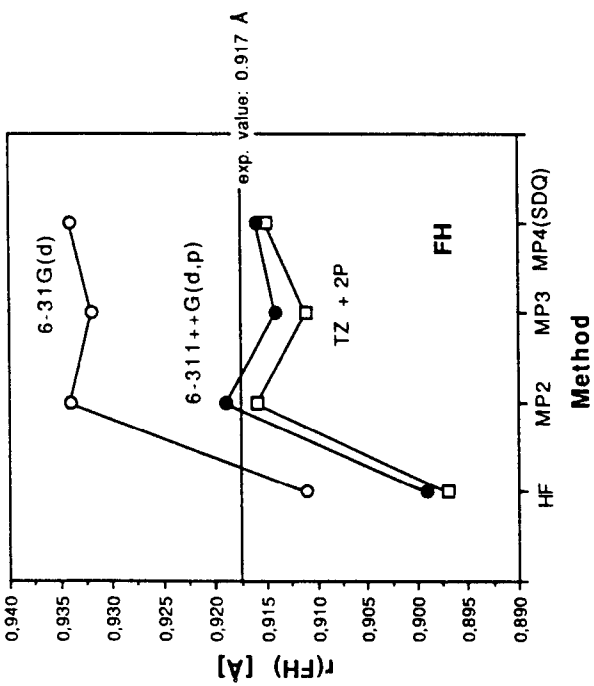

Figure 13a. Dependence of calculated equilibrium geometries on method and basis set. FH, bond length.

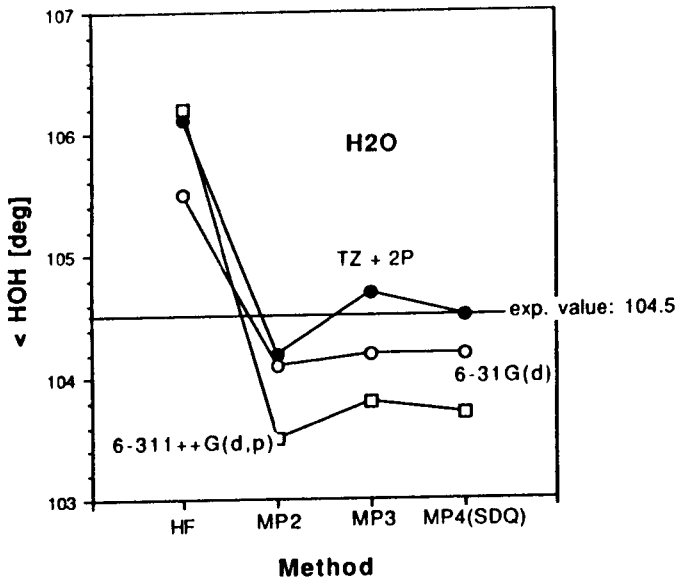

Figure 13c. Dependence of calculated equilibrium geometries on method and basis set. H_2O, bond angle HOH.

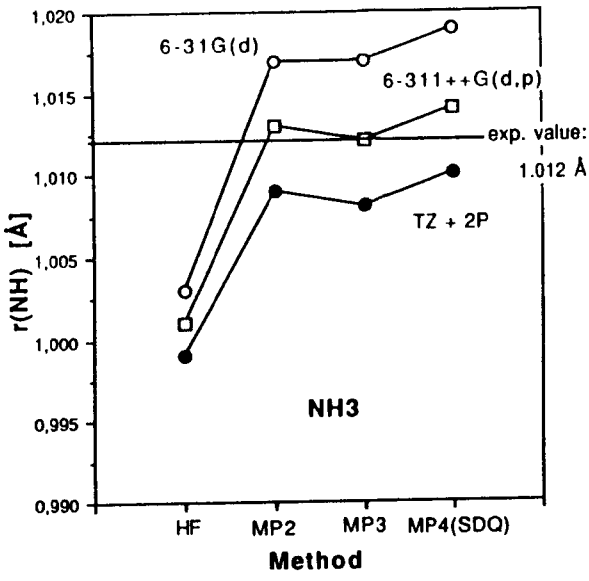

Figure 13d. Dependence of calculated equilibrium geometries on method and basis set. NH_3, bond length NH.

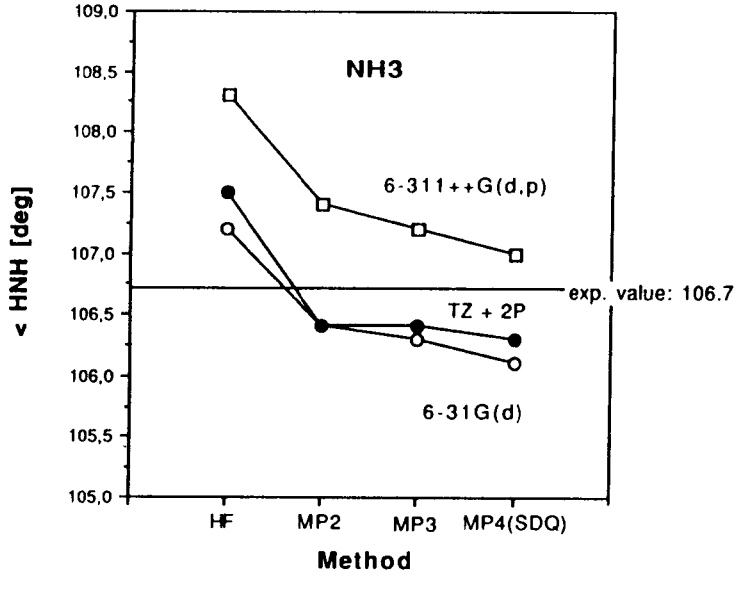

Figure 13e. Dependence of calculated equilibrium geometries on method and basis set. NH_3, bond angle HNH.

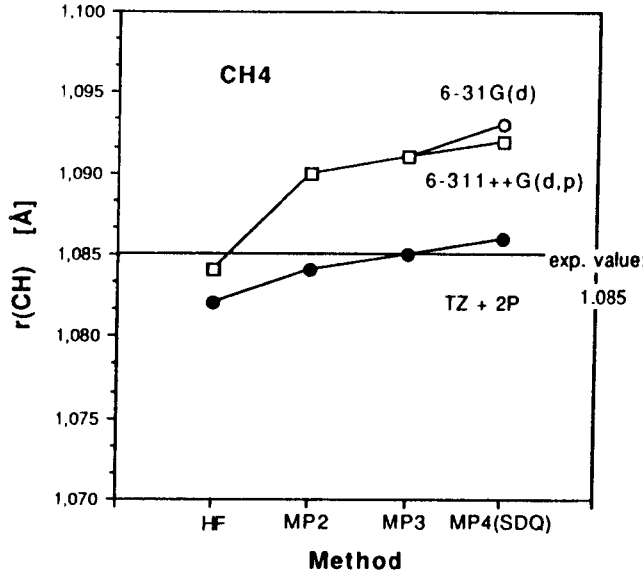

Figure 13f. Dependence of calculated equilibrium geometries on method and basis set. CH_4, bond length CH.

Tables 2 and 3) of FH (Figure 13a), H_2O (Figure 13b and c), NH_3 (Figure 13d and e) and CH_4 (Figure 13f) are shown. Theoretical values have been obtained with three different basis sets, 6-31G(d), 6-311++G(d,p) and (9s5p2d/5s2p)[5s3p2d/3s2p], which are of VDZ+(P), VTZ+P+diff, and VTZ +2P quality [118]. The diffuse basis functions added to the second basis are used to describe the distribution of the lone pair electrons at F, O, and N more accurately. Calculations have been carried out at the HF, MP2, MP3, and MP4 level of theory, where in the later case only SDQ excitations have been considered since T excitations are known to be of minor importance for molecules with just single bonds [119].

For all AH_n molecules investigated, similar trends in calculated equilibrium geometries are found. Trends in calculated AH bond lengths are opposite to trends in calculated HAH bond angles, i.e. a large bond length implies a small HAH bond angle and vice versa. As in the case of the response properties discussed in the previous section, correlation corrections to the calculated geometrical parameters depend only slightly on the basis set used.

Typical of all calculations is that HF underestimates the AH bond length by 0.01 - 0.02 Å. Two observations can be made in this connection. (a) Compared to the experimental value the HF value of r_e(AH) is the smaller, the larger the difference in the electronegativities between A and H and, hence, the AH bond polarity is. (b) With increasing size of the basis set the HF value decreases thus increasing the difference between experimental and theoretical r_e value.

MP2 leads to an increase of the AH bond length by 0.01-0.02 Å. In this way VTZ+P+diff or VTZ+2P values come close to the experimental r_e value while VDZ+P values become clearly too large. MP3 on the other hand reduces the value of the AH bond length back in the direction of the HF value. However, the reduction of r_e(AH) is much smaller than the increase calculated at the MP2 level. Also, the reduction of the AH bond length becomes the smaller the smaller the AH bond polarity and the smaller the basis set is. The MP3/6-31G(d) result for NH_3 and all the MP3 results for CH_4 already lead to a slight increase of the AH bond length.

At MP4(SDQ), again an increase of the calculated AH bond length is obtained. Since this increase is almost as large as the relative changes obtained at the MP3 level, MP4(SDQ) values are close to MP2 ones (exceptions: CH_4 and MP4(SDQ)/6-31G(d) result for NH_3). As a consequence, most MP4(SDQ) bond lengths obtained with the two VTZ basis sets agree with the experimental r_e values.

It would be difficult to distinguish between the quality of MP2 and

Table 2. Calculated equilibrium geometries, dipole moments, harmonic vibrational frequencies, and infrared intensities for HF, H_2O, NH_3, and CH_4. Bond lengths are given in Å, angles in deg, dipole moments (μ) in Debye, frequencies (ω) in cm^{-1}, and intensities (I) in km/mol.

	6-31G(d)				6-311++G(d,p)				TZ2P				
Basis	HF	MP2	MP3	MP4(SDQ)	HF	MP2	MP3	MP4(SDQ)	HF	MP2	MP3	MP4(SDQ)	exp.
Hydrogen Fluoride(HF)													
r(FH)	0.911	0.934	0.932	0.934	0.897	0.916	0.911	0.915	0.899	0.919	0.914	0.916	0.917[a]
μ	1.972	1.948	1.941	1.935	2.026	1.969	1.857	1.954	1.934	1.860	1.862	1.853	1.819[b]
ν	4357	4042	4071	4031	4493	4202	4286	4219	4471	4153	4229	4181	4139[c]
I	141.4	91.3	84.6	77.8	191.7	142.0	131.3	124.4	149.5	102.9	100.5	93.9	99.8[d]
Water (H_2O)													
r(OH)	0.947	0.969	0.967	0.968	0.941	0.959	0.955	0.958	0.941	0.958	0.954	0.956	0.958[e]
α(HOH)	105.5	104.1	104.2	104.2	106.2	103.5	103.8	103.7	106.1	104.2	104.7	104.5	104.5[e]
μ	2.199	2.199	2.188	2.179	2.196	2.189	2.164	2.164	2.020	1.984	1.977	1.971	1.855[f]
ν_1	4189	3919	3930	3893	4244	4007	4053	4005	4228	3980	4018	3980	3943[g]
ν_2	4071	3778	3809	3765	4143	3889	3960	3900	4128	3861	3921	3876	3832[g]
ν_3	1827	1734	1750	1745	1727	1627	1665	1653	1760	1657	1686	1680	1649[g]
I_1	58.1	39.2	31.3	26.3	87.9	63.5	52.0	47.6	68.6	49.8	42.8	38.1	44.6[g]
I_2	18.2	5.6	4.9	3.2	25.5	13.2	11.2	9.2	14.3	5.9	5.5	4.2	2.2[g]
I_3	107.3	88.9	89.8	86.3	85.4	57.7	59.3	56.9	98.7	74.7	77.7	74.9	53.6[g]

[a] K.P. Huber and G. Herzberg, *Constants of Diatomic Molecules* (Van Nostrand Reinhold, New York 1979).
[b] A.L. McCellan, *Tables of Experimental Dipole Moments* (Freeman, San Francisco, 1963).
[c] D.R. Stull and H. Prophet, *JANAF Thermochemical Tables* (NBS, Washington, 1971).
[d] A.S. Pine, A. Fried, and J.W. Elkins, *J. Mol. Spectrosc.* **109** (1985) 30.
[e] A.R. Hoy, I.M. Mills, and G. Strey, *Mol. Phys.* **24** (1972) 1265.
[f] S.A. Clough, Y. Beers, G.P. Klein, and L.S. Rothman, *J. Chem. Phys.* **59** (1973) 2254.
[g] B. A. Ziles and W.B. Person, *J. Chem. Phys.* **59** 2254 (1973).

Continuation of Table 2.

Basis	HF	MP2	MP3	MP4(SDQ)	HF	MP2	MP3	MP4(SDQ)	HF	MP2	MP3	MP4(SDQ)	exp.
			6-31G(d)				6-311++G(d,p)				TZ2P		
Ammonia (NH_3)													
r(NH)	1.003	1.017	1.017	1.019	1.001	1.013	1.012	1.014	0.999	1.009	1.008	1.010	1.013[a]
α(HNH)	107.2	106.4	106.3	106.1	108.3	107.4	107.2	107.0	107.5	106.4	106.4	106.3	106.7[a]
μ	1.920	1.965	1.955	1.958	1.723	1.733	1.736	1.736	1.682	1.718	1.703	1.703	1.472[b]
ν_1	3822	3661	3648	3611	3825	3689	3672	3659	3808	3672	3694	3642	3577[c]
ν_2	3689	3504	3519	3470	3696	3537	3555	3523	3689	3538	3562	3524	3506[c]
ν_3	1850	1756	1758	1753	1793	1666	1719	1678	1800	1705	1680	1716	1691[c]
ν_4	1209	1160	1172	1178	1098	1065	1107	1095	1135	1088	1090	1110	1022[c]
I_1	0.9	1.4	0.0	0.3	10.7	12.5	5.5	3.5	6.9	8.3	3.5	1.9	3.8[d]
I_2	0.3	0.1	0.3	0.7	0.2	1.5	1.9	2.7	0.0	0.1	0.4	0.7	7.6[d]
I_3	42.7	39.9	39.3	36.2	55.2	49.7	45.1	43.4	39.1	31.6	31.1	29.4	25[d]
I_4	218.3	188.3	183.8	174.3	232.4	208.8	197.5	192.2	192.9	159.6	156.4	152.1	127[d]
Methane (CH_4)													
r(CH)	1.084	1.090	1.091	1.093	1.084	1.090	1.091	1.092	1.082	1.084	1.085	1.086	1.086[e]
ν_1	3301	3251	3230	3203	3252	3217	3204	3183	3254	3218	3199	3177	3157[e]
ν_2	3197	3113	3104	3079	3150	3079	3079	3060	3153	3085	3080	3061	3026[e]
ν_3	1703	1625	1614	1607	1667	1570	1567	1566	1672	1605	1603	1600	1583[e]
ν_4	1488	1413	1409	1403	1453	1361	1367	1367	1457	1375	1381	1380	1367[e]
I_1	119.5	58.0	67.0	75.1	125.8	60.0	71.6	79.2	82.9	27.9	38.5	45.1	64[f]
I_4	30.8	48.8	48.3	44.7	35.9	44.8	39.5	36.2	35.8	47.0	42.1	38.9	33[f]

[a] W.S. Benedict and E.K. Pyler, *Can. J. Phys.* **35** (1957) 1235.
[b] M.D. Marshall and J.S. Muenter, *J. Mol. Spetrosc.* **85** (1981) 322.
[c] J.L. Duncan and I.M. Mills, *Spectrochim. Acta* **29** (1964) 523.
[d] K. Kim, *J. Quant. Spectrosc. Radiat. Trans.* **33** (1985) 611; T. Koops, T. Visser, and W.M.A. Smith, *J. Mol. Struct.* **44** (1966) 3561.
[e] D.L. Gray and A.G. Robiette, *Mol. Phys.* **37** (1979) 1901.
[f] D.E. Jennings and A.G. Robiette, *J. Mol. Spectrosc.* **94** (1982) 369; M. Dang-Nhu, A.S. Pine, and A.G. Robiette, *J. Mol. Spectrosc.* **77** (1979) 57.

Table 3. Calculated geometrical parameters for various multiple bonded molecules. Bond distances are given in Å, and angles in deg.

Basis	HF	MP2	MP3	MP4(SDQ)	HF	MP2	MP3	MP4(SDQ)	exp.
			6-31G(d)				TZ2P		
Acetylen(C_2H_2)									
r(CC)	1.185	1.216	1.205	1.211	1.180	1.208	1.197	1.201	1.203[a]
r(CH)	1.057	1.066	1.066	1.068	1.054	1.060	1.059	1.062	1.061[a]
Carbon Monoxide (CO)									
r(CO)	1.114	1.150	1.134	1.146	1.104	1.137	1.121	1.133	1.128[b]
Formaldehyde (H_2CO)									
r(CO)	1.184	1.220	1.209	1.216	1.178	1.211	1.198	1.206	1.203[c]
r(CH)	1.092	1.104	1.103	1.107	1.092	1.098	1.098	1.100	1.099[c]
α(HCH)	115.7	115.6	115.9	115.6	116.1	116.4	116.4	116.3	116.5[c]
Hydrogen Cyanide (HCN)									
r(CN)	1.133	1.176	1.157	1.166	1.124	1.164	1.145	1.153	1.153[d]
r(CH)	1.059	1.069	1.069	1.071	1.057	1.062	1.061	1.063	1.065[d]
Fluorine (F_2)									
r(FF)	1.345	1.421	1.414	1.425	1.335	1.414	1.402	1.415	1.412[e]
Hydrogen Peroxide (H_2O_2)									
r(OO)	1.397	1.468	1.452	1.464	1.390	1.459	1.440	1.451	1.464 [f]
r(OH)	0.949	0.976	0.971	0.974	0.943	0.964	0.958	0.961	0.965 [f]
α(OOH)	102.1	98.7	99.7	99.3	102.8	99.4	100.7	100.2	99.4[f]
θ(HOOH)	116.0	121.2	121.1	120.9	109.4	110.8	110.8	110.9	111.8[f]

[a] A. Baldacci, S. Ghersetti, S.C. Hurlock, and K.N. Rao, *J. Mol. Spectrosc.* **59** (1976) 116.
[b] K.P. Huber and G. Herzberg, *Constants of Diatomic Molecules* (Van Nostrand Reinhold, New York 1979).
[c] K. Yamada, T. Nakagawa, K. Kuchitsu, and Y. Morino, *J. Mol. Spectrosc.* **38** (1971) 70.
[d] G. Winnewisser, A.G. Maki, and R.D. Johnson, *J. Mol. Spectrosc.* **39** (1971) 149.
[e] E.A. Colbourn, M. Dagenais, A.E. Douglas, and J.W. Raymonds, *Can. J. Phys.* **54** (1976) 1343.
[f] J. Koput, *J. Mol. Spectrosc.* **115** (1986) 438.

MP4(SDQ) results on the one side and between 6-311++G(d,p) and TZ+2P results on the other side if just the bond lengths of AH_n molecules would be considered. However, comparison of the calculated HAH angles with experimental values clearly reveals that the best results are obtained at the MP4(SDQ) level using the TZ+2P basis set. For a reliable description of bond angles a second set of polarization function seems to be more important than diffuse functions. This is also true in the case of the CH bond length of CH_4 where the VTZ+2P values are slightly better than the VTZ+P+diff values.

The relative changes of the calculated geometrical parameters can easily be understood when considering the extent of electron correlation included at the different levels of theory. For example, at the HF level only exchange correlation is considered. Accordingly, electrons can concentrate around the nuclei and in the bonding region thus increasing electron-nucleus attraction and, thereby, the stability of the molecule. In the case of an AH_n molecule with a strongly electronegative atom A electrons accumulate in the nuclear region of A. As a consequence, nucleus A is largely shielded by the surrounding negative charge, nuclear repulsion between A and the H atom(s) is decreased, and a relatively short internuclear AH distance results. This effect is the more pronounced the larger the electronegativity of A is and the more negative charge can be concentrated in the nuclear region. Also, concentration of electronic charge is limited by the number of basis functions describing the region around the nuclei. Accordingly, the underestimation of the r_e value of polar AH bonds depends on the bond polarity and the basis set employed.

If electron correlation is considered, negative charge is no longer concentrated around the nuclei and in the bonding region. These areas are depleted relative to the HF electron distribution. As a consequence, the nuclei are partially deshielded, nuclear repulsion is increased, and longer AH bond lengths result. Of course, the extent of depletion of electronic charge and the increase of nuclear repulsion depend on how many correlation effects are included in the calculation. Electron pair correlation dominates these effects and, therefore, MP2 leads to the strongest corrections. Coupling of pair correlations at MP3 reduces MP2 corrections. MP4(SDQ) brings in new correlation effects due to S, D, and Q excitations thus increasing correlation corrections back to the MP2 values.

Obviously, trends in geometrical parameters are similar to those observed for multipole moments and other one-electron properties. This is not astonishing since the equilibrium geometry is defined by vanishing forces on the nuclei. These, on the other hand, are response properties which depend

on the changes in the response density. However, since the basis set depends on the position of the nuclei, additional terms have to be considered when calculating forces (compare e.g. eq. (3.60)).

Explanation of the trends in calculated bond lengths can easily be extended to those obtained for computed bond angles. In Figure 14, theoretical values of the HOH bond angle are plotted against the corresponding values of the OH bond length. There is a linear relationship between the two geometrical parameters in the way that the larger bond length implies a smaller bond angle. A similar relationship can also be found for NH_3 and other AH_n molecules. According to the electrostatic model of charge distribution used to explain trends in calculated bond lengths, accumulation of charge in the nuclear region of A is accompanied by a short bond length. It also leads to a relatively large positive charges at the H atoms. As a consequence, Coulomb repulsion between the H atoms becomes large thus forcing the HAH angle to widen. Accordingly, a short AH bond length implies a large HAH bond angle and vice versa.

The same explanations can be used to discuss trends in calculated geometrical parameters of two-heavy atoms. Figure 15 gives results for acetylene, C_2H_2, Figure 16 for formaldehyde, CH_2O, Figure 17 for hydrogen cyanide, HCN, Figure 18 for hydrogen peroxide, H_2O_2, and Figure 19 for F_2. In all these cases, bond lengths AH and AB as well as bond angles ABH show the same dependence on method and basis set as the geometrical parameters of molecules AH_n do. Apart from this, the following additional observations can be made:

(1) Changes due to the inclusion of correlation effects are now much stronger, namely up to 0.08 Åfor bonds OO and FF, up to 0.03 Åfor the OH bond in H_2O_2, and $3-4°$ for the angle OOH. This can be explained by considering the fact that now two heavy atoms rather than one concentrate negative charge around their nuclei thus leading to a relative strong change in nuclear repulsion between them.

(2) Geometrical parameters such as dihedral angles depend strongly on the basis set but not so much on the method used (Figure 18d). In the case of H_2O_2, a basis set such as 6-31G(d) which leads to more positively charged H atoms, predicts a larger dihedral angle while a more balanced charge distribution obtained with the TZ+2P basis predicts a smaller dihedral angle. On the other hand, changes in the distribution of electronic charge due to correlation effects seem to be too small to strongly affect H,H interactions that are more than 2 bonds apart.

(3) Equilibrium geometries depicted in Figures 15 to 17 clearly indicate the superiority of the MP4(SDQ) method compared to MP3 or MP2. Also,

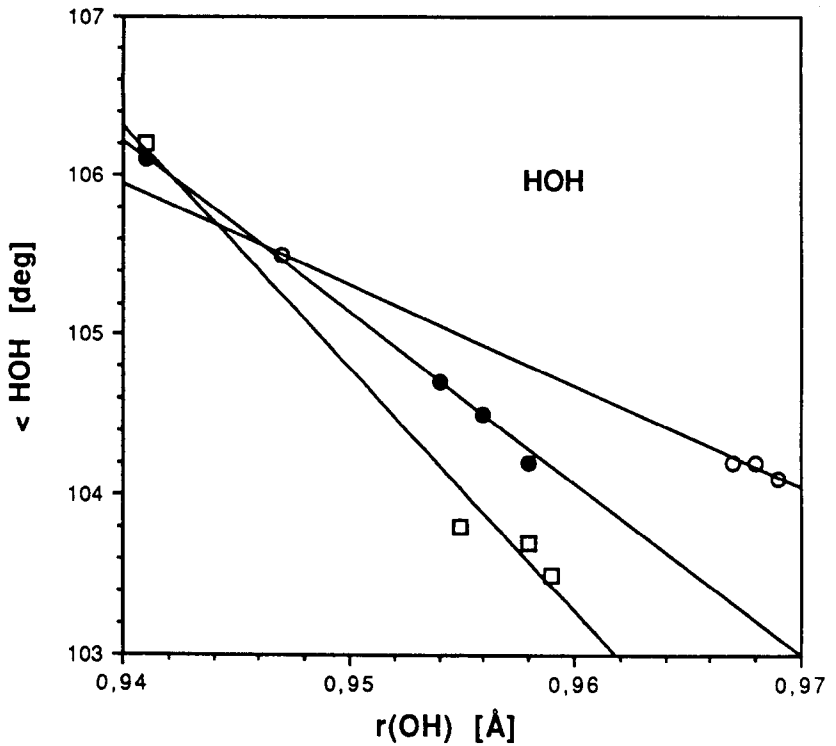

Figure 14. Relationship between geometrical parameters: H_2O - Calculated values of the bond angles HOH vs. calculated bond lengths OH.

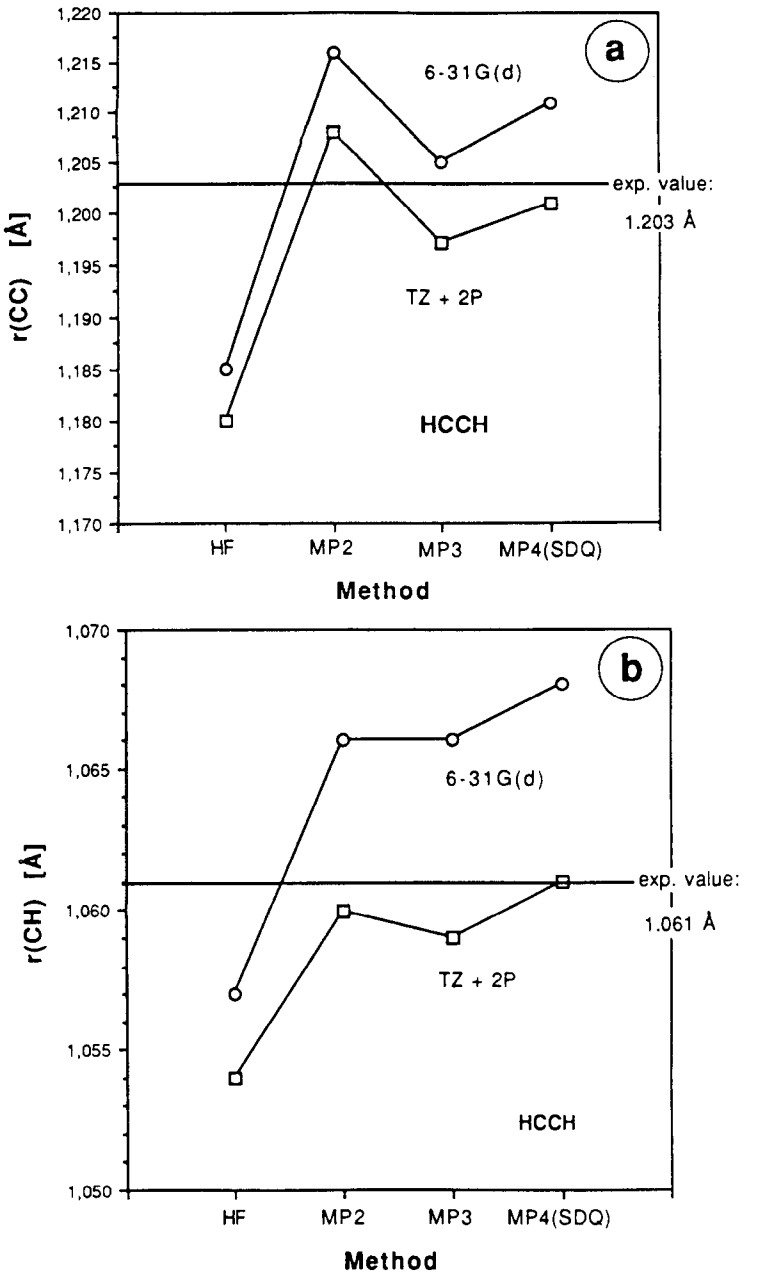

Figure 15. Dependence of calculated equilibrium geometries on method and basis set. Acetylene, HCCH: (a) CC bond length. (b) CH bond length.

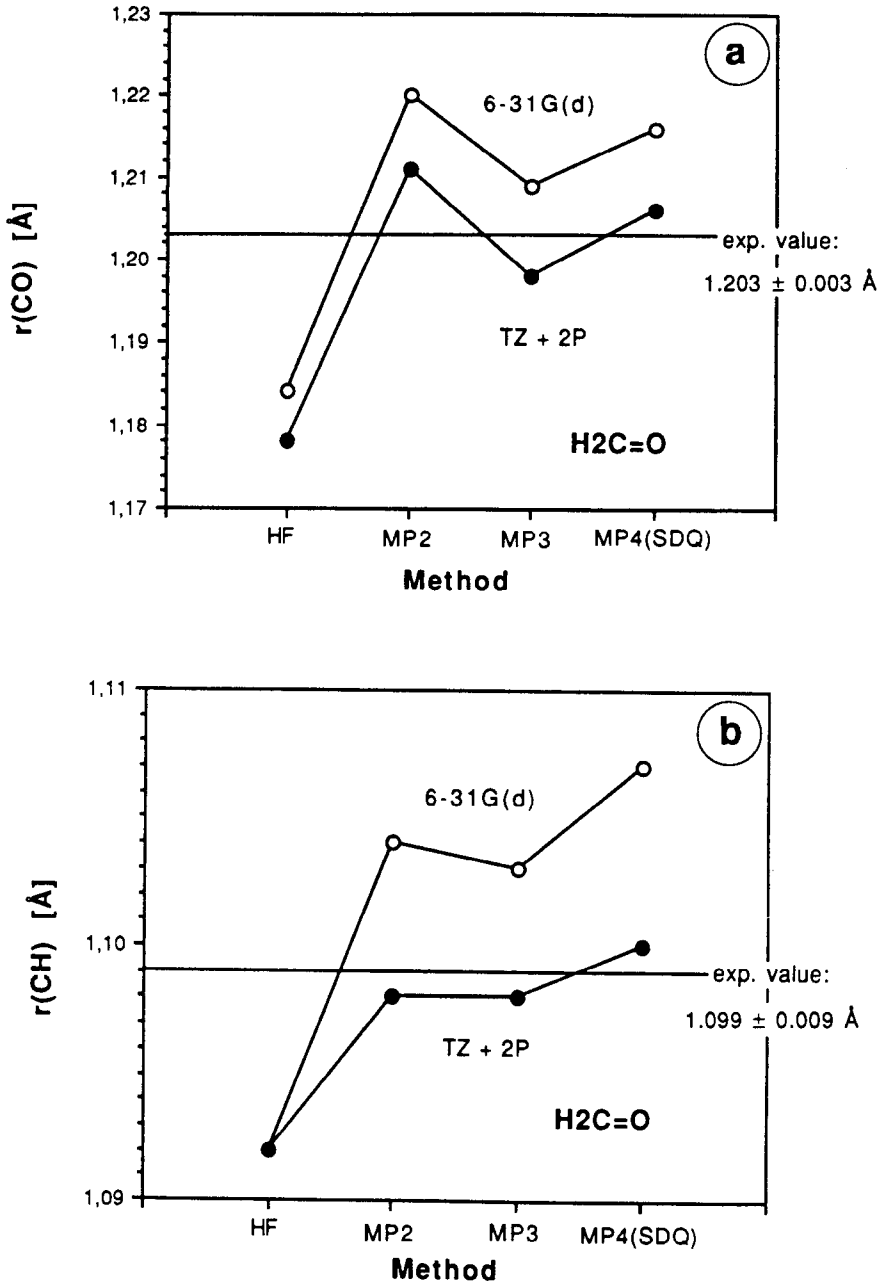

Figure 16. Dependence of calculated equilibrium geometries on method and basis set. Formaldehyde, CH_2O: (a) CO bond length. (b) CH bond length.

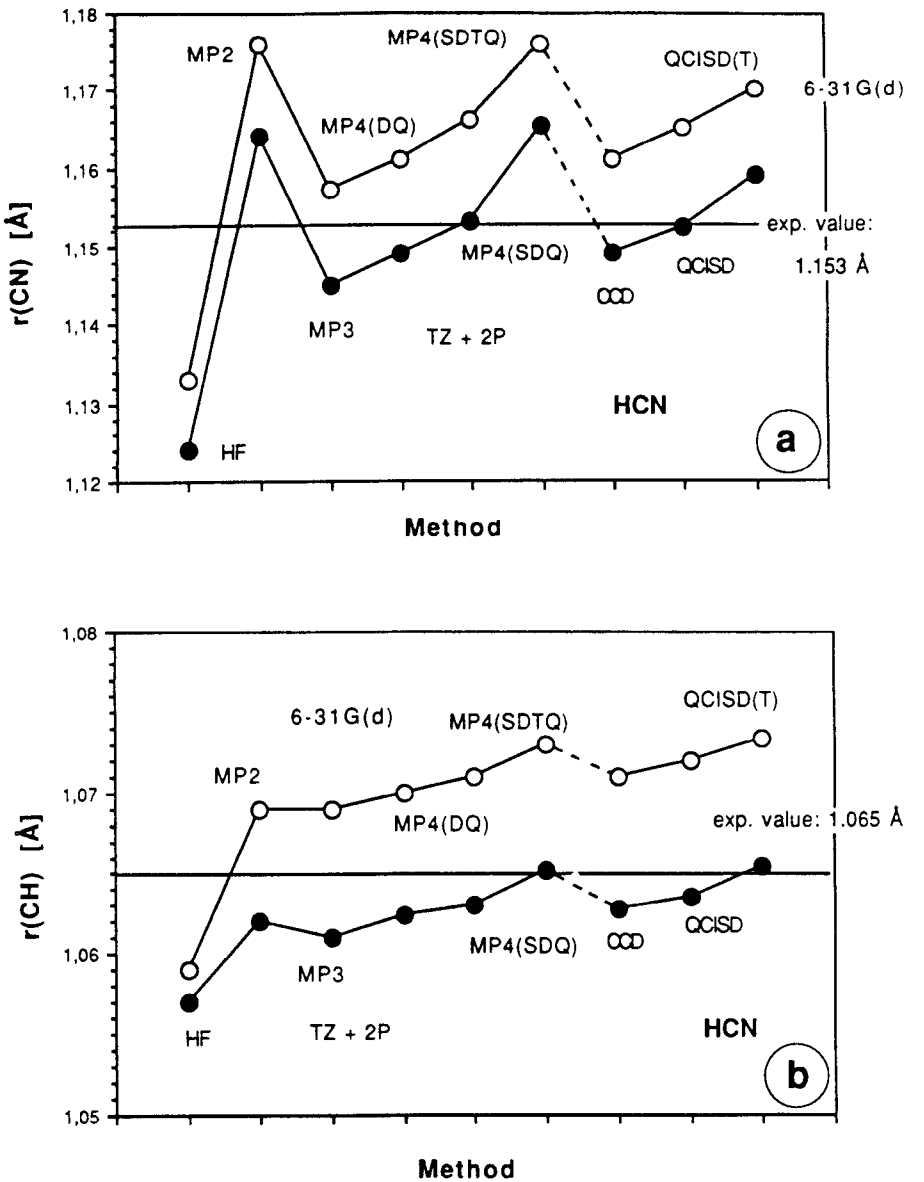

Figure 17. Dependence of calculated equilibrium geometries on method and basis set. Hydrogen cyanide, HCN: (a) CN bond length. (b) CH bond length.

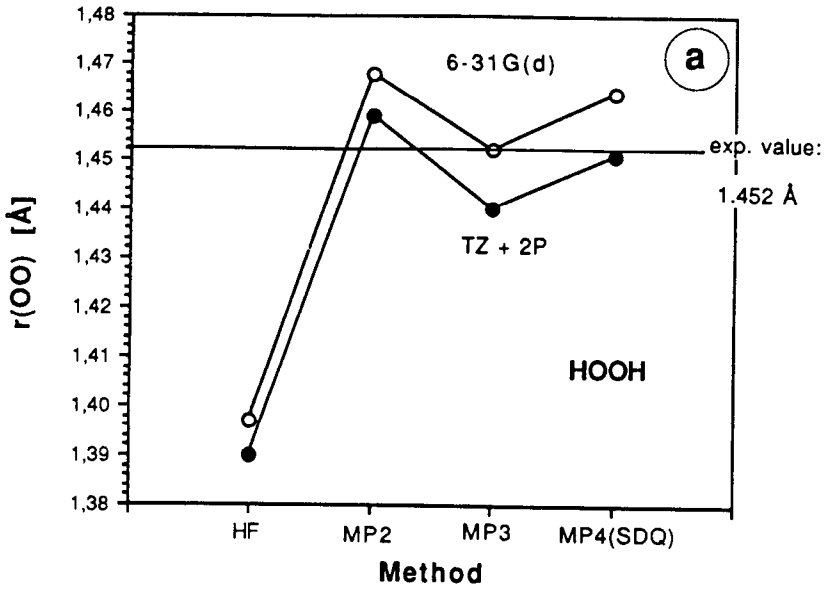

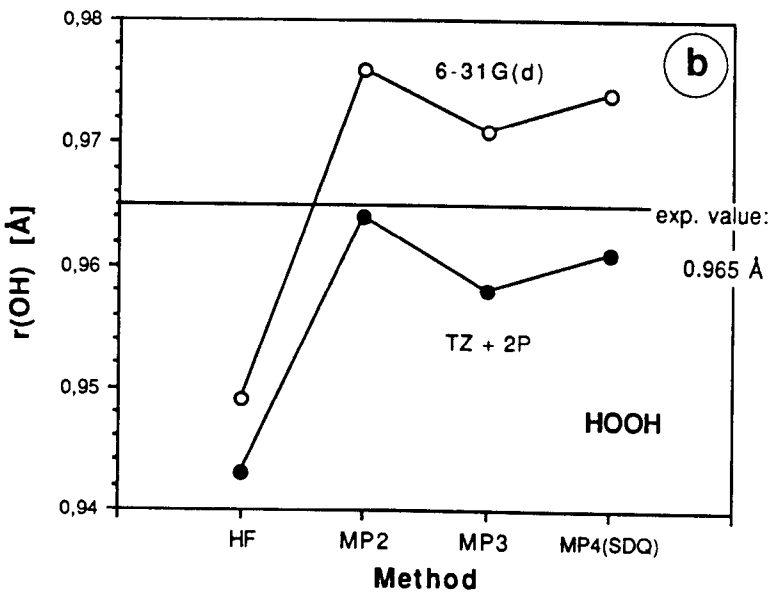

Figure 18. Dependence of calculated equilibrium geometries on method and basis set. Hydrogen peroxide, HOOH: (a) OO bond length. (b) OH bond length.

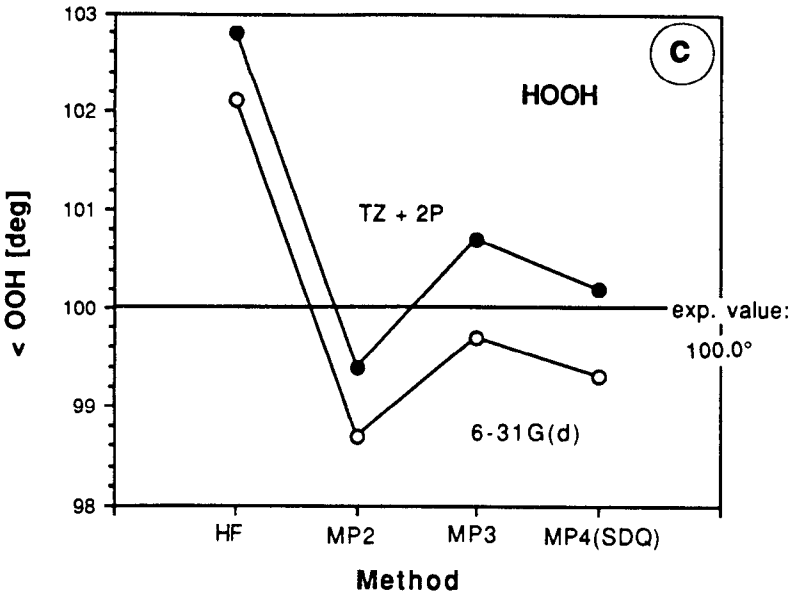

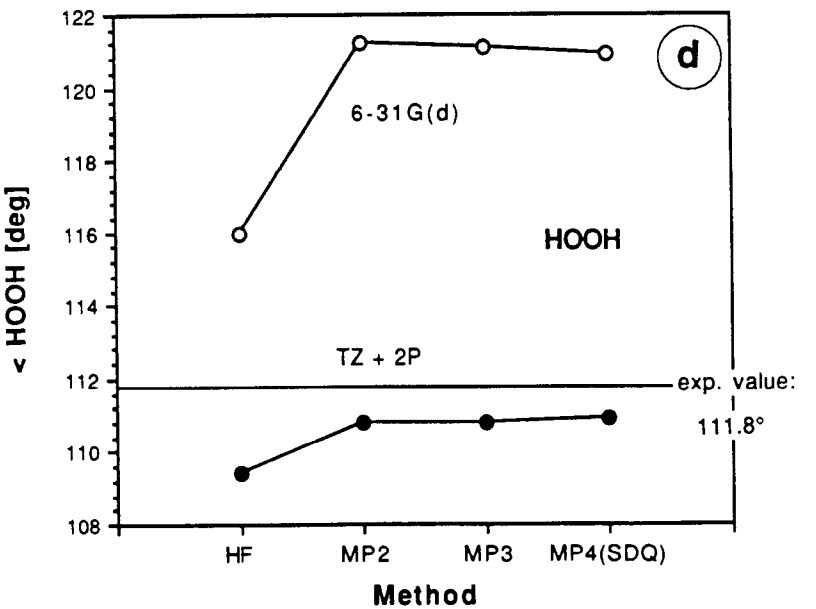

Figure 18. Dependence of calculated equilibrium geometries on method and basis set. Hydrogen peroxide, HOOH: (c) OOH bond angle. (d) HOOH dihedral angle.

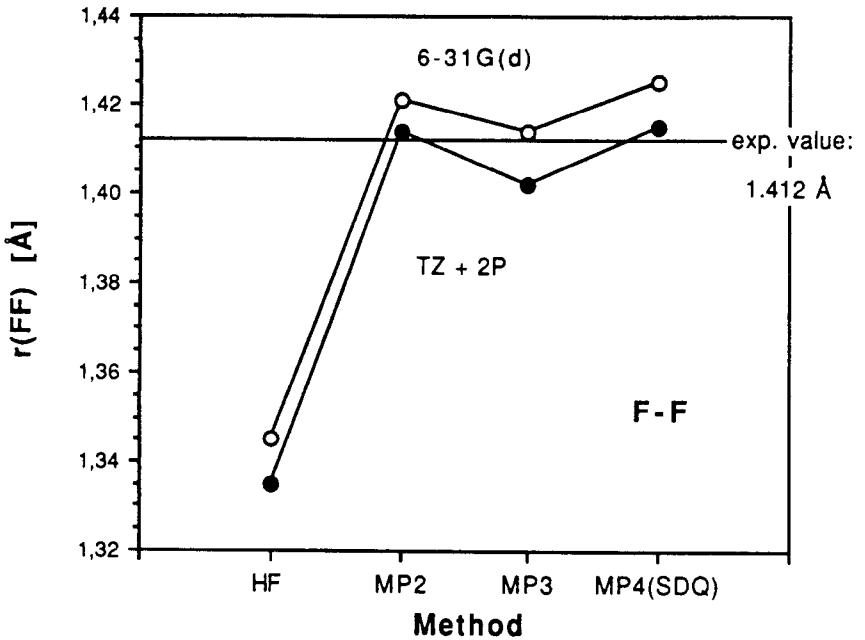

Figure 19. Dependence of calculated equilibrium geometries on method and basis set. F_2: FF bond length.

results underline the necessity of using a TZ+2P basis set to obtain accurate geometrical parameters. Previous investigations that have stressed the accuracy of MP3 or MP2 results [120] are misleading since they were due to a fortuitous cancellation of basis set and correlation errors. Of course, an even higher accuracy of calculated geometrical parameters is obtained by applying higher orders of MP perturbation theory or using CC or QCI methods.

For HCN (Figure 17), results obtained with methods that account for T effects, namely MP4(SDTQ) and QCISD(T), are also shown. It is well-known that T effects are important in the case of multiple bonds [119] and, therefore, one would expect an improvement of calculated geometries when going from MP4(SDQ) to MP4(SDTQ) or from QCISD to QCISD(T). Surprisingly, this is not the case. The CN bond length is predicted too long when T excitations are included. One could interpret this result as reflecting deficiencies of the TZ+2P basis set used. On the other hand, it has been found that T effects are significantly overestimated at the MP4(SDTQ) level of theory [93]. Furthermore, a detailed analysis of QCI in terms of perturbation theory reveals that the same is true to some extent with regard to QCISD(T) results [121]. The calculated values for the CN bond length reflect this as do the results shown in Figures 9 (charge and dipole moment of CS) and 11 (dipole moment of CO). Therefore, precautions have to be taken when accounting for T effects. A more balanced assessment of T effects is obtained at the CCSD(T), QCISD(TQ), CCSD(TQ) or CCSDT level of theory [121].

In Figure 20, the computed LiH bond length in dependence of method and basis set is shown as an example of a geometrical parameter that follows not the usual trends discussed above. The 6-31G(d) values of r(LiH) increase from HF to MP4(SDQ) while the 6-311++G(d,p) values decrease in the same direction. The LiH bond possesses partial ionic character according to the charge distribution Li^+H^-. At the HF/6-311++G(d,p) level of theory the ionicity of the LiH bond is exaggerated leading to a rather long bond distance of 1.61 Å(see Figure 20). At the MP level covalent biradical structures $Li^{\cdot}H^{\cdot}$ are mixed into the ground state wave function thus leading to a shorter bond length close to the experimental value (Figure 20). Clearly, the 6-31G(d) basis set is not sufficient to describe these changes correctly. This basis assigns 15 basis functions to Li and just 2 to H even though both atoms possess the same number of electrons (2) in an ionic structure, and, therefore, leads to an unbalanced description of the electron density distribution.

In summary all trends in calculated equilibrium geometries can be easily understood on the basis of changes in the response densities and on the basis of simple electrostatic models. As with other response properties, at

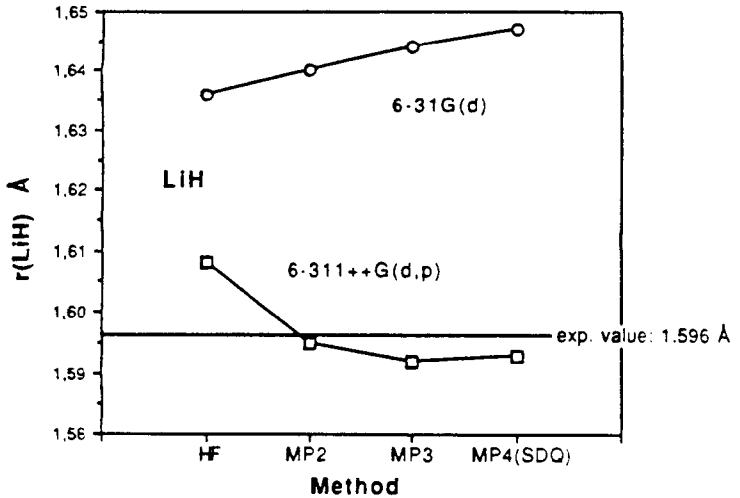

Figure 20. Dependence of calculated equilibrium geometries on method and basis set. LiH bond length.

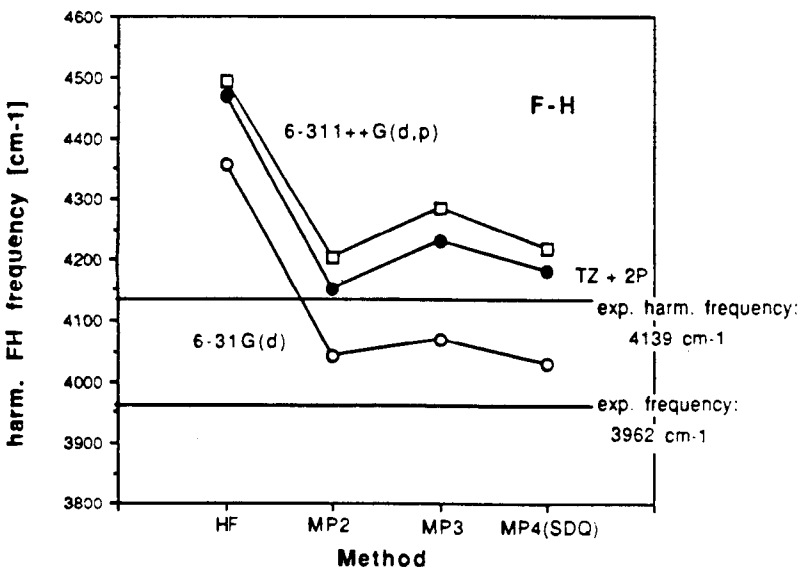

Figure 21. Dependence of calculated harmonic frequencies on method and basis set. FH stretching frequency.

least MP4(SDQ) and a TZ+P basis set is required to calculate accurate geometrical parameters.

5.3 Vibrational Spectra

In Figures 21, 22, 23, and 24 calculated harmonic frequencies ω of FH, H_2O, NH_3, and CH_4 are compared with experimental ones. Clearly, the theoretical ω values reflect a strong dependence on the computed equilibrium geometries.

(1) A short (long) bond length implies a large (small) value for the corresponding stretching frequency(ies) (compare Figures 13a and 21, 13b, 22a, and 22b, 13d and 23a, 13f and 24a).

(2) A large (small) bond angle, which can be considered to be the result of a short (large) bond length, implies a large (small) value of the corresponding bending frequency(ies) (compare Figures 13c and 22c, 13e, 23b, and 23c).

The harmonic frequency is proportional to the curvature of the potential surface at the equilibrium geometry in the direction of the corresponding internal coordinate. Therefore, on first sight it may be surprising that calculated frequencies directly depend on the theoretical values of the geometrical parameters. However, the potential surface in the direction of a bond distance AB (AH) becomes steeper if the AB (AH) distance is shortened and, hence, the corresponding bond strengthened. Accordingly, the stretching frequencies increase with a shortening of the bond. Widening of an angle ABC (HAH), on the other hand, indicates that there is increased electrostatic repulsion between A and C (or the H atoms) which makes the angle stiffer and, thereby, increases the bending frequency.

Figures 21 - 24 also show that MP4(SDQ)/TZ+2P is not sufficient to get accurate harmonic frequencies. In most cases calculated values are still too large. Obviously, higher order correlation effects have to be included to improve the accuracy of calculated values.

Finally, in Figure 25 theoretical and experimental IR intensities of the three vibrational modes of H_2O are compared. Since, there are not so many accurately determined IR intensities available from experiment the discussion is limited here to one example. This example, however, shows that agreement of calculated data with experimental values is even poorer as in the case of the harmonic frequencies. HF intensities are too large by up to 50 km/mol and more. Stepwise inclusion of correlation effects leads to a continuous decrease of intensities. Similar trends are also observed for other molecules. However, dependence on method and basis set may change more strongly

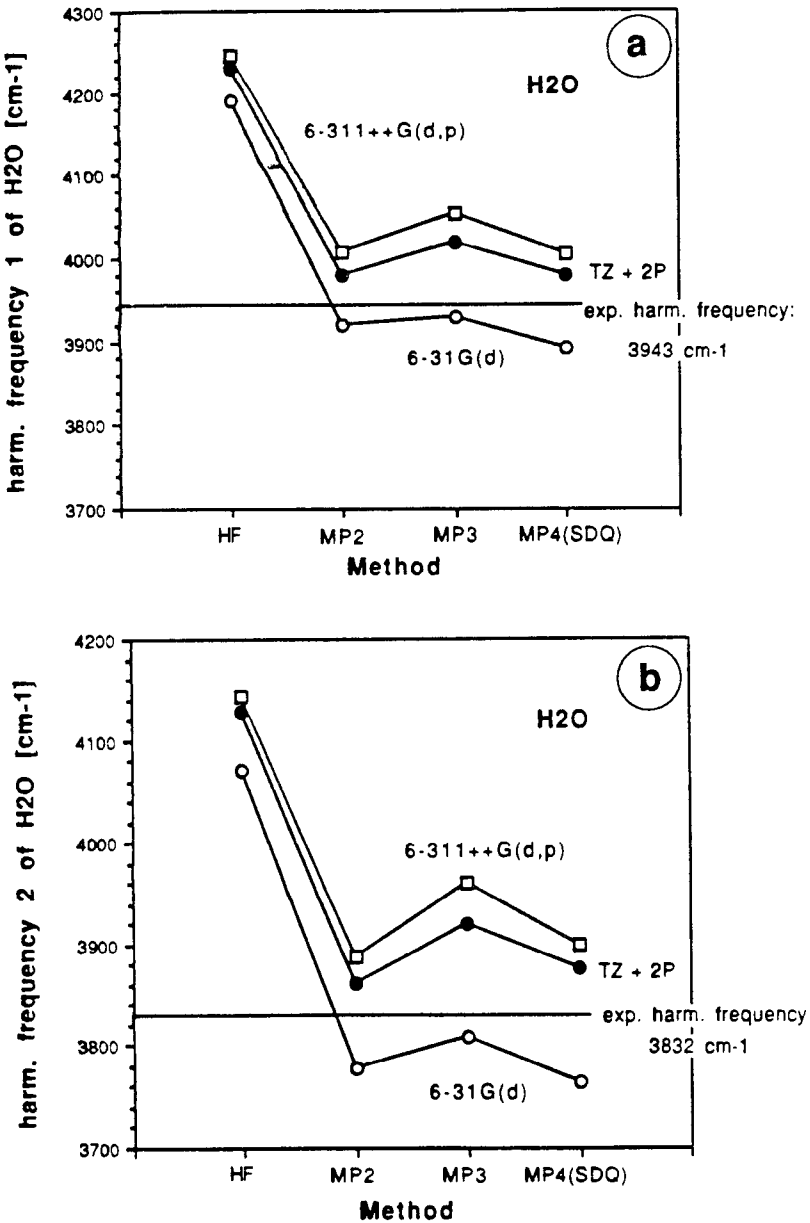

Figure 22. Dependence of calculated harmonic frequencies on method and basis set. H_2O : (a) asymmetric OH stretching frequency. (b) symmetric OH stretching frequency.

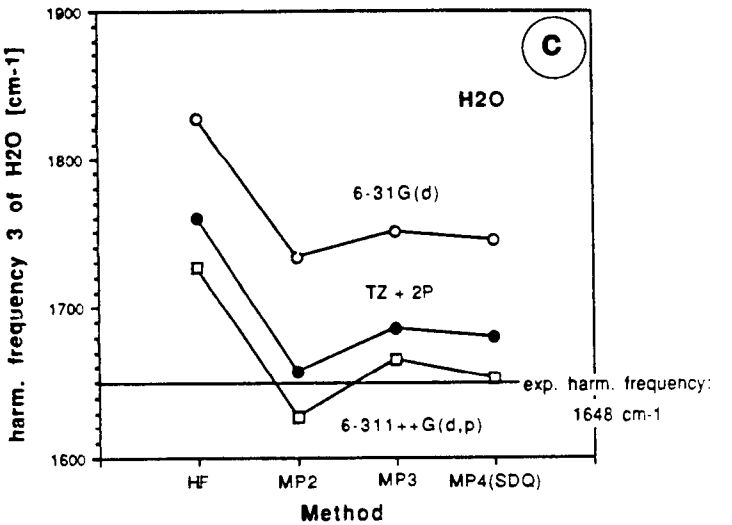

Figure 22. Dependence of calculated harmonic frequencies on method and basis set. H_2O : (c) HOH bending frequency.

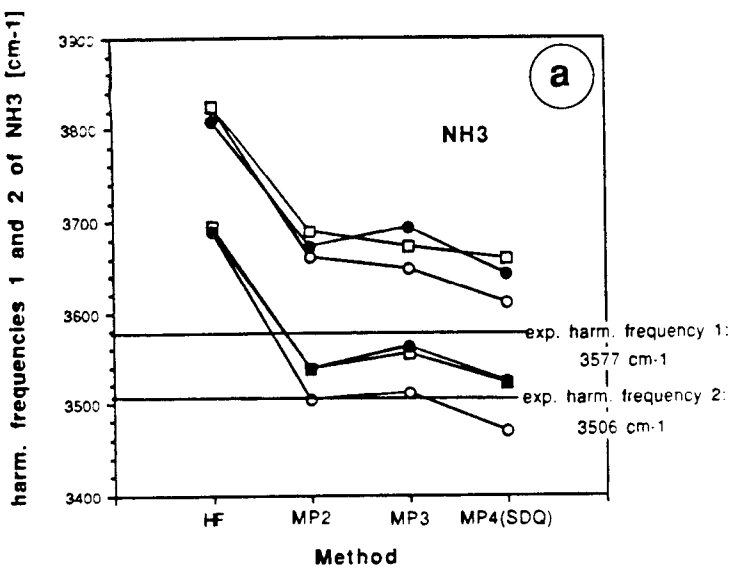

Figure 23. Dependence of calculated harmonic frequencies on method and basis set. NH_3 : (a) asymmetric and symmetric NH stretching frequency.

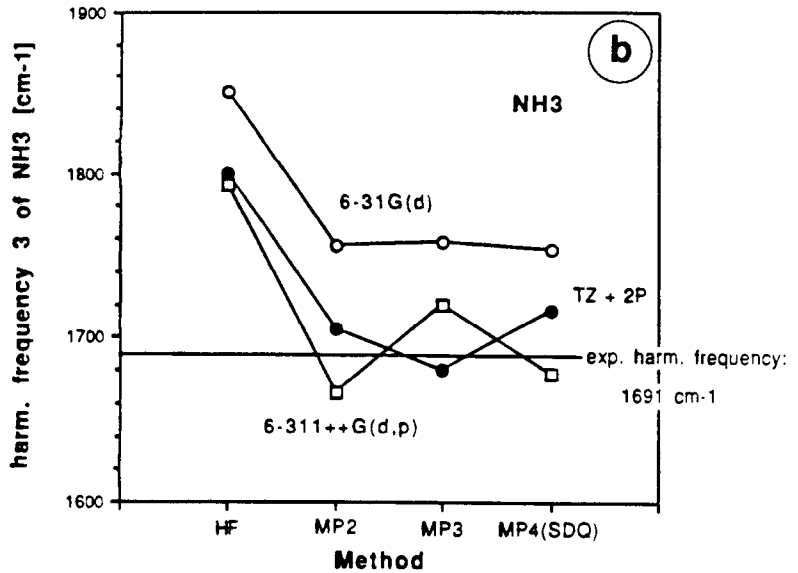

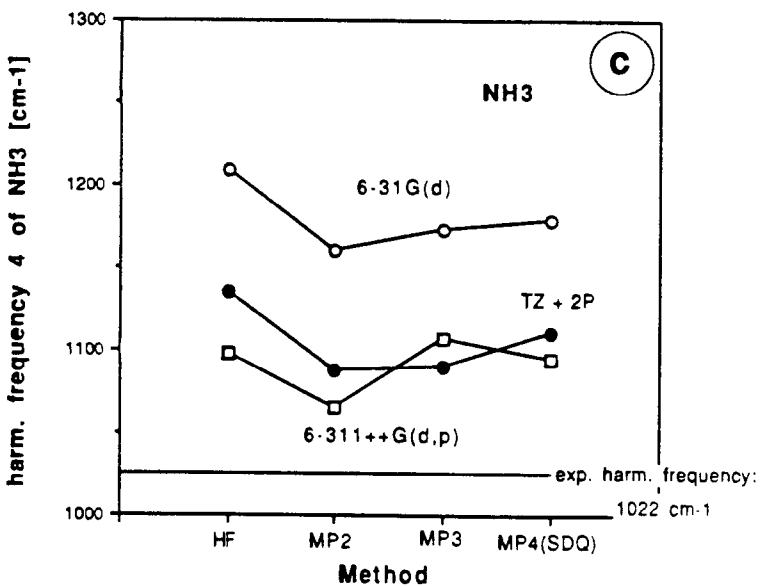

Figure 23. Dependence of calculated harmonic frequencies on method and basis set. NH_3 : (b) asymmetric HNH bending frequency. (c) symmetric HNH bending frequency.

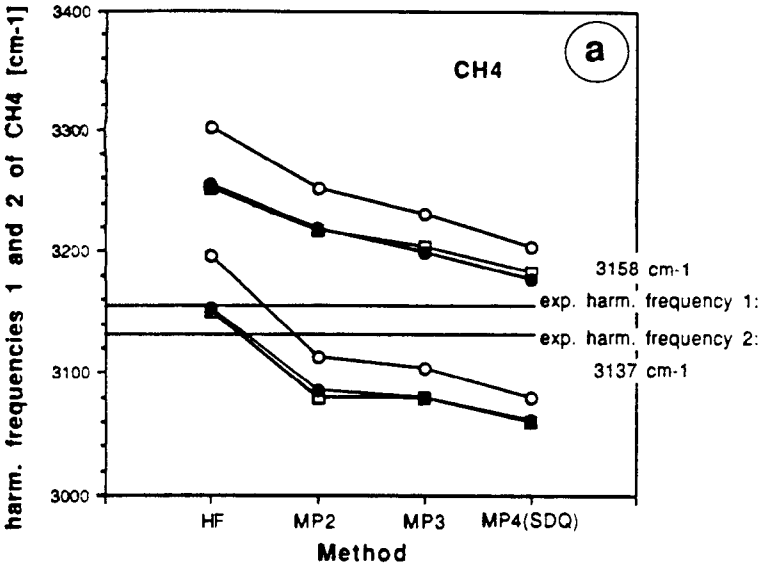

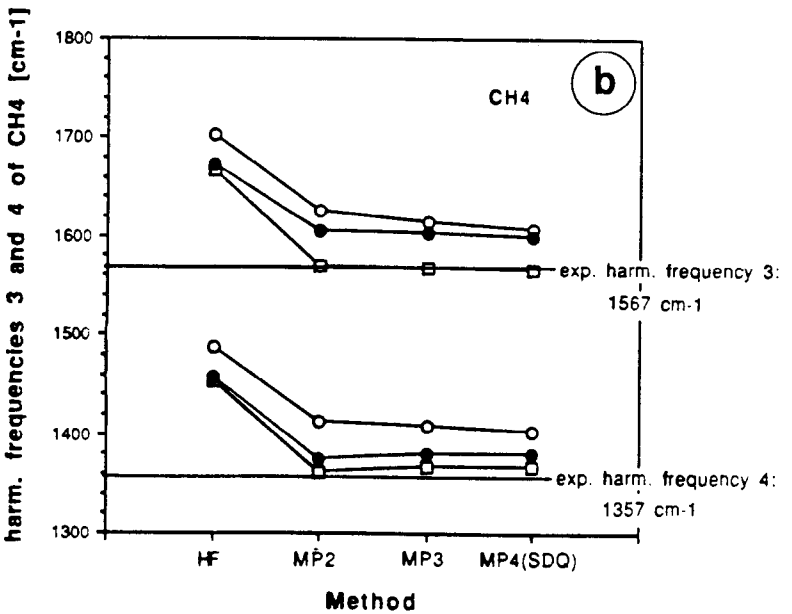

Figure 24. Dependence of calculated harmonic frequencies on method and basis set. CH_4 : (a) asymmetric and symmetric CH stretching frequency. (b) asymmetric and symmetric HCH bending frequency.

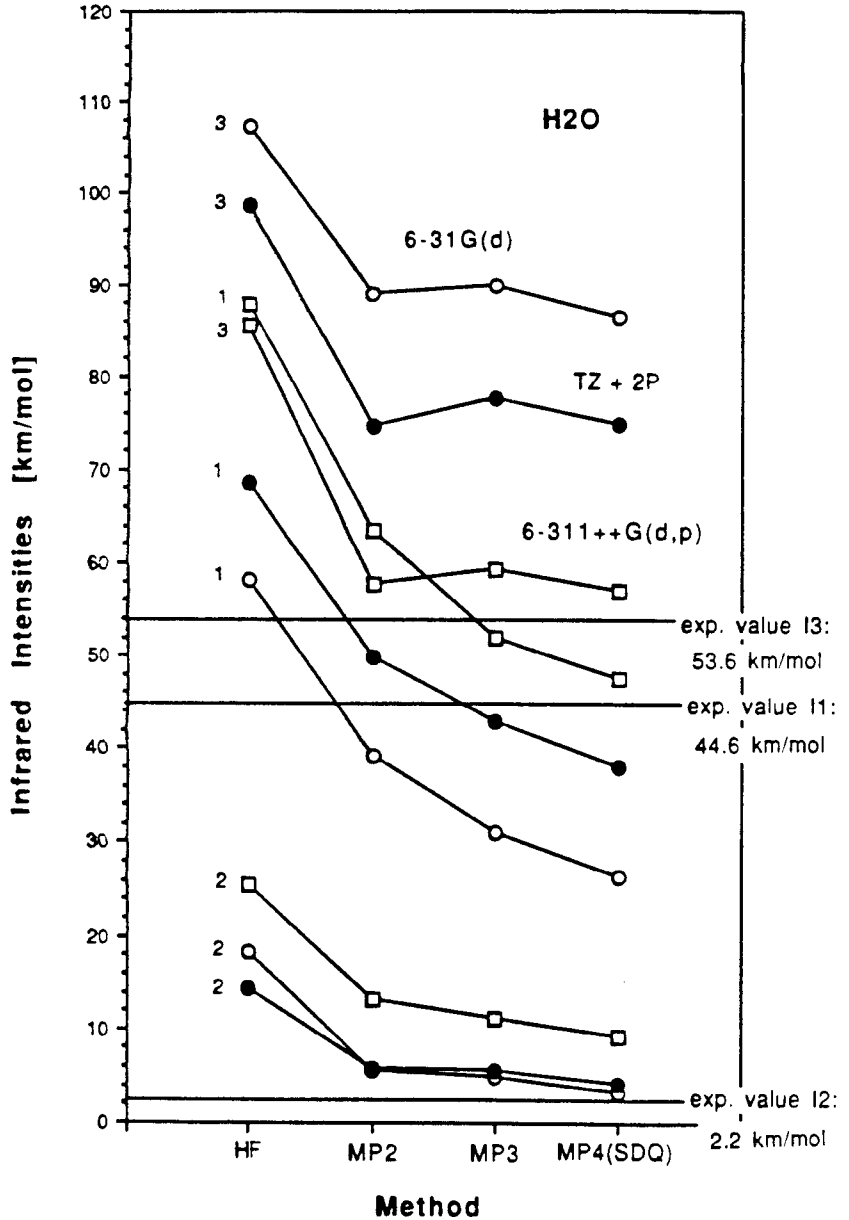

Figure 25. Dependence of calculated infra red (IR) intensities on method and basis set. H_2O.

than observed for geometrical parameters and vibrational frequencies. In any case, it seems that diffuse basis functions are probably more important than a second set of polarization functions (see Figure 25).

IR intensities are derived from dipole moment derivatives with regard to Cartesian coordinates. Assuming that dipole moment derivatives change similarly as dipole moments with method and basis set, HF and MP intensities can be discussed. At the HF level, the OH bond polarity and, thereby, the molecular dipole moment are exaggerated, obviously causing also enlarged IR intensities (Figure 25). Correlation effects reduce bond polarities and molecular dipole moment. The same is reflected by the computed IR intensities. In the case of H_2O, the best values are obtained at the MP4(SDQ)/6-311++G(d,p) level of theory. However, this may change from molecule to molecule as is shown by Figure 26 which compares calculated and experimental intensities for CH_4. Clearly, for harmonic frequencies and IR intensities it is much more difficult to predict trends in calculated ab initio data from response densities.

6. Concluding Remarks

Analytical energy gradients have opened a new avenue for the routine calculation of many molecular properties. They are particularly important for correlation corrected ab initio methods since they provide the basis for an understanding of the influence of correlation effects on calculated one-electron properties, geometries, vibrational spectra, etc.. In this article we have sketched the development of the theory of analytical gradients where we have put special emphasis on single-determinant ab initio methods. On first sight it may look as a demanding and tedious enterprise to develop for each method analytical derivatives of the molecular energy. However, as we have shown in this article, there are many similarities and relationships between the analytical derivatives for the various methods that can be used to reach a unified theory of analytical derivatives. Further developments in the area of analytical derivatives can be expected and are needed. One can predict that an important criterion of ab initio methods to be developed in the future will be the availability and the economy of analytical gradient calculations for the method in question.

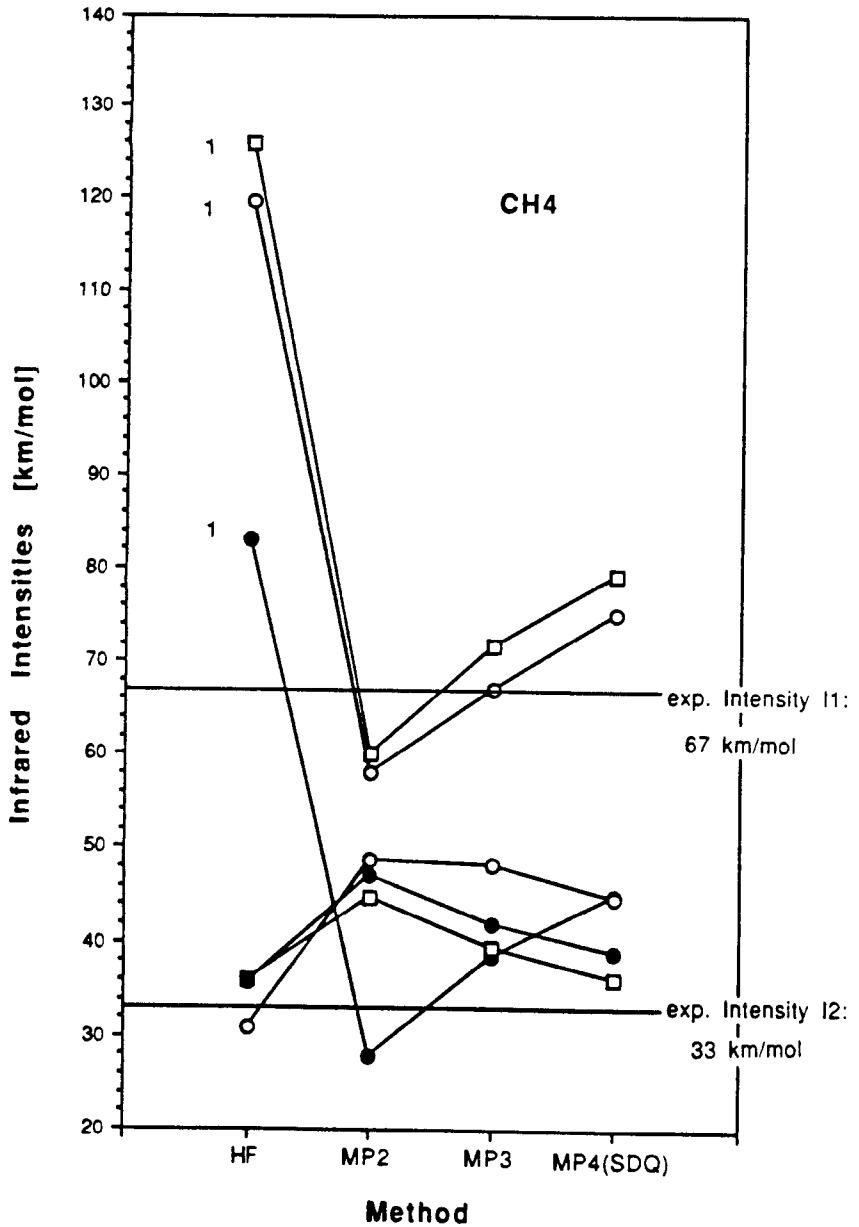

Figure 26. Dependence of calculated infra red (IR) intensities on method and basis set. CH_4.

Acknowledgement

The authors acknowledge helpful discussions with Dr. Elfi Kraka and Mrs. Zhi He. This work was supported by the Swedish Natural Science Research Council (NFR), Stockholm, Sweden. Calculations have been carried out with the CRAY XMP/48 of the Nationellt Superdatorcentrum (NSC), Linköping, Sweden. DC thanks the NSC for a generous allotment of computer time.

Appendix 1

The B and C terms in the CPQCISD equations are given by [72] :

$$B_i^{a(\lambda)} = -\sum_b \frac{\partial \varepsilon_{ab}}{\partial \lambda} a_i^b + \sum_j \frac{\partial \varepsilon_{ij}}{\partial \lambda} a_j^a + \sum_j \sum_b \frac{\partial \langle ja \| ib \rangle}{\partial \lambda} a_j^b + \frac{1}{2} \sum_j \sum_{b,c} \frac{\partial \langle ja \| bc \rangle}{\partial \lambda} a_{ij}^{bc} + \frac{1}{2} \sum_{j,k} \sum_b \frac{\partial \langle jk \| ib \rangle}{\partial \lambda} a_{jk}^{ab} - \frac{1}{2} \sum_{j,k} \sum_{b,c} \frac{\partial \langle jk \| bc \rangle}{\partial \lambda} \{a_i^b a_{jk}^{ca} + a_j^a a_{ik}^{cb} + 2 a_j^b a_{ik}^{ac}\}, \tag{A1.1}$$

$$\begin{aligned} B_{ij}^{ab(\lambda)} = & -\frac{\partial \langle ij \| ab \rangle}{\partial \lambda} - \sum_c \{\frac{\partial \varepsilon_{ac}}{\partial \lambda} a_{ij}^{cb} + \frac{\partial \varepsilon_{bc}}{\partial \lambda} a_{ij}^{ac}\} \\ & + \sum_k \{\frac{\partial \varepsilon_{ik}}{\partial \lambda} a_{kj}^{ab} + \frac{\partial \varepsilon_{jk}}{\partial \lambda} a_{ik}^{ab}\} - \frac{1}{2} \sum_{c,d} \frac{\partial \langle ab \| cd \rangle}{\partial \lambda} a_{ij}^{cd} - \frac{1}{2} \sum_{k,l} \frac{\partial \langle kl \| ij \rangle}{\partial \lambda} a_{kl}^{ab} \\ & + \sum_k \sum_c \{\frac{\partial \langle kb \| jc \rangle}{\partial \lambda} a_{ik}^{ac} + \frac{\partial \langle ka \| jc \rangle}{\partial \lambda} a_{jk}^{cb} + \frac{\partial \langle kb \| ic \rangle}{\partial \lambda} a_{kj}^{ac} + \frac{\partial \langle ka \| ic \rangle}{\partial \lambda} a_{kj}^{cb}\} \\ & - \frac{1}{4} \sum_{k,l} \sum_{c,d} \frac{\partial \langle kl \| cd \rangle}{\partial \lambda} \{a_{ij}^{cd} a_{kl}^{ab} - 2[a_{ij}^{ac} a_{kl}^{bd} + a_{ij}^{bd} a_{kl}^{ac}] \\ & \qquad - 2[a_{ik}^{ab} a_{jl}^{cd} + a_{ik}^{cd} a_{jl}^{ab}] + 4[a_{ik}^{ac} a_{jl}^{bd} + a_{ik}^{bd} a_{jl}^{ac}]\} \\ & - \sum_c \{\frac{\partial \langle ab \| cj \rangle}{\partial \lambda} a_i^c - \frac{\partial \langle ab \| ci \rangle}{\partial \lambda} a_j^c\} \\ & - \sum_k \{-\frac{\partial \langle kb \| ij \rangle}{\partial \lambda} a_k^a + \frac{\partial \langle ka \| ij \rangle}{\partial \lambda} a_k^b\}, \end{aligned} \tag{A1.2}$$

$$\sum_j \sum_b C^{a,b}_{i,j} \frac{\partial a^b_j}{\partial \lambda} = (\varepsilon_a - \varepsilon_i)\frac{\partial a^a_i}{\partial \lambda} - \sum_j \sum_b \langle ja \| ib \rangle \frac{\partial a^b_j}{\partial \lambda} + \frac{1}{2} \sum_{j,k} \sum_{b,c} \langle jk \| bc \rangle \{ a^{cd}_{jk} \frac{\partial a^b_i}{\partial \lambda} + a^{cb}_{ik} \frac{\partial a^a_j}{\partial \lambda} + 2 a^{ac}_{ik} \frac{\partial a^b_j}{\partial \lambda} \}, \tag{A1.3}$$

$$\sum_{j<k} \sum_{b<c} C^{a,bc}_{i,jk} \frac{\partial a^{bc}_{jk}}{\partial \lambda} = -\frac{1}{2} \sum_j \sum_{b,c} \langle ja \| bc \rangle \frac{\partial a^{bc}_{ij}}{\partial \lambda} - \frac{1}{2} \sum_{j,k} \sum_b \langle jk \| ib \rangle \frac{\partial a^{ab}_{jk}}{\partial \lambda} + \frac{1}{2} \sum_{j,k} \sum_{b,c} \langle jk \| bc \rangle \{ \frac{\partial a^{ca}_{jk}}{\partial \lambda} a^b_i + \frac{\partial a^{cb}_{ik}}{\partial \lambda} a^a_j + 2 \frac{\partial a^{ac}_{ik}}{\partial \lambda} a^b_j \}, \tag{A1.4}$$

$$\sum_k \sum_c C^{ab,c}_{ij,k} \frac{\partial a^c_k}{\partial \lambda} = \sum_c \{ \langle ab \| cj \rangle \frac{\partial a^c_i}{\partial \lambda} - \langle ab \| ci \rangle \frac{\partial a^c_j}{\partial \lambda} \} + \sum_k \{ -\langle kb \| ij \rangle \frac{\partial a^a_k}{\partial \lambda} + \langle ka \| ij \rangle \frac{\partial a^b_k}{\partial \lambda} \}, \tag{A1.5}$$

$$\begin{aligned} \sum_{k<l} \sum_{c<d} C^{ab,cd}_{ij,kl} \frac{\partial a^{cd}_{kl}}{\partial \lambda} &= (\varepsilon_a + \varepsilon_b - \varepsilon_i - \varepsilon_j) \frac{\partial a^{ab}_{ij}}{\partial \lambda} + \frac{1}{2} \sum_{c,d} \langle ab \| cd \rangle \frac{\partial a^{cd}_{ij}}{\partial \lambda} \\ &+ \frac{1}{2} \sum_{k,l} \langle kl \| ij \rangle \frac{\partial a^{ab}_{kl}}{\partial \lambda} - \sum_k \sum_c \{ \langle kb \| jc \rangle \frac{\partial a^{ac}_{ik}}{\partial \lambda} \\ &+ \langle ka \| jc \rangle \frac{\partial a^{cb}_{ik}}{\partial \lambda} + \langle kb \| ic \rangle \frac{\partial a^{ac}_{kj}}{\partial \lambda} + \langle ka \| ic \rangle \frac{\partial a^{cb}_{kj}}{\partial \lambda} \} \\ &+ \frac{1}{4} \sum_{k,l} \sum_{c,d} \langle kl \| cd \rangle \{ \frac{\partial a^{cd}_{ij}}{\partial \lambda} a^{ab}_{kl} + a^{cd}_{ij} \frac{\partial a^{ab}_{kl}}{\partial \lambda} \\ &- 2[a^{ac}_{ij} \frac{\partial a^{bd}_{kl}}{\partial \lambda} + a^{bd}_{ij} \frac{\partial a^{ac}_{kl}}{\partial \lambda} + \frac{\partial a^{ac}_{ij}}{\partial \lambda} a^{bd}_{kl} + \frac{\partial a^{bd}_{ij}}{\partial \lambda} a^{ac}_{kl}] \\ &- 2[a^{ab}_{ik} \frac{\partial a^{cd}_{jl}}{\partial \lambda} + a^{cd}_{ik} \frac{\partial a^{ab}_{jl}}{\partial \lambda} + \frac{\partial a^{ab}_{ik}}{\partial \lambda} a^{cd}_{jl} + \frac{\partial a^{cd}_{ik}}{\partial \lambda} a^{ab}_{jl}] \\ &+ 4[a^{ac}_{ik} \frac{\partial a^{bd}_{jl}}{\partial \lambda} + a^{bd}_{ik} \frac{\partial a^{ac}_{jl}}{\partial \lambda} + \frac{\partial a^{ac}_{ik}}{\partial \lambda} a^{bd}_{jl} + \frac{\partial a^{bd}_{ik}}{\partial \lambda} a^{ac}_{jl}] \}, \end{aligned} \tag{A1.6}$$

The final z-vector equations within QCISD theory are given by

$$(\varepsilon_a - \varepsilon_i) z^a_i + w[z]^a_i + v[z]^a_i = 0 \tag{A1.7}$$

and

$$(\varepsilon_a + \varepsilon_b - \varepsilon_i - \varepsilon_j) z^{ab}_{ij} + w[z]^{ab}_{ij} + v[z]^{ab}_{ij} + y[z]^{ab}_{ij} = \langle ij \| ab \rangle, \tag{A1.8}$$

that means by a form which is very similar to the original QCISD equations. The arrays $w[z]^a_i$ and $w[z]^{ab}_{ij}$ are very similar to the arrays w^a_i and w^{ab}_{ij}. The only difference is that while w^a_i and w^{ab}_{ij} are calculated using the amplitudes a^a_i and a^{ab}_{ij} the arrays $w[z]^a_i$ and $w[z]^{ab}_{ij}$ are evaluated using the z-amplitudes z^a_i and z^{ab}_{ij} :

$$w[z]^a_i = -\sum_j \sum_b \langle ja \| ib \rangle z^b_i - \frac{1}{2} \sum_j \sum_{b,c} \langle ja \| bc \rangle z^{bc}_{ij} - \frac{1}{2} \sum_{j,k} \sum_b \langle jk \| ib \rangle z^{ab}_{jk}, \tag{A1.9}$$

$$\begin{aligned} w[z]^{ab}_{ij} &= \sum_c \{ \langle ab \| cj \rangle z^c_i - \langle ab \| ci \rangle z^c_j \} + \sum_k \{ -\langle kb \| ij \rangle z^a_k + \langle ka \| ij \rangle z^b_k \} \\ &+ \frac{1}{2} \sum_{c,d} \langle ab \| cd \rangle z^{cd}_{ij} + \frac{1}{2} \sum_{k,l} \langle kl \| ij \rangle z^{ab}_{kl} - \sum_k \sum_c \{ \langle kb \| jc \rangle z^{ac}_{ik} \\ &+ \langle ka \| jc \rangle z^{cb}_{ik} + \langle kb \| ic \rangle z^{ac}_{kj} + \langle ka \| ic \rangle z^{cb}_{kj} \}. \end{aligned} \tag{A1.10}$$

The array $v[z]^a_i$ is obtained from v^a_i by substituting the two-electron integrals by the double excitation amplitudes a^{ab}_{ij}, the double excitation amplitudes by the two-electron integrals $\langle ij \| ab \rangle$ and by replacing the single excitation amplitudes a^a_i by z^a_i :

$$v[z]^a_i = \frac{1}{2} \sum_{j,k} \sum_{b,c} a^{bc}_{jk} \{ z^b_i \langle jk \| ca \rangle + z^a_j \langle ik \| cb \rangle + 2 z^b_j \langle ik \| ac \rangle \}. \tag{A1.11}$$

The array $v[z]^{ab}_{ij}$ is derived in a similar way from the quadratic array v^{ab}_{ij} :

$$\begin{aligned} v[z]^{ab}_{ij} &= \frac{1}{4} \sum_{k,l} \sum_{c,d} a^{cd}_{kl} \{ \langle ij \| cd \rangle z^{ab}_{kl} + z^{cd}_{ij} \langle kl \| ab \rangle \\ &- 2[\langle ij \| ac \rangle z^{bd}_{kl} + \langle ij \| bd \rangle z^{ac}_{kl} + z^{ac}_{ij} \langle kl \| bd \rangle + z^{bd}_{ij} \langle kl \| ac \rangle] \\ &- 2[\langle ik \| ab \rangle z^{cd}_{jl} + \langle ik \| cd \rangle z^{ab}_{jl} + z^{ab}_{ik} \langle jl \| cd \rangle + z^{cd}_{ik} \langle jl \| ab \rangle] \\ &+ 4[\langle ik \| ac \rangle z^{bd}_{jl} + \langle ik \| bd \rangle z^{ac}_{jl} + z^{ac}_{ik} \langle jl \| bd \rangle + z^{bd}_{ik} \langle jl \| ac \rangle] \}. \end{aligned} \tag{A1.12}$$

The only new term in the z-vector equations in comparision with the original QCISD equation is the array $y[z]_{ij}^{ab}$ which is defined as

$$y[z]_{ij}^{ab} = \sum_k \sum_c a_k^c \{\langle ij\|ca\rangle z_k^b + \langle ij\|bc\rangle z_k^a + \langle kj\|ba\rangle z_i^c + \langle ik\|bc\rangle z_j^c + \langle kj\|cb\rangle z_i^a + \langle kj\|ac\rangle z_i^b + \langle ik\|cb\rangle z_j^a + \langle ik\|ac\rangle z_j^b\}. \quad \text{(A1.13)}$$

There is no corresponding term to $y[z]_{ij}^{ab}$ in the QCISD equations. This is because the excitations $\mathbf{T_1 T_2}$ are only included in the equations for the singles, but not considered in the equations for the doubles.

Appendix 2

Here, formulas for the arrays X_1, X_2, ... ,X_6, Y_1, and Y_2 are given.

$$\text{MP2}: X_1^{MP2}(ijab) = \frac{1}{2}a(ij,ab)$$

$$Y_1^{MP2}(ij) = -\frac{1}{2}\sum_k \sum_{a,b} a(ik,ab)a(jk,ab)$$

$$Y_2^{MP2}(ab) = \frac{1}{2}\sum_{i,j} \sum_c a(ij,ac)a(ij,bc)$$

$$\text{MP3}: X_1^{MP3}(ij,ab) = \frac{1}{2}d(ij,ab)$$

$$X_2^{MP3}(ijkl) = \frac{1}{8}\sum_{a,b} a(ij,ab)a(kl,ab)$$

$$X_3^{MP3}(iajb) = -\sum_k \sum_c a(jk,ac)a(ik,bc)$$

$$X_4^{MP3}(abcd) = \frac{1}{8}\sum_{i,j} a(ij,ab)a(ij,cd)$$

$$Y_1^{MP3}(ij) = -\frac{1}{2}\sum_k \sum_{a,b} \{a(ik,ab)d(jk,ab) + d(ik,ab)a(jk,ab)\}$$

$$Y_2^{MP3}(ab) = \frac{1}{2}\sum_{i,j} \sum_c \{a(ij,ac)d(ij,bc) + d(ij,ac)a(ij,bc)\}$$

$$\text{MP4}: X_1^{MP4}(ij,ab) = \frac{1}{2}\{e(ij,ab) + x(ij,ab)\}$$

$$X_2^{MP4}(ijkl) = \frac{1}{8}\sum_{a,b} \{a(ij,ab)d(kl,ab) + d(ij,ab)a(kl,ab)\}$$

$$X_3^{MP4}(iajb) - \sum_k \sum_c \{a(jk,ac)d(ik,bc) + d(jk,ac)a(ik,bc)\}$$

$$X_4^{MP4}(abcd) = \frac{1}{8}\sum_{i,j} \{a(ij,ab)d(ij,cd) + d(ij,ab)a(ij,cd)\}$$

$$X_5^{MP4}(ijka) = -\sum_b d(k,b)a(ij,ba) + 2r(ijk,a)$$

$$X_6^{MP4}(iabc) = \sum_j d(j,a)a(ji,bc) + 2s(i,abc)$$

$$Y_1^{MP4}(ij) = -\frac{1}{2}\sum_k \sum_{a,b} \{a(ik,ab)[e(jk,ab) + \frac{1}{2}x(jk,ab)] + [e(ik,ab) + \frac{1}{2}x(ik,ab)a(jk,ab)\}$$
$$- \sum_a d(i,a)d(j,a) - \frac{1}{2}\sum_k \sum_{a,b} d(ik,ab)d(jk,ab)$$
$$-\frac{1}{12}\sum_{k,l} \sum_{a,b,c} d(ikl,abc)d(jkl,abc)$$

$$Y_2^{MP4}(ab) = \frac{1}{2}\sum_{i,j} \sum_c \{a(ij,ac)[e(ij,bc) + \frac{1}{2}x(ij,bc)] + [e(ij,ac) + \frac{1}{2}x(ij,ac)]a(ij,bc)\}$$
$$+ \sum_i d(i,a)d(i,b) + \frac{1}{2}\sum_{i,j} \sum_c cd(ij,ac)d(ij,bc)$$
$$+\frac{1}{12}\sum_{i,j,k} \sum_{c,d} d(ijk,acd)d(ijk,bcd)$$

$$\text{QCISD}: X_1^{QCISD}(ijab) = \frac{1}{4}\{a_{ij}^{ab} - z_{ij}^{ab} - x_{ij}^{ab}\}$$

$$X_2^{QCISD}(ijkl) = -\frac{1}{16}\sum_{a,b}\{z_{ij}^{ab}a_{kl}^{ab} + z_{kl}^{ab}a_{ij}^{ab}\}$$

$$X_3^{QCISD}(iajb) = \frac{1}{2}\sum_{k}\sum_{c}\{a_{jk}^{ac}z_{ik}^{bc} + z_{jk}^{ac}a_{ik}^{bc}\} + \frac{1}{2}\{z_i^b a_j^a + a_i^b z_j^a\}$$

$$X_4^{QCISD}(abcd) = -\frac{1}{16}\sum_{i,j}\{z_{ij}^{ab}a_{ij}^{cd} + z_{ij}^{cd}a_{ij}^{ab}\}$$

$$X_5^{QCISD}(ijka) = \frac{1}{2}\sum_{b}\{a_{ij}^{ba}z_k^b + z_{ij}^{ba}a_k^b\}$$

$$X_6^{QCISD}(iabc) = \frac{1}{2}\sum_{j}\{a_{ji}^{bc}z_j^a + z_{ji}^{bc}a_k^b\}$$

$$Y_1^{QCISD}(ij) = -\frac{1}{2}\sum_{a}\{a_i^a z_j^a + a_j^a z_i^a\} - \frac{1}{4}\sum_{k}\sum_{a,b}\{a_{ik}^{ab}z_{jk}^{ab} + z_{ik}^{ab}a_{jk}^{ab}\}$$

$$Y_2^{QCISD}(ab) = \frac{1}{2}\sum_{i}\{a_i^a z_i^b + z_i^a a_i^b\} + \frac{1}{4}\sum_{i,j}\sum_{c}\{a_{ij}^{ac}z_{ij}^{bc} + z_{ij}^{ac}a_{ij}^{bc}\}$$

$$\text{QCISD(T)}: X_1^{QCISD(T)}(ijab) = X_1^{QCISD}(ijab) + \frac{1}{2}u_{ij}^{ab}$$

$$X_2^{QCISD(T)}(ijkl) = X_2^{QCISD}(ijkl)$$

$$X_3^{QCISD(T)}(iajb) = X_3^{QCISD}(iajb)$$

$$X_4^{QCISD(T)}(abcd) = X_4^{QCISD}(abcd)$$

$$X_5^{QCISD(T)}(ijka) = X_5^{QCISD}(ijka) + 2r_{ijk}^a$$

$$X_6^{QCISD(T)}(iabc) = X_6^{QCISD}(iabc) + 2s_i^{abc}$$

$$Y_1^{QCISD(T)}(ij) = Y_1^{QCISD}(ij) + \frac{1}{24}\sum_{k,l}\sum_{a,b,c}\{d_{ijk}^{acd}[d_{ijk}^{bcd} + \tilde{d}_{ijk}^{bcd}] + d_{jkl}^{abc}[d_{ikl}^{abc} + \tilde{d}_{ikl}^{abc}]\}$$

$$Y_2^{QCISD(T)}(ab) = Y_2^{QCISD}(ab) + \frac{1}{24}\sum_{i,j,k}\sum_{c,d}\{d_{ijk}^{acd}[d_{ijk}^{bcd} + \tilde{d}_{ijk}^{bcd}] + d_{ijk}^{bcd}[d_{ijk}^{acd} + \tilde{d}_{ijk}^{acd}]\}.$$

All formulas are given here in such a way that symmetries between the four indices p, q, r, and s of the corresponding integral derivative can be used. For example, in the case of the integral $\langle ij\|ab\rangle$ the following symmetry relations hold

$$\langle ij\|ab\rangle = -\langle ji\|ab\rangle = -\langle ij\|ba\rangle = \langle ji\|ba\rangle$$

and in the same way

$$X_1(ijab) = -X_1(jiab) = -X_1(ijba) = X_1(jiba).$$

References

[1] See, e.g. (a) H.F. Schaefer III, *Quantum Chemistry, the Development of Ab initio Methods in Molecular Electronic Structure Theory* (Clarendon Press, Oxford, 1984); (b) C.E. Dykstra, *Ab initio Calculations of the Structures and Properties of Molecules* (Elsevier, Amsterdam, 1988); (c) R.S. Mulliken and W.C. Ermler, *Polyatomic Molecules, Results of ab initio Calculations* (Academic Press, New York, 1981); (d) R.S. Mulliken and W.C. Ermler, *Diatomic Molecules, Results of ab initio Calculations* (Academic Press, New York, 1977)

[2] See, for example, *Theoret. Chim. Acta* **71** (1987) 89 - 245 ; **72** (1987) 71-173, where papers from the Symposium on Computational Quantum Chemistry and Parallel Processors held in Edmonton, Canada, were published.

[3] W.J. Hehre, L. Radom, P.v. R. Schleyer, and J.A. Pople. *Ab Initio Molecular Orbital Theory* (Wiley, New York, 1986).

[4] P.Jørgensen and J. Simons, eds. *Geometrical Derivatives of Energy Surfaces and Molecular Properties* (Reidel, Dordrecht, 1986).

[5] (a) H.F. Schaefer and Y. Yamaguchi *J. Mol. Struct. (THEOCHEM)* **135** (1986) 369; (b) P. Pulay, *Adv. Quant. Chem.* **67** (1987) 241.

[6] H.B. Schlegel, *Adv. Quant. Chem.* **67** (1987) 249.

[7] B.A. Hess Jr., L.J. Schaad, P. Carsky, and R. Zahradnik, *Chem. Rev.* **86** (1986) 709.

[8] J.F. Gaw and N.C. Handy in *Geometrical Derivatives of Energy Surfaces and Molecular Properties*,P.Jørgensen and J. Simons, eds. (Reidel, Dordrecht, 1986), p. 79.

[9] R.D. Amos, *Adv. Quant. Chem.* **67** (1987) 99.

[10] S. Califano, *Vibrational States* (Wiley, New York, 1976).

[11] E.B. Wilson, J.C. Decius, P.C. Cross, *Molecular Vibrations* (Dover, New York, 1981).

[12] P. Pulay in *Modern Theoretical Chemistry, Vol. 3*, ed. H.F. Schaefer III (Plenum Press, New York, 1977).

[13] P. Pulay in *The Force Concept in Chemistry*, ed. B.M. Deb (van Nostrand Reinhold, New York 1983).

[14] P. Pulay, *Mol. Phys.* **17** (1969) 197.

[15] P. Pulay, *Mol. Phys.* **18** (1970) 473.

[16] H.F. King and M. Dupuis, *J. Comp. Phys.* **21** (1976) 144; M. Dupuis, J. Rys, and H.F. King, *J. Chem. Phys.* **65** (1976) 111.

[17] H.B. Schlegel, J.S. Binkley, and J.A. Pople, *J. Chem. Phys.* **80** (1984) 1976.

[18] J.A. Pople, R. Krishnan, H.B. Schlegel, and J.S. Binkley, *Intern. J. Quantum Chem. Symp.* **13** (1979) 225.

[19] R. McWeeny, *Rev. Mod. Phys.* **32** (1960) 335; R. McWeeny, *Phys.Rev.* **126** 1028.

[20] R.M. Stevens, R.M. Pitzer, and W.N. Lipscomb, *J. Chem. Phys.* **38** (1963) 550.

[21] J. Gerratt and I.M. Mills, *J. Chem. Phys.* **49** (1968) 1719.

[22] N.C. Handy and H.F. Schaefer III, *J. Chem. Phys.* **81** (1984) 5031.

[23] B.R. Brooks, W.D. Laidig, P. Saxe, J.D. Goddard, Y.Yamaguchi, and H.F. Schaefer III, *J. Chem. Phys.* **72** (1980) 4652.

[24] R. Krishnan, H.B. Schlegel, and J.A. Pople, *J. Chem. Phys.* **72** (1980) 4654.

[25] J.D. Goddard, N.C. Handy, and H.F. Schaefer III, *J. Chem. Phys.* **71** (1979) 1525.

[26] S. Kato and K. Morokuma, *Chem. Phys. Letters* **65** (1979) 19.

[27] J.F. Gaw, Y. Yamaguchi, and H.F. Schaefer III, *J. Chem. Phys.* **81** (1984) 6395.

[28] R.N. Camp, H.F. King, J.W. McIver, and D Mullally, *J. Chem. Phys.* **79** (1983) 1088.

[29] Y. Yamaguchi, Y. Osamura, G. Fitzgerald, and H.F. Schaefer III, *J. Chem. Phys.* **78** (1983) 1607.

[30] D.J. Fox, Y. Osamura, M.R. Hoffmann, J.F. Gaw, G. Fitzgerald, Y. Yamaguchi, and H.F. Schaefer III, *Chem. Phys. Letters* **102** (1983) 17.

[31] R.D. Amos, *Chem. Phys. Letters* **108** (1985) 185.

[32] R.D. Amos, *Chem. Phys. Letters* **124** (1986) 376.

[33] M.J. Frisch, Y. Yamaguchi, J.F. Gaw, H.F. Schaefer III, and J.S. Binkley, *J. Chem. Phys.* **84** (1986) 531.

[34] C. Møller and M.S. Plesset, *Phys. Rev.* **46** (1934) 618.

[35] I. Shavitt, in *Modern Theoretical Chemistry, Vol. 3*, ed. H.F. Schaefer III (Plenum Press, New York, 1977).

[36] J. Čížek, *J. Chem. Phys.* **45** (1966) 4256; *Advan. Chem. Phys.* **14** (1966) 35.

[37] R.J. Bartlett, *Ann. Rev. Phys. Chem.* **32** (1981) 359; J. Paldus in *New Horizons of Quantum Chemistry*; R.J. Bartlett, C.E. Dykstra, and J. Paldus in *Advanced Theories and Computational Approaches to the Electronic Structure of Molecules*; R.J. Bartlett, J. Phys. Chem. **93** (1989) 1697.

[38] J.A. Pople, J.S. Binkley, and R. Seeger, *Intern. J. Quantum Chem. Symp.* **10** (1976) 1.

[39] R. Krishnan and J.A. Pople, *Intern. J. Quantum Chem.* **14** (1978) 91.

[40] R. Krishnan, M.J. Frisch, and J.A. Pople, *J. Chem. Phys.* **72** (1980) 4244.

[41] J.S. Binkley, M.J. Frisch, D.J. DeFrees, K. Raghavachari, R.A. Whiteside, H.B. Schlegel, E.M. Fluder, and J.A. Pople, *GAUSSIAN82*, Carnegie-Mellon University, Pittsburgh (1985).

[42] S.R. Langhoff and E.R. Davidson, *Intern. J. Quantum Chem.* **8** (1974) 61.

[43] (a) C.W. Gillies, J.Z. Gillies, R.D. Suenram, F.J. Lovas, E. Kraka, D. Cremer, *J. Am. Chem. Soc.* **113** (1991) 2412; (b) D. Cremer, to be published.

[44] See for example T.J. Lee, R.B. Remington, Y. Yamaguchi, and H.F. Schaefer III, *J. Chem. Phys.* **89** (1988) 408.

[45] H.B. Schlegel, *J. Chem. Phys.* **84** (1986) 4530; H.B. Schlegel, *J. Phys. Chem.* **92** (1988) 3075.

[46] P.J. Knowles and N.C. Handy, *J. Chem. Phys.* **88** (1988) 6991.

[47] K. Wolinski and P. Pulay, *J. Chem. Phys.* **90** (1989) 3647.

[48] K. Anderssen, P. Å. Malmqvist, B.O. Roos, A.J. Sadlej, and K. Wolinski, *J. Phys. Chem.* **94** (1990) 5403.

[49] J.A. Pople, R. Krishnan, H.B. Schlegel, and J.S. Binkley, *Intern. J. Quantum Chem.* **14** (1978) 545.

[50] R.J. Bartlett and G.D. Purvis III, *Intern. J. Quantum Chem.* **14** (1978) 561.

[51] G.D. Purvis III and R.J. Bartlett, *J. Chem. Phys.* **76** (1982) 1910.

[52] J.A. Pople, M. Head-Gordon, and K. Raghavachari, *J. Chem. Phys.* **87** (1987) 5968.

[53] G.E. Scuseria and H.F. Schaefer III, *J. Chem. Phys.* **90** (1989) 3700.

[54] J. Paldus, J.Čížek, and B. Jeziorski, *J. Chem. Phys.* **90** (1989) 4356.

[55] K. Raghavachari, J.A. Pople, E.S. Replogle, and M. Head-Gordon, *J. Phys. Chem.* **94** (1990) 5579.

[56] P. Jørgensen and J. Simons, *J. Chem. Phys.* **79** 91983) 334.

[57] G. Fitzgerald, R. Harrison, W.D. Laidig, and R.J. Bartlett, *J. Chem. Phys.* **82** (1985) 4379.

[58] J. Gauss and D. Cremer, *Chem. Phys. Letters* **138** (1987) 131.

[59] J.E. Rice and R.D. Amos, *Chem. Phys. Letters* **122** (1985) 585.

[60] E.A. Salter, G.W. Trucks, G. Fitzgerald, and R.J. Bartlett, *Chem. Phys. Letters* **141** (1987) 61.

[61] I.L. Alberts and N.C. Handy, *J. Chem. Phys.* **89** (1988) 2107.

[62] G. Fitzgerald, R.J. Harrison, and R.J. Bartlett, *J. Chem. Phys.* **85** (1986) 5143.

[63] J. Gauss and D. Cremer, *Chem. Phys. Letters* **153** (1988) 303.

[64] G.W. Trucks, J.D. Watts, E.A. Salter, and R.J. Bartlett, *Chem. Phys. Letters* **153** (1988) 490.

[65] J.D. Watts, G.W. Trucks, and R.J. Bartlett, *Chem. Phys. Letters* **164** (1989) 502.

[66] G. Fitzgerald, R.J. Harrison, W.D. Laidig, and R.J. Bartlett, *Chem. Phys. Letters* **117** (1985) 433.

[67] L. Adamowicz, W.D. Laidig, and R.J. Bartlett, *Intern. J. Quantum Chem. Symp.* **18** (1984) 245.

[68] A.C. Scheiner, G.E. Scuseria, J.E. Rice, T.J. Lee, and H.F. Schaefer III, *J. Chem. Phys.* **87** (1987) 433.

[69] Y.S. Lee and R.J. Bartlett, *J. Chem. Phys.* **80** (1983) 4371; Y.S. Lee, S.A. Kucharski, and R.J. Bartlett, *J. Chem. Phys.* **81** (1984) 5906; *J. Chem. Phys.* **82** (1984) 5761.

[70] G.E. Scuseria and H.F. Schaefer III, *Chem. Phys. Letters* **146** (1988) 23.

[71] J. Gauss, J.F. Stanton, and R.J. Bartlett, *J. Chem. Phys.*, in press.

[72] J. Gauss and D. Cremer, *Chem. Phys. Letters* **150** (1988) 280.

[73] J. Gauss and D. Cremer, *Chem. Phys. Letters* **163** (1989) 549.

[74] S. Kucharski and R.J. Bartlett, *Adv. Quant. Chem.* **18** (1986) 281.

[75] S. Kucharski, J. Noga, and R.J. Bartlett, *J. Chem. Phys.* **90** (1989) 7282.

[76] P. Pulay, *Chem. Phys. Letters* **73** (1980) 393; *J. Comp. Chem.* **3** (1982) 556.

[77] G.D. Purvis and R.J. Bartlett, *J. Chem. Phys.* **75** (1981) 1284; G.W. Trucks, J. Noga, and R.J. Bartlett, *Chem. Phys. Letters* **145** (1988) 548.

[78] C.E. Dykstra and J.D. Augspurger, *Chem. Phys. Letters* **145** (1988) 545.

[79] G.E. Scuseria, T.J. Lee, and H.F. Schaefer III, *Chem. Phys. Letters* **130** (1986) 236.

[80] It should be noted that QCISDT is no longer a size consistent method (see e.g. ref [54]) Therefore, an iterative inclusion of triple excitations in QCI theory is not as straightforward as in CC theory, where the full CCSDT model [81] and various approximations to it [82] can be easily formulated in a size consistent way.

[81] J. Noga and R.J. Bartlett, *J. Chem. Phys.* **86** (1987) 7041; J.D. Watts and R.J. Bartlett, *J. Chem. Phys.* **93** (1990) 6104.

[82] J. Noga, R.J. Bartlett, and M. Urban, *Chem. Phys. Letters* **134** (1987) 126.

[83] K. Raghavachari, G.W. Trucks, J.A. Pople, and M. Head-Gordon, *Chem. Phys. Letters* **157** (1989) 479.

[84] K. Raghavachari, G.W. Trucks, J.A. Pople, and E. Replogle, *Chem. Phys. Letters* **158** (1989) 207.

[85] L.A. Curtiss and J.A. Pople, *J. Chem. Phys.* **90** (1989) 2833.

[86] L.A. Curtiss and J.A. Pople, *J. Chem. Phys.* **90** (1989) 2522; *J. Chem. Phys.* **90** (1989) 4314; *J. Chem. Phys.* **91** (1989) 4189.

[87] For other CC methods, which include connected quadruple excitations, see for example S. Kucharski and R.J. Bartlett, *Chem. Phys. Letters* **158** (1989) 550.

[88] N.C. Handy, R.D. Amos, J.F. Gaw, J.E. Rice, and E.D. Simandiras, *Chem. Phys. Letters* **120** (1985) 151.

[89] R. Moccia, *Chem. Phys. Letters* **5** (1970) 260.

[90] E.A. Salter, G.W. Trucks, and R.J. Bartlett, *J. Chem. Phys.* **90** (1989) 1752.

[91] G.W. Trucks, E.A. Salter, J. Noga, and R.J. Bartlett, *Chem. Phys. Letters* **150** (1988) 37.

[92] G.W. Trucks, E.A. Salter, C. Sosa, and R.J. Bartlett, *Chem. Phys. Letters* **147** (1988) 359.

[93] E. Kraka, J. Gauss, and D. Cremer, *J. Mol. Struct. (THEOCHEM)* , in

press.

[94] J. Gauss, E. Kraka, F. Reichel, and D. Cremer, *COLOGNE*, University of Cologne, Cologne (1989) and University of Göteborg, Göteborg (1990).

[95] D. Cremer and E. Kraka, *COLOGNE84*, University of Cologne, Cologne (1984).

[96] J. Gauss, Ph.D. Thesis, University of Cologne, Cologne (1988).

[97] J. Almlöf, K. Faegri,Jr., and K. Korsell, *J. Comp. Chem.* **3** (1982) 385.

[98] D. Cremer and J. Gauss, *J. Comp. Chem.* **7** (1986) 274.

[99] F. Reichel, Diploma Thesis, University of Cologne, Cologne (1988).

[100] F.W. Bobrowicz and W.A. Goddard III, *Modern Theoretical Chemistry Vol.3*, ed. H.F. Schaefer III (Plenum Press, New York, 1977).

[101] L.R. Kahn, P. Baybutt, and D.G. Truhlar, J. Chem. Phys. **65** (1976) 3826.

[102] D. Cremer, *J. Phys. Chem.* **94** (1990) 5502.

[103] R.F.W. Bader, T.S. Slee, D. Cremer, and E. Kraka, *J. Am. Chem. Soc.* **105** (1985) 5061.

[104] D. Cremer and E. Kraka, *Croat. Chem. Acta* **57** (1985) 1265.

[105] D. Cremer in *Modelling of Structure and Properties of Molecules*, ed. Z.B. Maksic (Ellis Horwood, Chichester, 1988).

[106] M. Dupuis and H.F. King, *Int. J. Quant. Chem.*, **11** (1977) 613.

[107] P. Carsky, B.A. Hess, Jr., and L.J. Schaad, *J. Comp. Chem.* **5** (1984) 280.

[108] J.F. Stanton, J. Gauss, J.D. Watts, and R.J. Bartlett, *J. Chem. Phys.* **94** (1991) 4334.

[109] Y. Osamura, Y. Yamaguchi, P. Saxe, D.J. Fox, M.A. Vincent, and H.F. Schaefer III, *J. Mol. Struct. (THEOCHEM)* **103** (1983) 183.

[110] P. Pulay, *J. Chem. Phys.* **78** (1983) 5043.

[111] M. Yoshimine, *J. Comp. Phys.* **11** (1973) 449.

[112] R.D. Nelson, Jr., D.R. Lide, Jr., and A.A. Maryott, *Selected Values of Electric Dipole Moments for Molecules in the Gas Phase*, NSRDS-NBS **10**, Washington 1967.

[113] A.K. Siu and E.R. Davidson, *Intern. J. Quantum Chem.* **4** (1970) 233; S. Green *Chem. Phys.* **54** (1971) 827; S. Green, *Adv. Chem. Phys.* **25** (1974) 179.

[114] D. Cremer, M. Krüger, and H. Dreizler, to be published.

[115] N. Ensllin, W. Bertozzi, S. Kowalski, C.P. Sargent, W. Turchinetz, C.F. Williamson, S.P. Fivozinsky, J.W. Lightbody, and S. Penner, *Phys. Rev. (C)* **9** (1974) 1705; H. Winter and H.J. Andr, *Phys. Rev. (A)* **21** (1980) 581.

[116] D. Sundholm, P. Pyykkö, L.Laakoonen, and A.J. Sadlej, *Chem. Phys.* **101** (1986) 219; I. Cernusak, G.H.F. Diercksen, and A.J. Sadlej, *Chem. Phys.* **101** (1986) 45; S. Gerber and H. Huber, *Chem. Phys.* **134** (1989) 279.

[117] F.C. de Lucia and W. Gordy, *Phys. Rev.* **187** (1969) 58.

[118] 6-31G(d) and 6-31G(d,p): P.C. Hariharan and J.A. Pople, *Theoret. Chim. Acta* **28** (1973) 213. 6-311G(d,p): R. Krishnan, J.S. Binkley, R. Seeger, and J.A. Pople, *J. Chem. Phys.* **72** (1980) 650; MC-311G(d,p): A.D. McLean and G.S. Chandler, *J. Chem. Phys.* **72** (1980) 5639. 6-311++G(d,p): T. Clark, J. Chandrasekhar, G.W. Spitznagel, and P. v. R. Schleyer, *J. Comp. Chem.* **4** (1983) 294. [5s3p2d/3s2p]: T. Dunning, Jr., *J. Chem. Phys.* **53** (1970) 2823. Exponents of the polarisation functions: K. Somasundram, R.D. Amos, and N.C. Handy, *Theoret. Chim. Acta* **69** (1986) 491.

[119] T.J. Lee, R.B. Remington, Y. Yamaguchi, and H.F. Schaefer III, *J. Chem. Phys.* **89** (1988) 408. R. Krishnan, M.J. Frisch and J. A. Pople, *J. Chem. Phys.* **72** (1980) 4244.

[120] See, e.g., W.J. Hehre, L. Radom, P.v. R. Schleyer, and J. A. Pople, *Ab Initio Molecular Orbital Theory*, (John Wiley, New York, 1986) and references cited therein.

[121] Zhi He and D. Cremer, *Intern. J. Quantum Chem. Symp.*, in press.

[122] S. Miertus and J. Tomasi, *Chem. Phys.* **65** (1982) 239.

[123] M. Schindler and W. Kutzelnigg, *J. Chem. Phys.* **76** (1982) 1919.

[124] E. Kraka, D. Cremer, and S. Nordholm in *Molecules in Science and Biomedicine*, Z. Maksic, Edt., Ellis Horwood, 1991, in press.